# Role of methylglyoxal in the pathogenesis of insulin resistance

A Thesis Submitted to the College of Graduate Studies and Research in Partial Fulfillment of the Requirement for the Degree of Doctor of Philosophy
in the Department of Pharmacology
University of Saskatchewan
Saskatoon

By

**Xuming Jia, M.Sc; M.D.**

# PERMISSION TO USE

In presenting this thesis in partial fulfillment of the requirements for a Ph.D. degree from the University of Saskatchewan, I agree that the libraries of this university may make it freely available for inspection. I further agree that permission for copying of this thesis in any manner, in whole or in part, for scholarly purposes may be granted by the professor or professors who supervised my thesis work or, in their absence, by the Head of the Department or the Dean of the College in which my thesis work was done. It is understood that any copying or publication or use of this thesis or parts thereof for financial gain shall not be allowed without my written permission. It is also understood that due recognition shall be given to me and to the University of Saskatchewan in any scholarly use which may be made of any material in my thesis.

Requests for permission to copy or make other use of material in this thesis in whole or in part should be addressed to:

Head of the Department of Pharmacology

Health Science Building, 107 Wiggins Road

University of Saskatchewan

Saskatoon SK

S7N 5E5 Canada

## ABSTRACT

Methylglyoxal (MG) is a reactive metabolite presents in all biological systems. The accumulation of MG in diabetic patients and animals has been long recognized. Recently, studies have shown that MG levels are elevated in hypertensive rats. However, the pathological effects of MG in diabetes and related insulin resistance syndrome such as obesity are currently unknown. In the present study, the role of MG in the pathogenesis of insulin resistance was investigated.

First, it was observed that MG induced structural and functional changes of insulin. Incubation of human insulin with MG *in vitro* yielded MG-insulin adducts, as evidenced by additional peaks observed upon mass spectrometric (MS) analysis. Tandem MS analysis of insulin B-chain adducts confirmed attachment of MG at an arginine residue. [$^3$H]-2-deoxyglucose uptake ([$^3$H]-2-DOG) by 3T3-L1 adipocytes was significantly and concentration-dependently decreased after treatment with MG-insulin adducts, in comparison with the effect of native insulin at the same concentration. A significant decrease of glucose uptake induced by MG-insulin adducts was also observed in L8 skeletal muscle cells. Unlike native insulin, MG-insulin adducts did not inhibit insulin release from pancreatic β-cells. The degradation of MG-insulin by cultured liver cells was also decreased. In conclusion, MG modifies insulin by attaching to internal arginine residue in the β-chain of insulin. The formation of this MG-insulin adduct decreases insulin-mediated glucose uptake, impairs autocrine control of insulin secretion, and decreases insulin clearance. These structural and functional abnormalities of the insulin molecule may contribute to the pathogenesis of insulin resistance.

Second, the effects of MG on the insulin signaling pathway were investigated. After 9 weeks of fructose treatment, an insulin resistant state was developed in Sprague-Dawley (SD) rats, demonstrated as increased triglyceride and insulin levels, elevated blood pressure, and decreased insulin-stimulated glucose uptake by adipose tissue. A close correlation between insulin resistance and the elevated MG accumulation in adipose and skeletal muscle tissues was observed. The insulin resistant state and the elevated MG level were reversed by the MG scavenger, N-acetyl cysteine (NAC) and metformin. In cultured adipose cells, MG treatment impaired insulin signaling as measured by decreased tyrosine phosphorylation of insulin-receptor substrate-1 (IRS-1) and the decreased kinase activity of phosphatidylinositol 3-kinase (PI3K). The ability of NAC to block MG-impairment of PI3K activity and IRS-1 phosphorylation further confirmed the role of MG in the development of insulin resistance. In cultured skeletal muscle cells, MG treatment significantly reduced the expression of IRS-1 and PI3K at the mRNA level. Similar to adipose cells, MG also decreased tyrosine phosphorylation of IRS-1 and PI3K activity. We also examined the mechanism of metformin to inhibit AGEs. Using mass spectrometry, stable metformin-MG adducts were identified.

In addition, we investigated the causative effect of MG in the pathogenesis of obesity, another form of insulin resistance. This study revealed a previously unrecognized effect of MG in stimulating adipogenesis by up-regulating Akt signaling. Further study suggested that MG accumulation stimulates the phosphorylation of Akt and its effectors p21 and p27. The activated Akt pathway then increased the activity of Cdk2 and accelerates the cell cycle progression and proliferation of pre-adipocytes. The effects of MG were efficiently reversed by both alagebrium, and Akt inhibitor SH-6.

Overall, the current study investigated the effect of MG during the pathogenesis of insulin resistance syndrome. MG, as the most potent precursor of AGEs, impairs the activity of insulin signaling pathway by glycating the insulin molecule and other insulin signaling proteins. Moreover, this study observed a previously unrecognized causative effect of MG in the proliferation of adipocytes by up-regulating the Akt signaling pathway. The results from this study offer new mechanisms to explain the development of insulin resistance and to prevent the related diseases.

# ACKNOWLEDGEMENTS

I would first like to express my deepest gratitude to my supervisor Dr. Lingyun Wu for providing me with a great research opportunity. Her invaluable guidance is a great help not only in the completion of this project but also in my future academic pursuits. I greatly appreciate the wonderful time of working with her. Her mastery of science and devotion to research set a role model to me, and I will be conscious of her example in my whole life.

I would also like to thank the members of my supervisory committee, Dr. Kash Desai, Dr. Venkat Gopal, Dr. Robert McNeill, Dr. Andrew Ross, Dr. John Tuchek, Dr. Tom Wilson, and Dr. Peter Yu for their selfless supports, helpful insights and useful suggestions for the progression of my research.

My gratitude is extended to all the members of Dr. Wu's laboratory and all thank all my friends in the Department of Pharmacology for their friendship and providing a friendly and productive environment. I greatly appreciate the financial support from the Heart and Stroke Foundation of Canada and Arthur Smyth Award of University of Saskatchewan.

My special thanks go to my parents, Jingye Jia and Guihua Wang, and my sister, Qingqing Jia, for their unconditional love, understanding, help and encouragement in every possible way. I am deeply indebted to my dear husband, Dr. Yu Fu, for his love and understanding through these years. Finally, thanks to my son, Jiachen (who arrived during my thesis writing), for the joy and the happiness he brings to my life.

**To my family**

# TABLE OF CONTENTS

**CHAPTER SIX: METHYLGLYOXAL MEDIATES ADIPOCYTE PROLIFERATION AND CONTRIBUTES TO THE DEVELOPMENT OF OBESITY**

# LIST OF TABLES

# LIST OF FIGURES

# LIST OF ABBREVIATION

| | |
|---|---|
| AG | Aminoguanidine |
| AGEs | Advanced glycation end products |
| AMO | Acetol monooxygenase |
| BAT | Brown adipose tissue |
| BCA | Bicinchoninate |
| BMI | Body mass index |
| C/EBP | CCAAT/enhance binding protein |
| Cdks | Cyclin-dependent kinases |
| CEL | Nε-Carboxyethyl lysine |
| Cip | Cdk inhibitory protein |
| CML | Nε-`Carboxymethyl lysine |
| DCFH-DA | 5-(and 6)-carboxy-2',7'-dichlorodihydrofluoresceindiacetate |
| DHAP | Dihydroxyacetone phosphate |
| DMEM | Dulbecco's modified Eagle's medium |
| DTT | Dithiothreitol |
| ELISA | Enzyme-linked immunosorbent assay |
| ER | Endoplasmic reticulum |
| ERK | Extracellular signal-regulated kinase |
| F2,6BP | Fructose-2,6-bisphosphate |
| G3P | Glyceraldehyde-3-phosphate |
| GLUT | Glucose transporter |
| GOLD | Glyoxal lysine dimmer |
| GSH | Reduced glutathione |
| GSK3 | Glycogen synthase kinase 3 |
| [$^3$H]-2-DOG | [$^3$H]-2-deoxyglucose |
| HDL-cholesterol | High-density lipoprotein cholesterol |
| HPLC | High-performance liquid chromatography |
| IGF-I | Insulin-like growth factor-I |
| IKK-β | Inhibitor κB kinase-β |
| IL-6 | Interleukin-6 |
| iNOS | Inducible nitric oxide synthase |
| $IP_3$ | Inositol 1,4,5-triphosphate |
| IPGTT | Intraperitoneal glucose tolerance test |
| IR | Insulin receptor |
| IRS | Insulin receptor substrate |
| JNK | c-jun NH2-terminal kinase |
| Kip | Kinase inhibitor protein |
| LC-MS | Liquid chromatography-mass spectrometry |
| M phase | Mitosis phase |
| MALDI-TOF MS | Matrix-assisted laser desorption/ionization-time of flight mass |

| | |
|---|---|
| | spectrometry |
| MG | methylglyoxal |
| MG-H1 | Hydroimidazolone Nε-(5-hydro-5-methyl-4-imidazolon-2yl)-ornithine |
| MOLD | Methylglyoxal lysine dimmer |
| MS | Mass spectrometry |
| MS/MS | Tandem mass spectrometry |
| mTOR | Mammalian target of rapamycin |
| MTT | 3-(4,5-dimethylthiazol-2-yl)-2,5-diphenyltetrazolium bromide |
| NAC | N-acetlyl ysteine |
| NEFA | Non-esterified fatty acid |
| NF-κB | Nuclear factor- κB |
| o-PD | o-phenylenediamine |
| Ox | oxidation |
| p-Akt | Phosphor-akt |
| PBS | Phosphate buffer saline |
| PCR | Polymerase chain reaction |
| PDK1 | Protein kinase 3-phosphoinositide dependent protein kinase-1 |
| PFK-1 | Phosphofructokinase-1 |
| PI | Propidium iodide |
| PI3K | Phosphatidylinositol 3-kinase |
| $PIP_2$ | PI 4,5-bisphosphate |
| $PIP_3$ | $PtdIns(3,4,5)P_3$ |
| PK | Pyruvate kinase |
| p-p21 | Phosphor-p21 |
| p-p27 | Phosphor-p27 |
| PTB | Phenacyl thiazolium bromide |
| PTEN | Phosphatase and tensin homologue |
| PTPase | Protein-tyrosine phosphatease |
| RAGE | Receptor for advanced glycation end products |
| Rb | Retinoblastoma protein |
| ROS | Reactive oxygen species |
| S phase | Synthesis phase |
| SD | Sprague-Dawley rat |
| SHR | Spontaneously hypertensive rats |
| SREBP-1 | Sterol regulatory element binding protein-1 |
| SSAO | Semicarbazide-sensitive amine oxidase |
| TNF-α | Tumor necrosis factor-α |
| TPI | Triosephosphate isomerase |
| VEGF | Vascular endothelial growth factor |
| WAT | White adipose tissue |
| WKY | Age-matched Wistar-Kyoto rats |

# CHAPTER ONE

# INTRODUCTION

## 1.1. Insulin resistance

Insulin resistance is a state in which the biological functions of insulin are impaired. An increased amount of insulin is required for the cells of the body to produce a given biological response under insulin resistant state. Although the resistance to insulin can happen in different tissues, the three most important tissues that usually linked to the development of metabolic insulin resistance are skeletal muscle, liver and adipose tissue. Under insulin resistance state, the physiological metabolism of the body is largely altered. For example, insulin resistance increased hydrolysis of triglycerides in stored in adipocytes and resulted in the elevated accumulation of free fatty acids in the blood plasma. As the skeletal muscle cells are responsible for uptaking majority of the circulating glucose, insulin resistance in skeletal muscle tissue reduces glucose uptake from circulating system. In liver, insulin resistance leads to a reduced glycogen synthesis and an enhanced glucose production. Therefore, insulin resistance is involved in different forms of diseases including obesity, dyslipidemia, hypertension and athrosclerosis. Increased levels of plasma insulin and glucose resulted by insulin resistance are reported to be the origin of various metabolic syndromes and related complications. In particular, the impaired insulin function will ultimately elevate blood glucose level and contribute to the pathogenesis of type 2 diabetes mellitus. Furthermore, increased insulin levels result in the retention of sodium and fluid, which leads to hypertension and congestive heart failure. A study (Gallistl et al., 2000) showed that overweight children with high blood

levels of insulin are likely to have high levels of homocysteine, a substance which appears to raise the risk of cardiovascular diseases, stroke, and birth defects. Since insulin induces cellular proliferation, its effect on the pathogenesis of cancer is also suspected (Boyd, 2003).

### 1.1.1. Insulin

Insulin is a hormone with a molecular weight of approximately 6000 Daltons produced and secreted exclusively by pancreatic β-cells. It is essential in regulating the metabolism of carbohydrates and fat in the body. The primary amino acid sequence and the unique covalent structure of insulin were identified over 50 years ago (Sanger and Tuppy, 1951). The pathway behind the biosynthesis of insulin in pancreatic β cells, specifically as a proinsulin precursor, was also determined in the same era (Steiner et al., 1969). Although insulin is one of the most studied molecules in biochemistry and physiology field, there are many details of the mechanisms behind its secretion and signaling still remain unidentified.

#### 1.1.1.1. Structure of insulin

Circulating and biologically active insulin is monomeric which contains two polypeptide chains, chain A and chain B. In most species, these two chains have 21 amino acids and 30 amino acids, respectively (Figure 1-1A). They are covalently tethered together by two disulfide bridges between A chian and B chain (residues A7 to B7, and A20 to B19) and the additional disulfide bridge within A chain (residues A6 to A11). The positions of these disulfide bonds are highly conserved in all mammalian

forms of insulin. Insulin has a tendency to dimerize in solution and further associates into hexamers in the presence of Zinc ion (Smith, 1971). The hexamer form is the form in which insulin stored in the beta cells and secreted into the blood stream.

Insulin has a compact three-dimensional structure. Although the amino acid sequence of insulin differs among different species, this basic conformation is present in all members of the insulin peptide family (Figure 1-1*B*). This is due to the conserved positions of the three disulfide bonds and the conserved amino acid residues of both ends of the A chain and the C-terminal sequence of the B chain. The hydrophobic residues that form the core of insulin contribute to its stability. The molecular structure is further stabilized by the three disulfide bridges (two between A chian and B chain and one within A chain). The insulin monomer has two extensive nonpolar surfaces around its core. The first one buried in insulin dimer and contributes to the formation of an antiparallel beta sheet structure. The other one is more extensive and is buried when insulin hexamer is formed. Insulin uses these hydrophobic surfaces for the receptor binding and self-assembly into dimmers and hexamers.

#### 1.1.1.2. <u>Biosynthesis of insulin</u>

Insulin is synthesized in the β cells of the pancreatic islets. It is origianaly produced as a single chain precursor called preproinsulin. After the insulin mRNA is translated into preproinsulin in the ribosomes of the rough endoplasmic reticulum, its signal peptide is cleaved and forms proinsulin. The proinsulin is then transported to the Golgi apparatus and wrapped into secretory granules located close to the cell membrane.

**A**

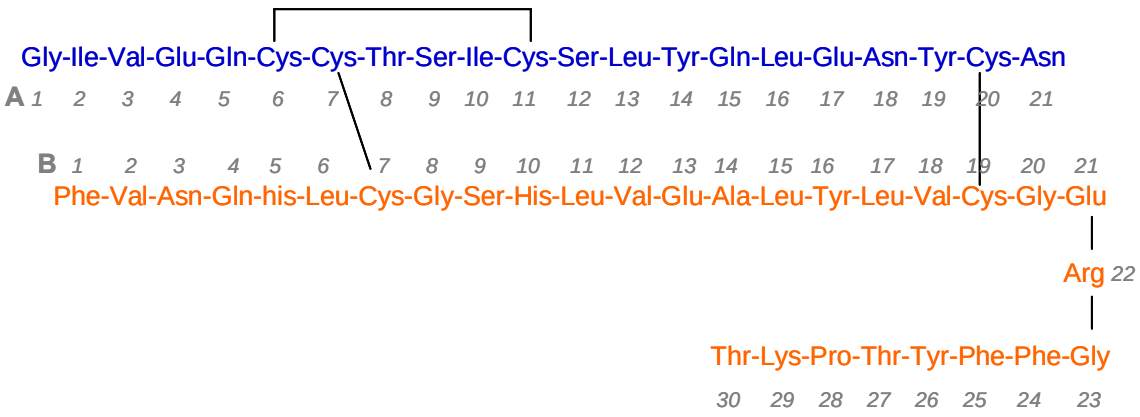


**B**

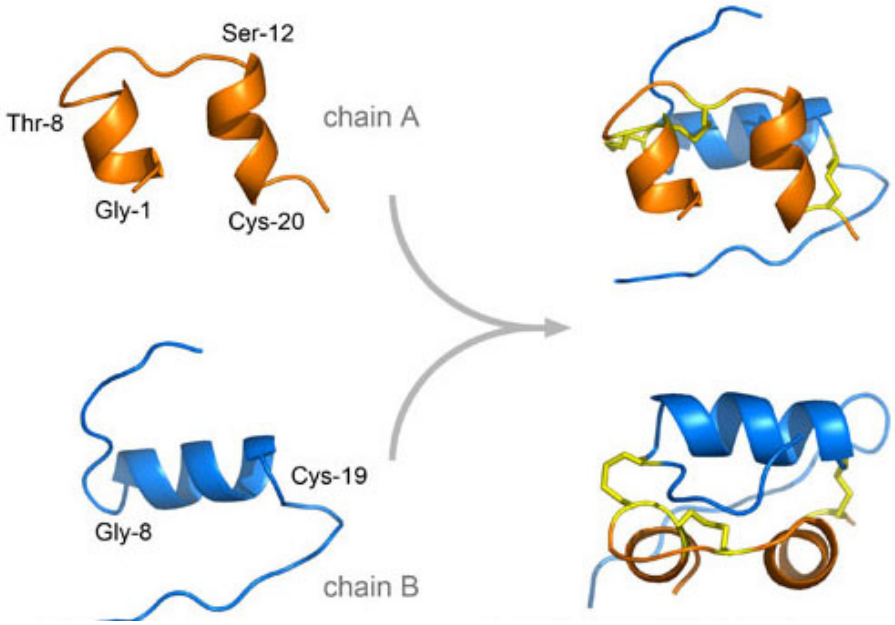


**Figure 1-1. Sequence and structure of human insulin.** ***A***) The A chain of human insulin is shown in blue and the B chain is shown in orange. The disulfide bridges are shown as black bonds connecting the cysteine residues. ***B***) shows quaternary structure of insulin. The two chains are assembled via post-translational modification that includes disulfide bridge formation (shown in yellow) and removal of the C-peptide. This figure is obtained from www.betacell.org.

Proinsulin has three domains including an amino-terminal B chain, a carboxy-terminal A chain and a connecting C-peptide between A chain and B chain. Some specific endopeptidases excised the C-peptide in the endoplasmic reticulum, thereby producing the mature form of insulin. Both of the C-peptide and the mature insulin are packaged into secretory granules and accumulate in the cytoplasm. When the pancreatic β cells are stimulated by increased blood glucose level or other factors, insulin is then secreted by exocytosis and diffuses into islet capillary blood. At the same time, equal molar of C-peptide is secreted into circulation with insulin. Around 50% of the insulin and C-peptide are then delivered into the portal venous system which leads them directly to the liver while the remainder is distributed throughout the body (Polonsky, 1995).

#### 1.1.1.3. The regulation of insulin secretion

Insulin secretion is stimulated by various agents including glucose, metabolites of fatty acid such as acetone and acetoacetic acid, and amino acids (arginine, lysine). However, it is especially sensitive to the increased blood glucose level. Glucose elicits a biphasic release of insulin which consists of an immediate insulin release and a sustained insulin secretion. The immediate release of insulin is due to the release of pre-synthesized insulin stored in secretory granules. This is followed by a more prolonged release of newly synthesized insulin.

The pancreatic islet cells are connected by tight cell-cell junctions, which play an important role in synchronizing insulin secretion by controling the transport of ions, metabolites, messenger molecules from one cell to another. When glucose enters the β cells via glucose transporter GLUT2, it is activated and phosphorylated by glucokinase

and leads to ATP production. The enhanced intracellular ATP synthesis therefore closes ATP-dependant potassium channels and shuts down the potassium exit. Consequently, the voltage-dependant calcium channels are depolarized opened. The increased intracellular calcium concentration activates phospholipase C, which catalyzes the membrane phospholipid phosphatidyl inositol 4,5-bisphosphate into inositol 1,4,5-triphosphate ($IP_3$) and diacylglycerol (DAG). The binding of $IP_3$ to its receptor on ER membrane launches the discharge of $Ca^{2+}$ from the ER and thus further raises intracellular $Ca^{2+}$ concentration. Subsequently, the previously synthesized insulin from the secretory vesicles is secreted.

When the glucose level returns to the normal physiologic value, insulin release from the β cells slows down or being terminated. If blood glucose level decreases further to lower than normal value, glucagon is released from pancreatic Langerhans' α cells and forces glycogenolysis in the liver, thus enhances the circulating glucose level. By regulating blood glucose level, hyperglycemic hormones prevent the occurrence of life-threatening hypoglycemia. In addition to food intake, the β cells are also influenced by the autonomic nervous system. For example, norepinephrine is released in response of stress thus inhibites insulin secretion and leads to increased blood glucose levels.

#### 1.1.1.4. Clearance and degradation of insulin

In view of the significant effect of insulin in lowering blood glucose level, it is critical for the fine regulation of the biological function of insulin. One of the regulated processes that linked to insulin action is to degrade and clear the circulating insulin.

Impairment of insulin clearance results in different diseases including Type 2 diabetes (Duckworth et al., 1998).

The uptake of insulin is mainly through a receptor mediated specific process at physiological concentrations. At higher concentrations, non-receptor mediated insulin uptake plays a more important role. Same as in the initiation of insulin signaling, the first step in insulin degradation is to bind to the insulin receptor. This receptor mediated insulin uptake and degradation undergo in all of the insulin-sensitive tissues such as liver, adipose and skeletal muscle (Duckworth et al., 1998). However, liver and kidney are the primary site of insulin clearance (Sato et al., 1991). The molecular mechanism behind insulin clearance and degradation has been extensively studied. The most popular model for insulin degradation includes three steps: receptor binding, receptor-mediated internalization of insulin and insulin degradation. The receptor-bound insulin spends different time in different tissues. The endogenously secreted insulin spend much longer time binding to hepatic insulin receptor than to the insulin receptor in skeletal mucle tissue and adipose tissue (Hovorka et al., 1993). Binding to insulin receptor does not necessarily lead to the degradation of insulin. Namely, not all receptor-bound insulin is internalized into endosomes. In fact, a significant portion of insulin return back to the circulation with full or partial biological function. Some of this partially degraded insulin retains receptor binding and biological activity. As they are also immunoreactive to anti-insulin antibody, this partially degraded insulin still contributes to measurable insulin levels. The uptake of insulin is altered by nutrient intake and the insulin level in the circulation. Shortly after internalization, endosomes acidify and result in dissociation of insulin from IR. This is followed by degradation of insulin by insulin degradation enzyme

(IDE) through multipal pathways. insulin that not cleared by liver and kidney is eventually removed by other insulin-sensitive cells, such as skeletal muscle cells, adipocytes (Ardevol et al., 1996; Jochen et al., 1989), fibroblasts (Baldwin et al., 1981), monocytes (Powers et al., 1980), lymphocytes (Buffington et al., 1986) and gastrointestinal cells (Bai et al., 1995). The circulating insulin was degraded very fast by insulinase in liver and kidney. As a result, insulin has an extremely short half-life of about 6 minutes in systemic circulation. This short duration of action allows rapid changes in the circulating levels of insulin.

#### 1.1.1.5. Biological functions of insulin

As seen in Figure 1-2, the major biological function of insulin is to regulate the metabolism of glucose, protein and lipid. In addition, it modulates DNA synthesis and transcription, alters the expression of numerous mRNAs and stimulates growth.

##### 1.1.1.5.1. Regulation of protein synthesis

Insulin stimulates protein synthesis by promoting cellular uptake of amino acid and inhibiting protein degradation in different type of cells and tissues (Saltiel and Kahn, 2001). At molecular level, insulin promotes translational initiation and elongation of specific proteins by mTOR signalling pathway. The activation of mammalian target of rapamycin (mTOR) through Akt and the inactivation of TSC1–TSC2 promote each stage of protein synthesis including ribosome biogenesis, cap-dependent translational initiation and translational elongation (Proud, 2006). The mTOR is a kinase that shares homology.

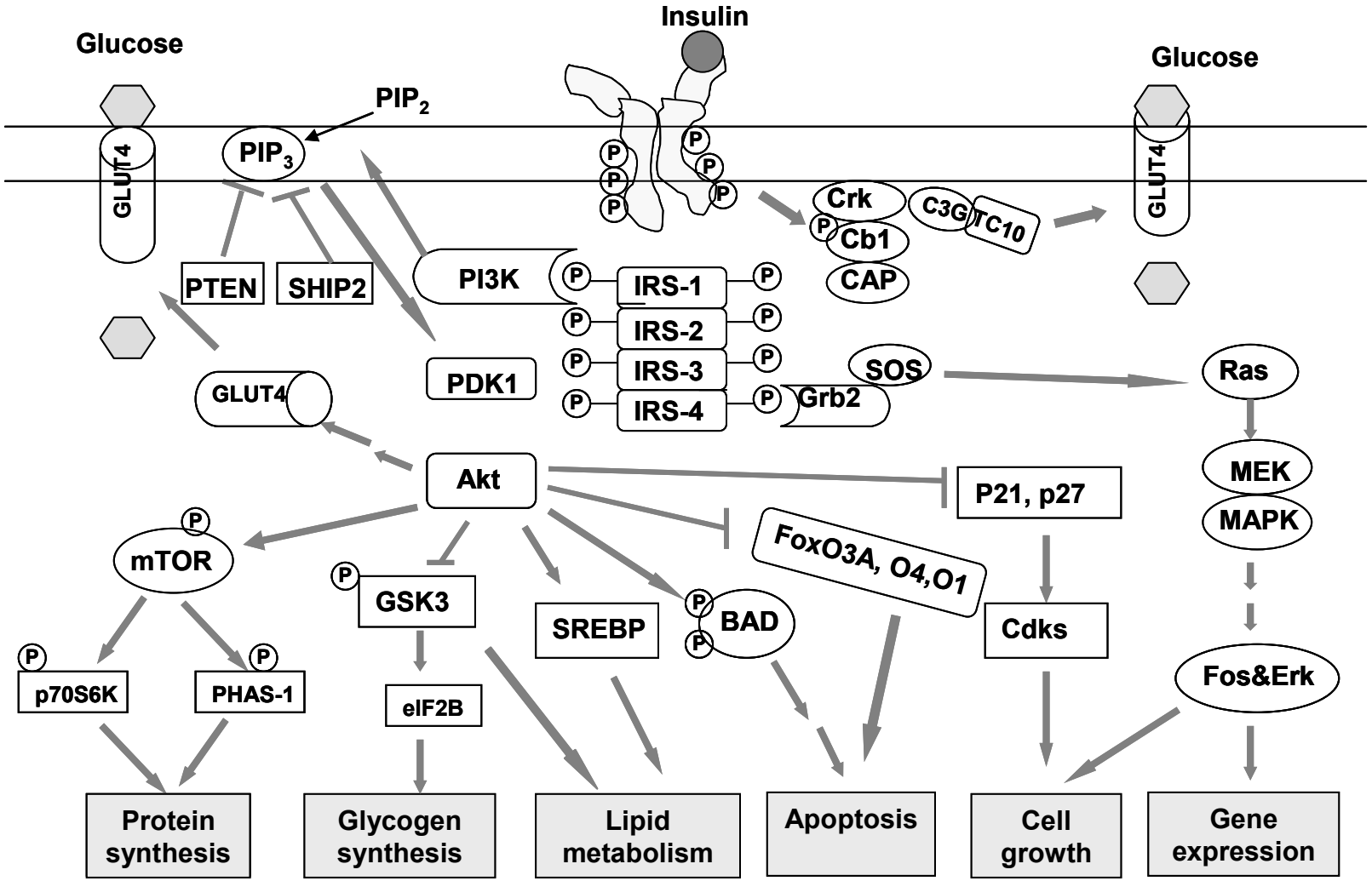
Insulin
Glucose
Glucose
PIP2
PIP3
GLUT4
GLUT4
PTEN
SHIP2
PI3K
IRS-1
IRS-2
IRS-3
IRS-4
Crk
Cb1
CAP
C3G
TC10
PDK1
GLUT4
SOS
Ras
Grb2
Akt
P21, p27
MEK
MAPK
mTOR
FoxO3A, O4,O1
GSK3
SREBP
BAD
Cdks
p70S6K
PHAS-1
eIF2B
Fos&Erk
Protein synthesis
Glycogen synthesis
Lipid metabolism
Apoptosis
Cell growth
Gene expression

**Figure 1-2. Schematic illustration of major biological effects of insulin**. Binding of insulin to its receptor activates its intrinsic tyrosine kinase activity and causes autophosphorylation of insulin receptor. The activation of insulin receptor phosphorylates IRS proteins and other docking proteins such as CAP and Crk on tyrosine residues. The phosphorylated IRS proteins therefore initiates signaling cascades and leads to the activation of multiple downstream effectors which ultimately transmit the insulin signal to a various intracellular pathways that regulates protein synthesis, glycogen synthesis, and lipogenesis. In addition, by inhibiting FoxO and cdk inhibory proteins including p21, p27, insulin also inhibits apoptosis and stimulates cell proliferation.

with similar catalytic domain of lipid kinases from the PI3K family. The activated mTOR causes phosphorylation and activation of p70S6K which in turn increases phosphorylation of eEF2 kinase and thus inititiate translation elongation. Because insulin induces p70S6K activity and increases phosphorylation on eEF2 kinase, the eEF2 becomes much more sensitive in response to insulin action (Asnaghi et al., 2004). Furthermore, the inactivation of GSK3, which is known for phosphorylating and inactivating glycogen synthase, increases the dephosphorylation of eIF2B and promote protein synthesis and storage of amino acids (Lizcano et al., 2002).

**1.1.1.5.2**. **Regulation of lipid synthesis**

Synthesis of fatty acids takes place in the cytoplasm of hepatocytes. The effect of insulin in liver is to promote fatty acids uptake and stimulates lipid synthesis, and at the same time inhibite lipolysis. Previous studies indicate that the insulin pathway mediating different metabolic effects (Kitamura et al., 1999; Kitamura et al., 1998) demonstrate differential degree of sensitivity to insulin. For example, a very low concentration of insulin is enough to induce the anti-lipolytic effect while a much higher insulin dose is required for the stimulation of glucose transport. As a result, the antilipolytic effect of insulin can still be active even when the glucose transport is impaired. It provides a molecular mechanism for insulin to maintain and expand the body adipose stores. The transcription factor ADD-1 (adipocyte determination and differentiation factor-1) and SREBP-1c (sterol regulatory element–binding protein-1c) play critical roles in regulating adipocyte gene expression (Foretz et al., 1999; Kim et al., 1998; Shimomura et al., 1999). The physiological role of insulin through SREBP-1c is to induce expression of lipogenic

genes and repressing the genes that involved in fatty acid oxidation. Meanwhile, insulin inhibits lipid catabolism through diminishing the cellular cAMP concentrationsf by activating cAMP specific phosphodiesterase in adipocytes (Kitamura et al., 1999).

#### 1.1.1.5.3. Regulation of cell growth and cell survival

Insulin is involved in the control of cell growth and cell survival by regulating some signal transduction proteins such as Growth factor receptor-bound protein 2 (Grb2) (Figure 1-2), an adaptor protein that contains SH3 domains that involved extensively in signal transduction and cell communication. Activated by phosphorylated IRS, Grb2 associates with the guanine nucleotide exchange factor SOS and stimulates the MAPK signaling pathway which leads to mitogenic responses (Ogawa et al., 1998). The activation of MAPK could also be triggered by Shc, another substrate for the IR. Once being phosphorylated, Shc associates with Grb2 and directly activate the MAPK pathway independently of IRS. In addition, insulin also reduces apoptosis through Akt pathway. In response to insulin action, the activated Akt phosphorylates and inhibits the activity of transcription factor FoxO3a, and in turn reduces apoptosis.

#### 1.1.1.5.4. Negative regulation and termination of insulin signaling

Termination of insulin signaling is basically achieved by internalizing the insulin-IR complex into endosomes and the degrading insulin by IDE (Bevan, 2001). Negative regulation of insulin signaling is necessary to maintain the normal physiological metabolism of the body. Meanwhile, it is also a major cause of insulin resistance. Insulin activates two major signaling pathways including the PI3K/Akt pathway and Ras-MAPK

pathways. These two pathways regulate metabolic processes and cell growth, respectively. Inhibitors of both pathways have been reported (Huang et al., 2009). The phosphatase and tensin homologue (PTEN, a 3' phosphatase) and the Src homology 2 family containing inositol 5'-phosphatase (SHIP, a 5' phosphatase) attenuates the $PIP_3$ signaling by degrading PIP3 to PIP2 (Lazar and Saltiel, 2006), and lead to the termination of PI3K/Akt pathway. Similarly, the negative regulation of Ras-MAPK is also through changing the expression and phosphorylation of target proteins.

### 1.1.2. Causes of insulin resistance

Pathogenesis of insulin resistance involves both genetic background and environmental influences. It could be a result of hereditary defects including the mutations of IR, glucose transporter and other signaling proteins. But most of insulin resistance is cause by certain acquired factors such as inadequate physical activity level, over-nutrition induced hyperglycemia (glucose toxicity), increased free fatty acids and the aging process (Lutsey et al., 2008). Cellular development of insulin resistance involves pre-receptor defects, receptor defects and post-receptor defects. Compare to the decreased bioavailability of insulin, defective insulin receptor and impaired insulin signaling are more frequently observed in individuals with insulin resistance. As obesity usually is associated with decreased IR number and failure in activating postreceptor insulin signaling cascade (such as reduced postreceptor tyrosine phosphorylation), obesity is regarded as the most common cause of insulin resistance.

#### 1.1.2.1. Pre-receptor reasons of insulin resistance

Pre-receptor defects is usually refered to reduced bioavailability of insulin in circulation. Some forms of insulin resistance can be resulted by the high titer and/or affinity of insulin antibodies. These insulin antibodies competitively bind to insulin and reduce the maximum action of insulin. Therefore, this type of insulin resistance is called immunological insulin resistance (Lupsa et al., 2009). IgG antibodies in response to exogenous insulin are often found in patients with insulin therapy (Hirano et al., 2008). Mutations in human insulin cause an autosomal-dominant insulin resistance syndrome. The mutated insulin may either reduce the binding capacity to its receptor or impair the subcellular trafficking and processing of the proinsulin in pancreatic β-cells. Patients with mutated insulin usually respond normally to exogenous insulin but shows increased fasting plasma insulin level due to delayed receptor-mediated clearance of the mutated insulin (Steiner et al., 1990). In addition to the mutation of insulin, there are also possibilities that certain reactive chemicals in the circulation could modify the structure of insulin and alter its biological function.

#### 1.1.2.2. Defects of insulin receptor resulting insulin resistance

Alterations in the expression, binding, phosphorylation and kinase activity of insulin receptor account for major types of insulin resistance.

The insulin receptor is a heterotetrameric glycoprotein that belongs to receptor tyrosine kinase super family. It consists of two α-subunits and two β-subunits which linked together by two disulphide bridges. The extracellular α-subunits contain insulin binding sites whereas the β-subunit is composed of an extracellular domain, a transmembrane domain, and an intracellular domain. The intracellular domain of β-

subunit possesses the intrinsic tyrosine kinase activity of IR. The entire insulin receptor is expressed in two isoforms, isoform A and isoform B. The isoform B contains a 12-amino-acid peptide at the COOH-terminus of the α-subunit while the isoform A lacks this insertion. The isoform B shows a two-fold higher affinity for insulin as compared to the A isoform (Kosaki et al., 1995). The different ligand binding affinity of these two isoforms results in different sensitivity to insulin and the subsequent biological function in both anabolism and metabolism (Kosaki and Webster, 1993). Increased expression of the B isoform in skeletal muscle has been positively correlated with both hyperglycaemia and hyperinsulinaemia. Thus, the different distribution abundance of these two isoforms in insulin target tissues may contribute to the pathogenesis of insulin resistant state (Mosthaf et al., 1991). Furthermore, it might explain the pathogenesis of tissue specific insulin resistance.

Mutations of IR may alter its expression, ligand binding and tyrosine kinase activity in insulin sensitive tissues (Taylor et al., 1990). A number of different genetic mutations of IR gene have been identified in patients with extreme insulin resistance syndrome. These mutations decrease the number of insulin receptors on cell surface by reducing the insulin-receptor mRNA levels or impairing the recruitment of receptors to cell membrane. Another type of IR mutation increases the insulin-IR affinity and impairs the dissociation of insulin from its receptor in the endosomal acidic pH. This defect inhibits the recycling of IR back to the plasma membrane and accelerates receptor degradation, which also lead to a decreased number of insulin receptors on the cell surface (Accili et al., 1989).

In addition to auto-phosphorylation on tyrosine residues, the activity of IR is also regulated by the serine/threonine phosphorylation of its β subunit. The serine/threonine thephosphorylation reduces the tyrosine kinase activity of IR. Under insulin resistant state, the chronic elevation of insulin might stimulate the phosphorylation level on certain serine residues of IR. As a result, the tyrosine kinase activity of IR decreases and thus exacerbates the insulin resistance state. Indeed, impaired phosphorylation of the IR in response to insulin has been observed in insulin sensitive tissues (skeletal muscle tissue, adipose tissue and liver) of morbidly obese individuals with/without Type 2 diabetes (Caro et al., 1987; Goodyear et al., 1995; Nolan et al., 1994).

#### 1.1.2.3. Defects of post-receptor insulin signaling in insulin resistance

Previous studies of the insulin resistant subjects suggested that the reduced insulin-mediated glucose transport in insulin sensitive tissues is mainly resulted by dysfunction of insulin signalling cascade such as the reduced expression and tyrosine phosphorylation of IRS proteins and PI3K/Akt (Brozinick et al., 2003; Goodyear et al., 1995; Kim et al., 1999). In the skeletal muscle tissues of obese and diabetic individuals, defects in insulin activation of PKC-ζ have also been observed. The defects in PKC-ζ activation were also observed in cultured myocytes and adipocytes from obese subjects (Sajan et al., 2004). Previous studies demonstrated contradictive results of the expression and activation of Akt in insulin resistance state. Although insulin-stimulated Akt phosphorylation was shown to be reduced in adipocytes and skeletal muscles of glucose intolerant type 2 diabetics patients compared with control subjects (Brozinick et al., 2003; Krook et al., 1998), other studies failed to detect alterations in insulin-induced Akt

activation in skeletal muscle of obese subjects with or without Type 2 diabetes (Kim et al., 1999). Impairment of insulin signaling may also results from the up-regulation of the insulin signaling inhibitors. The inhibitive effect of the intracellular enzyme protein-tyrosine phosphatases (PTPase) 1B and the transmembrane PTPase leukocyte antigen-related protein have been recognized by recent studies. It is observed that obese non-diabetic subjects exhibited increased expression and activity of PTPases in adipose tissue and skeletal muscle (Ahmad et al., 1997a; Ahmad et al., 1997b). In addition, IR tyrosine kinase inhibitor glycoprotein PC-1 was also found to be correlated with BMI value. The increased glycoprotein PC-1 expression dramatically reduced insulin sensitivity in adipose tissue (Frittitta et al., 1997). These PTPases have been identified as new targets to enhance insulin action in insulin-resistant diseases.

There is growing evidence associates chronic, low-grade inflammation with the insulin resistance state. Increased level of proinflammatory cytokines contribute to the pathogenesis of clinical features of insulin resistance syndrome including hyperinsulinemia, hyperlipidemia, decreased HDL cholesterol concentration and increased body mass index (BMI)/waist circumference (Pickup, 2004). For example, increased expression of inflammatory cytokines such as tumor necrosis factor-α (TNF-α) and interleukin-6 (IL-6) were detected in adipose tissue in obese subjects (Kern et al., 2001). TNF-α induces site-specific serine phosphorylation and decreases tyrosine phosphorylation of IRS-1. The alteration on IRS-1 phosphorylation dissociates the protein from IR and thus induces IRS protein degradation. Likewise, several other serine kinases have also been characterized for their activities in phosphorylation of IRS-1 at serine residues, such as Akt, mTOR, inhibitor κB kinase (IKK-β), c-Jun NH2-terminal

kinase (JNK), and extracellular signal-regulated kinase (ERK) (Draznin, 2006). Moreover, accumulation of intracellular metabolites of fatty acids including diacylglycerol and fatty acyl-CoAs were reported to induce site-specific serine phosphorylation of IRS-1 by activating PKCθ (Li et al., 2004). Nevertheless, it is uncertain whether the association of these inflammatory markers and acute reactants with insulin resistance is independent of measures of obesity and insulin resistance as they are already included in a risk prediction mode.

#### 1.1.2.4. Impaired GLUT expression and function

The insulin stimulated uptake and metabolism of glucose in insulin target cells are ultimately regulated by glucose transport, which is mediated by specific plasma membrane glucose transporters. GLUT-4 is a protein with 12-transmembrane domains which mediates the majority of insulin-stimulated gluose transport in peripheral tissues. Therefore, defect in the GLUT4 translocation machinery contribute to impaired insulin-stimulated glucose uptake in cardiac muscle, skeletal muscle, and adipose tissues (Garvey et al., 1998; Zierath et al., 1996).

Population studies did not find specific GLUT4 gene mutation that account for Type 2 diabetes in different human ethnic groups although the pre-translational suppression of GLUT4 gene expression was observed to diminish the content of GLUT4 protein (Gould and Bell, 1990). The morbidly obese people showed a reduced insulin-stimulated glucose transport in skeletal mucle, which at least partially due to the decreased GLUT4 expression (Dohm et al., 1991). However, GLUT4 protein expression in skeletal muscle is not altered in non-obese type 2 diabetic patients (Handberg et al.,

1990). Therefore, the insulin resistance at skeletal-muscle level is most likely resulted by defects in the insulin-signalling pathways that regulate GLUT4 translocation. Moreover, defects in the recruitment and transportation of GLUT4 to the plasma membrane may also be a major reason (Garvey et al., 1998). Indeed, more recent studies showed that decrease in serine phosphorylation of GLUT-4 contributes to insulin resistance state (Chiappe De Cingolani and Caldiz, 2004).

### 1.1.3. Insulin resistance and obesity

Although the strong correlation between obesity and Type 2 diabetes has been pointed out for decades and extensive studies have been carried out in this field, there are still many unidentified details to clarify the causative effect of obesity in inducing systemic insulin resistance. Furthermore, it is also assumed insulin resistance and hyperinsulinemia, other than being results of obesity, may also contribute to the development of obesity. This possibility needs to be clarified in future investigations.

#### 1.1.3.1. Definition for obesity

The terms 'overweight' and 'obesity' are referred to abnormally increased accumulation of fat. As the bodyweight is always corresponded to the height of adult people, the overweight and obesity ranges are usually determined by body mass index (BMI) which measures of body fat based on height and weight. BMI is calculated based on formula: BMI = (Weight in Kilograms / (Height in Meters) x (Height in Meters)). A BMI value between 25 and 29.9 indicates overweight of an adult person whereas a BMI value equal or greater than 30 indicates the development of obesity. However, although

BMI associates with the amount of body fat, it does not directly reflect the body fat accumulation and is not a proper indicator to show the increased distribution of abdominal fat. Therefore, other measurements including skinfold thickness, waist circumference and waist-to-hip circumference ratio have also been performed together with BMI caulculation to estimate body fat and body fat distribution. In addition, more efficient techniques including ultrasound, magnetic resonance imaging and computed tomography have been developed for a more accurate determination of body fat distribution.

#### 1.1.3.2. Epidemiology of obesity

As a major risk factor of many major health problems incuding carviovascular diseases, obesity has become a major concern especially in most developed countries. Most recent data shows an increased prevalence of obesity in different populations. The incidence of obesity varies by age, sex and race-ethnic group. According to the American Obesity Association (AOA), the number of obese population in the United States increased from 31.1% to 33.3% during the period of 2003 to 2005 among adult men. Among adult women, the incidence of obesity increased from 33.2% to 35.3%. In the same period, more than 16% of children and adolescents between 2 and 19 years old were found obese. The increasing rate of obesity in children and adolescents not only associates with health problems, but also become an important social problem. The increased incidence of obesity greatly increases the risk of many diseases and health complications, including cardiovascular disease, Type 2 diabetes. There are a significant number of genes identified in rare monogenic form obesity. In contrast, it is difficult to

identify the genes related to polygenic form obesity without observable simple Mendelian mode. Previous studies demonstrated that obesity increased the incidence of nonalcoholic fatty liver disease, cancers in various tissues, hypertension, and various metabolic syndromes including elevated total cholesterol, LDL cholesterol and triglycerides levels, liver steatosis and gallbladder disease. Furthermore, obesity is also an important causal factor of sleep apnea and respiratory problems, and even gynecological problems (such as abnormal menses, infertility).

#### 1.1.3.3. Etiology of obesity

Obesity usually develops chronically due to long-term energy imbalance resulted by excessive caloric consumption. It is a result of interaction between genetic background and environmental factors. Common obesity is more likely due to environment factors such as inadequate general activity level and calorie expenditure rate which results in an impaired oxidation of fat and excessive fat storage with non-reactive lipolysis in adipocytes. There are a few genes, namely melanocortin 4 receptor and brain-derived neurotrophic factor, have been shown involved in both monogenic obesity and common obesity cases (Qi and Cho, 2008; Xu et al., 2003). Leptin, encoded by *LEP* gene, plays a critical role in the regulation of energy balance through acting on both food intake and energy expenditure. The increased fat mass is determined by adipocyte hypertrophy and hyperplasia, which refered to as increased size and number of adipocytes, respectively. A significant larger population of adipocytes is only observed in early-onset obesity but not in normal adult onset obesity. The enlargement of adipocytes through increased fat deposit is thought to be responsible for the adult form obesity (Spalding et al., 2008).

There are two types of adipocytes found in mammalians known as white fat cells and brown fat cells. White fat cells are monovacuolar cells which have a flattened nucleus that situates at the periphery. They contain a large lipid droplet but only a thin layer of cytoplasm. A typical white fat cell is around 0.1mm in diameter with a variation in size from 0.05 mm to 0.2 mm. The fat stored in white fat cells is primarily triglycerides and cholesteryl esters in a semi-liquid state. In addition to store energy, mature white fat cells secrete fatty acids and cytokines like resistin, adiponectin and leptin (Fajas, 2003; Fonseca-Alaniz et al., 2007). These adipogenic factors work as paracrine factors and stimulate the proliferation of preadipocytes, thus increase the absolute number of fat cells (Hausman et al., 2001). More importantly, they show multiple functions in regulating immune and inflammation response. Unlike white fat cells, brown fat cells (plurivacuolar cells) are polygonal in shape. These cells have considerable cytoplasm with a round, eccentrically located nucleus. Instead of a large lipid droplet, the small lipid droplets scattered throughout the brown fat cell. The biological function of brown fat cells is to generate heat by uncoupling the respiratory chain of oxidative phosphorylation within mitochondria. The brown adipose tissue presents widespreadly in human infants but located only around the neck and large blood vessels of the thorax. The induction of active brown adipose tissue in adult people by therapeutic intervention may be applied for the treatment of obesity.

The cellular development of adipose tissue involves both cellular hypertrophy and hyperplasia. Hypertrophy increases the size of existing adipocytes due to surplus triglyceride accumulation resulted by a positive energy balance. Hyperplasia is also called adipogenesis. It includes both proliferation and differentiation of pre-adipocytes

which is resulted by the recruitment of new adipocytes from precursor cells into mature adipocytes. The increase in total fat cell number originating from adipocyte precursor cells is called proliferation. Traditionaly, adipose precursor cells, preadipocytes, are thought capable of replication while mature adipocytes are not. However, human preadipocyte studies indicate that partially differentiated cells remain capable of replication. Moreover, there were several reports of the replication of mature adipocytes *in vitro* (Hausman et al., 2001). Differentiation referred to the transition from undifferentiated fibroblast-like pre-adipocytes into mature round lipid-filled fat cells and is characterized by change in morphology from fibroblastic to unilocular appearance of the mature fat cell. Differentiation also is characterized by the expression of transcription factors in a regulatory cascade which result in the expression of adipose-associated genes and an increased lipogenic capacity of the cell.

The processes regulating proliferation have been extensively studied. The major factors that regulate adipocyte proliferation include hormonal factor, paracrine factor and neural factor. Thyroid hormones and glucocorticoids, for example, enhanced adipocyted development in rat models (Bray et al., 1992; Freedman et al., 1986; Hausman et al., 2001; Levacher et al., 1984). Under *in vitro* condition, glucocorticoid or its synthesized analogue dexamethasone, combined with insulin, stimulate recruitment and/or differentiation of pre-adipocyte by inducing the sequential expression of CCAAT/enhance binding protein transcription factors (C/EBPs) including the early expression of $C/EBP_{\beta}$, $C/EBP_{\delta}$ and the late expression of C/EBPα. The activation of adipogenic transcription factors and different cell cycle proteins drive the adipogenesis of pre-adipocytes (Yeh et al., 1995). Thyroxine (T4) were also found involving in the

development of adipose tissue by inducing fetal pre-adipocyte development and regulating the expression of insulin-like growth factor-I (IGF-I) and IGF binding proteins (Hausman et al., 2001). In addition to these hormones, recent investigation reported a role of sympathetic nervous system in adipocyte proliferation and lipolysis (Youngstrom and Bartness, 1998). The selective induction of pre-adipocyte proliferation is believed due to the stimulation of α2-adrenoceptors (Valet et al., 1998). Although the mechanism remains to be elucidated, the development of pre-adipocyte could also be regulated by adipocyte derived paracrine factors, such as leptin, resistin, IGF and IGF binding proteins, TGF-β, TNF-α and angiotensin II (Lau et al., 1996; Mohamed-Ali et al., 1998).

The cellular and molecular mechanisms of adipocyte differentiation have been studied using pre-adipocyte culture systems. The best characterized *in vitro* model of adipogenesis is the 3T3-L1 cell line, a substrain of the Swiss 3T3 fibroblast cell line (Green and Kehinde, 1975). The committed pre-adipocytes enter growth arrest couple times during adipogenesis so that they can maintain the capacity for growth but withdraw from the cell cycle before adipose conversion. The growth arrest is mainly brought about by the cooperative expression of two transcriptional factors, C/EBPα and PPARγ (Altiok et al., 1997). After growth arrest at confluence, pre-adipocytes receive mitogenic and adipogenic signals to continue through subsequent differentiation steps. By chronological changes in the expression of adipogenic markers at both mRNA and protein levels, the preadipocytes gradually differentiated into mature adipocytes with adipocyte phenotype. Expression of lipoprotein lipase mRNA has been cited as an early sign of adipocyte differentiation (Ailhaud, 1996; MacDougald and Lane, 1995). Similarly, SREBP-1c, a bHLH-leucine zipper protein that involved in cholesterol metabolism is also activated in

the early stage of differentiation (Kim and Spiegelman, 1996). In contrast, the early expression of C/EBP and PPAR is responsible for terminal differentiation by transactivation of adipocyte specific genes. During the terminal phase of differentiation, the cultured adipocytes markedly increase lipogenesis and acquire sensitivity to insulin. This is followed by increased activity and expression of the enzymes that associate with lipid metabolism such as ATP citrate lyase, acetyl-CoA carboxylase (ACC), glycerol-3-phosphate acyltransferase (GPAT) and fatty acid synthase (FAS) (Weiner et al., 1991). In addition to these triglyceride metabolism enzymes, mature adipocytes secrete certain adipose tissue-specific markers such as adipocyte specific fatty acid binding protein, aP2. The synchronized activation of aP2, GLUT4, and leptin follows the early PPARγ and C/EBP gene expression and leads to terminal differentiation of adipocytes. In contrast to these adipogenic factors, the adipocyte differentiation is negatively regulated by the expression and activity of several endogenous negative regulators including Pref-1 and Wnt-10b. These genes are highly expressed in undifferentiated 3T3-L1 cells and down-regulated upon addition of adipogenesis induction (Mei et al., 2002; Ross et al., 2000).

#### 1.1.3.4. Mechanism linking obesity and insulin resistance

Obesity is the most critical factor that contributes to the pathogenesis of metabolic diseases. The white adipose tissue releases variety of factors including non-esterified fatty acids (NEFA), glycerol, leptin, adiponectin, and proinflammatory cytokines. Under obese condition, the production of these products is increased. Increased NEFA release promptly induces the development of insulin resistance in humans within hours (Roden et al., 1996). On the other hand, insulin-mediated glucose uptake and glucose tolerance

improve with an acute decrease of NEFA (Santomauro et al., 1999). It was reported that the intracellular accumulation of NEFA could inhibite the activity of pyruvate dehydrogenase, phosphofructokinase and hexokinase II by competing with glucose for substrate oxidation (Randle et al., 1963). Furthermore, the elevated NEFA delivery or decreased intracellular fatty acid and its metabolites (diacyglycerol, fatty acyl-coenzyme and ceramides) cause serine/threonine phosphorylation on IRS-1/IRS-2. Subsequently, the downstream insulin signaling was diminished by a reduced PI3K activity. Another adipocyte-derived factor, retinol-binding protein-4, also induces insulin resistance through reducing PI3K signaling. It reduces PI3K activity in skeletal muscle tissue and increases gluconeogenesis in liver through a retinol-dependent pathway (Yang et al., 2005). In addition, products from macrophages and other cells that populate adipose tissue may also contribute to the development of insulin resistance. TNF-α and IL-6 act through receptor-mediated processes to stimulate both the c-Jun amino-terminal kinase (JNK) and the IKK-β/nuclear factor-κB(NF-κB) pathways, resulting in upregulation of potential mediators of inflammation that can lead to insulin resistance (Wellen and Hotamisligil, 2005). Moreover, the suppression of cytokine signaling proteins and inducible nitric oxide synthase (iNOS) mediate cytokine-induced insulin resistance by inducing the secretion of proinflammatory proteins, particularly monocyte chemoattractant protein-1 from adipocytes, endothelial cells and monocytes (Mooney et al., 2001; Picard et al., 2001). The impaired insulin signaling in the hypothalamus increases food consumption, increases lipolysis in adipocytes, decreseas the inhibition on glucose production in liver and reduces the glucose uptake in skeletal muscle tissue. As a

result, leading to an increased plasma levels of NEFA and other adipocyte-derived factors, and deteriorates insulin resistance state (Kahn et al., 2006).

## 1.2. Advanced glycation end products

Maillard reaction is a non-enzymatic modification of proteins by reducing sugars. It results in the formation of advanced glycation end products (AGEs) under *in vivo* conditions. There has been a growing body of evidence shows that formation and accumulation of AGEs and AGE precursors contribute to the development of insulin resistance in major insulin sensitive tissues such as liver, skeletal muscle and adipopose tissue.

### 1.2.1. Formation of AGEs

Maillard reaction was first described in 1912, which it is also called as glycation, browning reaction or "nonenzymatic glycosylation". It is a nonenzymatic chemical reaction involving three major steps. The first step of Maillard reaction is the condensation reaction between the carbonyl group of reducing sugars and the N-terminus or free-amino groups of proteins via a nucleophilic addition, which resulting in the rapid formation of a Schiff base (Figure 1-3). As the Schiff base products are extremely active, they form more stable Amadori products through intra-molecular re-arrangement and acid-base catalysis. During the lifetime of most cellular and plasma proteins, the levels of intermediate Amadori-products varied depend on the glucose concentrations and keep in equilibrium with glucose. Part of these Amadori-products undergo further oxidative reactions and irreversibly form AGEs. There is a growing population of chemically characterized AGE adducts found in human and experimental animals, such as pyrraline,

pentosidine, $N^{\varepsilon}$-(carboxymethyl)lysine (CML) (Ikeda et al., 1996), carboxyethyllysine (CEL) (Ahmed et al., 1997) and argpyrimidine (Oya et al., 1999) (Figure 1-4).

Formation of AGEs usually occurs slowly, which is the reason why the long-lived proteins of the extracellular matrix, collagen and elastin are especially susceptible to AGE accumulation. AGEs sometimes form covalent cross-links with other proteins, lipids, and DNA or RNA. By changing their natural structure, AGEs disrupt the normal activity of enzymes, hormones and alter immune function. For example, the AGE cross-links between endothelial proteins and oxidized LDL cholesterol give rise to the formation of atherosclerotic plaque in vasculature system. A variety of pathological conditions such as hyperglycemia induce the accumulation of AGEs to an above than normal level. These AGEs may constitute a chronic environmental risk factor for tissue injury (Goldberg et al., 2004). In addition, increased AGE formation is also observed in the state of insulin resistance, hyperlipidemia and pathological conditions with increased oxidative stress, decreased anti-oxidant activity and reduced renal clearance of AGE-precursors. However, whether these factors are the causative factors to induce AGE formation is still unclear.

The formation of AGEs is usually endogenous but can also be derived from exogenous sources, especially from food intake (Koschinsky et al., 1997). As AGEs are produced by Maillard products, foods cooked at high temperature generates more AGEs than natural sources. It is very likely that these AGEs products could be absorbed and incorporated in body components efficiently. Indeed, different investigations showed that dietary AGEs contribute significantly to the total circulating and tissue AGEs. Same as their endogenous counterpart, these exogenous AGEs induce variety of pathological

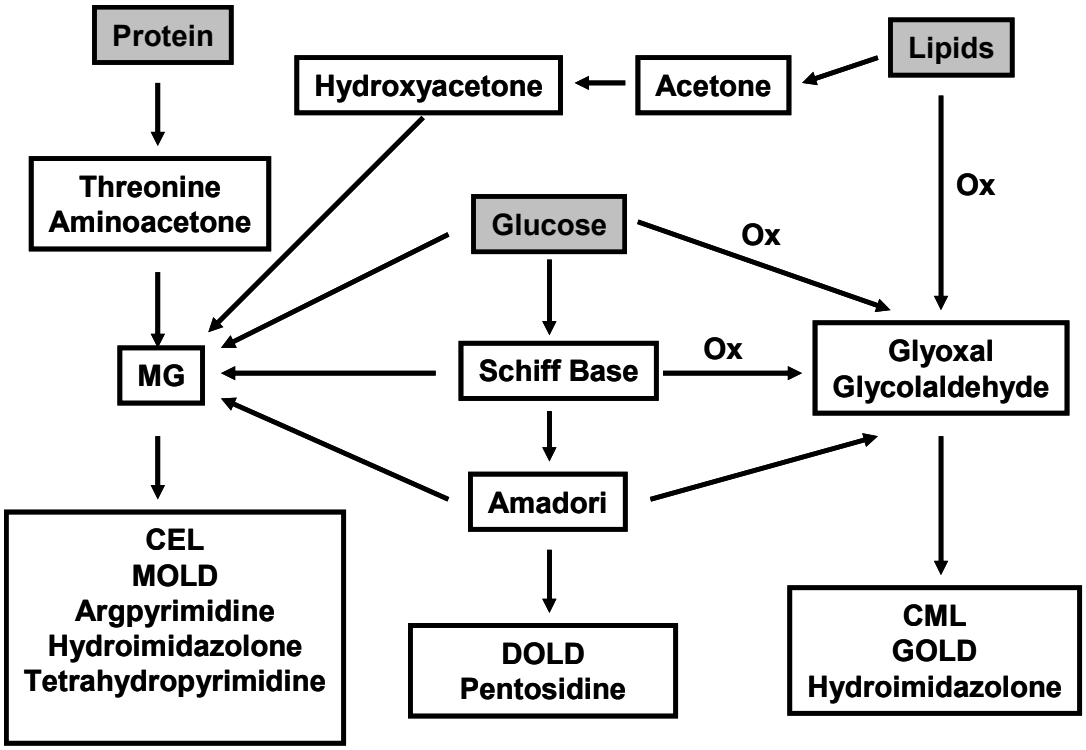


**Figure 1-3.** Simplified scheme of the Maillard reaction and the formation of some advanced glycation endproducts from glucose, protein and lipid.

CEL: Nε-(Carboxyethyl)lysine
CML: Nε-(Carboxymethyl)lysine
DOLD: 3-deoxyglucosone lysine dimer
GOLD: glyoxal lysine dimmer
MG: methylglyoxal
MOLD: methylglyoxal lysine dimer
Ox: oxidation

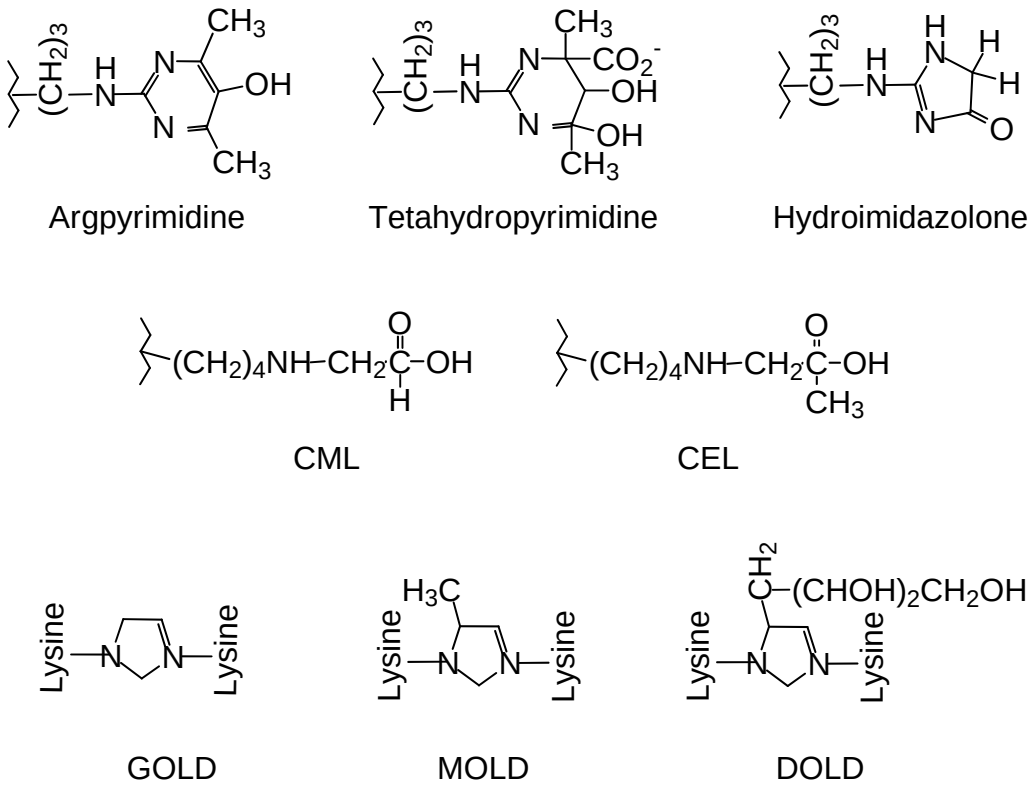


**Figure 1-4**. Chemical structure of major AGEs.

CEL: Nε-(Carboxyethyl)lysine
CML: Nε-(Carboxymethyl)lysine
DOLD: 3-deoxyglucosone lysine dimer
MOLD: methylglyoxal lysine dimmer
GOLD: glyoxal lysine dimmer

effects including potential risk of inflammation and vascular complications in insulin resistance. The significant effect of dietary AGEs in the development of insulin resistance has been evidenced by different animal experiments (Sandu et al., 2005).

The expression of proinflammation markers is increased with the dietary AGE consumption. In addition, the close correlation between endothelial dysfunction and exogenous AGEs was also shown in diabetic patients and animals (Stirban et al., 2006). These results suggest a causative role of dietary AGEs in inducing inflammation, insulin resistance and vascular dysfunction. However, because these dietary based studies usually use different type and amount of food to feed animals, the conclusions from these studies could be contradictive. Further investigations are required to differentiate between endogenous and exogenously derived AGEs and then relate them to specific pathological damage.

### 1.2.2. Receptor for AGEs

Cell surface receptors that binding AGEs include the scavenger receptor and the receptor for advanced glycation end products (RAGE). Scavenger receptor recognizes proteins that highly modified by glycation adducts, by which results in the clearance of these glycated proteins. RAGE are cell surface molecules that belongs to the IgG immunoglobulin superfamily (Neeper et al., 1992; Schmidt et al., 1994; Schmidt et al., 1993). It is composed of three immunoglobulin-like regions including one “V” type domain, two “C” type domains, a short transmembrane domain, and a cytoplasmic tail (Neeper et al., 1992; Schmidt et al., 1994; Schmidt et al., 1993). Unlike scavenger receptor, binding of AGEs to RAGE does not accelerate the clearance and degradation of

AGEs. Instead, engagement of RAGE results in activation of different intracellular signaling pathways. Because RAGE has multiple ligands, it binds not only AGEs but also different proteins such as proinflammatory cytokines, $Ca^{2+}$-binding S100 proteins and nuclear high mobility group protein box-1 (Dumitriu et al., 2005; Geroldi et al., 2006). This ability to bind different ligands implies novel roles for RAGE in a broad range of chronic diseases. By interacting with RAGE, AGEs trigger the activation of secondary messenger pathways such as protein kinase C and NF-κB. When activated, NF-κB is translocated to the nucleus where it increases transcription of a number of proteins, including intercellular adhesion molecule-1, E-selectin, endothelin-1, vascular endothelial growth factor (VEGF), and proinflammatory cytokines (Goldin et al., 2006; Schiekofer et al., 2003). Moreover, the expression of RAGE on T lymphocytes, monocytes and macrophages suggests its essential effect on immune responses under *in vivo* condition (Hofmann et al., 1999).

### 1.2.3. Pathological effects of AGEs

The accumulation of AGEs may alter the structural properties of tissue proteins and reduce their susceptibility to catabolism (Ahmed, 2005; Ceriello and Motz, 2004). In addition, RAGE–ligand interaction may directly induce the generation of reactive oxygen species *via* NADPH oxidases and/or other identified mechanisms (Lander et al., 1997; Wautier et al., 2001).

Since the 1980's, the pathophysiological significance of AGEs has attracted attention in medical science. AGEs accumulation has been linked to diabetes, especially various diabetes complications. Although diabetic complications is caused by multipal

factors, the accelerated formation of advanced glycation endproducts in diabetes as a result of chronic hyperglycemia has been considered to be a major cause. With the proceeding of diabetes and hyperglycemia, an accelerated intermolecular collagen cross-linking was formed with increased AGEs accumulation. As a result, the arterial and myocardial compliance is reduced and vascular shows stiffness. AGEs accumulate in different organs that damaged in diabetes, including kidney, retina, and vascular system (Ahmed, 2005; Baynes, 2001; Monnier et al., 1981; Singh et al., 2001; Smit and Lutgers, 2004). For example, the presence of argpyrimidine has been identified in arterial walls of the kidneys and lenses from diabetic patients (Bourajjaj et al., 2003). It has also been localized to atherosclerotic lesions and contribute to atherosclerosis by enhancing endothelial dysfunction, elevating vascular low-density lipoprotein (LDL) levels, promoting plaque destabilization, inducing neointimal proliferation, and inhibiting vascular repair in response to injury (Baynes and Thorpe, 2000; Stitt et al., 1997; Vlassara, 1996). Moreover, a large body of evidence has indicated the importance of AGEs in diseases such as inflammation (Basta et al., 2002), neurodegenerative disorders (Munch et al., 2002; Sasaki et al., 1998; Yan et al., 2001), hypertension (Wang et al., 2007b; Wang et al., 2004; Wang et al., 2008) and even cancer (Abe and Yamagishi, 2008). In hypertensive rat aortic tissues, immunohistochemical study showed an age-dependent increase in CEL and CML staining localized at the endothelial layer (Wang et al., 2005). The intensity of CEL and CML staining in aortic tissues was significantly higher in SHR than in age-matched WKY rats. Positive CEL and CML staining was even detected in aortic tissues from very young age (5-week old) SHR. As different type off AGEs have been found on lymphocytes, it is possible that AGEs are involved in

modulating interactions between cells and alters immune response including antigen presentation and T cell responses. (Poggioli et al., 2002). Futher studies suggested that AGEs accumulation reduced the ability of dendritic cells to stimulate primary T cell responses in spite of the accelerated cell development (Price et al., 2004). As a result, the AGE-enriched environment may enventually re-direct immune responses under *in vivo* conditions.

### 1.2.4. Clearance of AGEs

The modification of proteins by Maillard reaction involves complicated and sequential reactions. At the early-stage of Maillard reaction, some liable and reversible intermediates including fructosyl-lysine and fructosamines are formed. With further molecular rearrangement and oxidation reaction, these adducts turn into stable end-stage AGEs. The degradation of AGEs by proteolysis release glycated adducts with different molecular weights. The small free glycated adducts whose molecular weight is less than 500 Da are mainly excreted in urine in human objects (Gugliucci et al., 2007; Thornalley, 2005). However, the extracellularly-derived AGE proteins are usually very large in molecular weight. They have to be degraded into glycated-peptides or glycated free adducts before passing through the basal membrane of the renal corpuscle. Peripheral macrophage and liver sinusoidal endothelial cells and Kuppfer's cells have also been implicated involved in AGEs clearance. However, the physiological role of hepatic cells in AGEs degradation and clearance remains unclear.

### 1.2.5. Precursors of AGEs

In addition to glucose, a number of glycolytic intermediates such as glyoxal, methylglyoxal (MG) and deoxyglucosone, are known to form AGEs and called AGE precursors. Among these glycolytic intermediates, MG has recently received considerable attention as it is believed to be the most potent glycating agent (Shinohara et al., 1998; Westwood and Thornalley, 1995).

#### 1.2.5.1. Physical characterization of MG

MG ($CH_3$-CO-CH=O or $C_3H_4O_2$) is also known as pyruvaldehyde, pyruvic aldehyde, 2-oxopropanal, 2-ketoproprion-aldehyde or acetyl-formaldehyde. It is called dicarbonyl compound because of having two carbonyl groups.

Endogenous MG exists in two forms, free and bound. More than 99% of MG is estimated to be involved in reversible or irreversible interaction with proteins (Chaplen et al., 1998). This part of MG cannot freely move into or out of cells. In alkaline envinronment, MG undergoes an intramolecular Cannizzaro rearrangement with the formation of lactate. In aqueous solution it is polymerized and hydrated. At pH 7.0, MG exists in three forms including monohydrate, dihydrate and unhydrated forms (Creighton et al., 1988). The percentile distribution of these species is 56%, 44% and trace amount, respectively.

#### 1.2.5.2. Chemical reactions of MG

With both aldehydic and ketonic groups, MG becomes an extremely active molecule and reacts with compounds with either thiols and amine groups. Compared to the ketonic group, the aldehydic group is more susceptible to be attacked by other

functional groups (Leoncini, 1979). These reactions provide the chemical basis of the MG-induced modification on amino acids, proteins and nucleic acids, and thus explain the mode of action of this α-oxoaldehyde in biological systems (Kalapos, 1999).

When MG reacts with pyrimidines or purines, it produces interstrand crosslinks, especially in AT-rich regions in duplex DNA (Rahman et al., 1990). The MG-DNA adducts were detected in DNA extracts of peripheral human lymphocytes incubated with MG (Vaca et al., 1994). The reaction between MG and nucleic acids lead to both mutagenic and clastogenic effect. A variety of mutations including sister chromatid exchanges, single strand breaks and DNA-protein crosslinks were observed in plasmid or cells after preincubation with 0.1-200 μM MG and transfection into a mouse lymphoid cell line (Papoulis et al., 1995; Tucker et al., 1989). These MG-induced modifications occur even under physiological conditions (Figure 1-5). It reacts with arginine residues in proteins to form the non-fluorescent products 5-hydro-5-methylimidazolone and tetrahydropyrimidine, as well as the major fluorescent product argpyrimidine (Bourajjaj et al., 2003; Oya et al., 1999). Although MG reacts primarily with arginine under physiological concentration (<5 μM), MG–lysine adducts are also very common. CML,CEL and MOLD have been shown accumulate with the aging of animals and human (Ahmed et al., 1997; Baynes, 2001). As a typical Millard reaction, the reaction between MG and proteins includes both reversible phase and non-reversible phases. In the first phase, MG irreversibly binds to side-chain guanidine of arginine and ε-amine residue of lysine. Irreversible reactions result in the formation of different imidazole derivatives, arginyl-pirimidine, CML, and imidazolium crosslinks. In addition to arginine

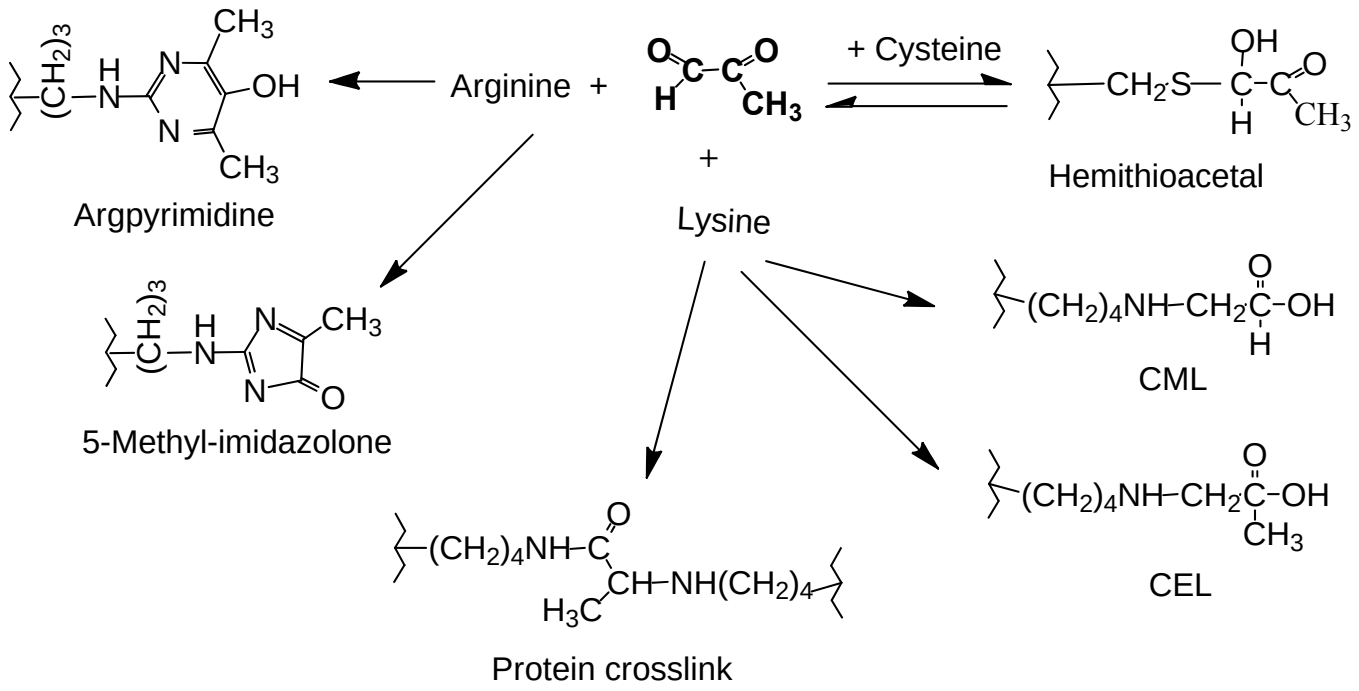


**Figure 1-5.** Formation of main MG adducts with cystine, arginine and lysine residue

CEL: Nε-(Carboxyethyl)lysine
CML: Nε-(Carboxymethyl)lysine

and lysine, MG reacts with cysteine residues and forms hemithioacetal. The reaction between MG and cysteine is irreversible (Kalapos, 2008).

### 1.2.5.3. Metabolism of MG

In mammals, MG is synthesized by bacteria of the gut or by the host itself. It can also be taken up from food. Both nonenzymatic and enzymatic reactions are responsible for endogenous MG formation. For the enzymatic reaction, MG is synthesized by three pathways: the glycolysis bypass, acetone metabolism and protein catabolism (Figure 1-6), which, involve methylgloxal synthase, cytochrome P450, and amino oxidases, respectively (Chang and Wu, 2006; Kalapos, 1994). Methylgloxal synthase was first found in prokaryotic cells and then in mammalian cells (Ray and Ray, 1981). Its activity is inhibited by inorganic phosphate and it was suggested that this enzyme regulates glycolysis depending on the availability of intracellular $P_i$ (Cooper, 1984). MG is also formed from acetone by cytochrome P450 IIE1 isoenzymes. With consumption of $NADPH + H^+$, this enzyme catalyses the sequential formation of hydroxyacetone and MG (Koop and Casazza, 1985). Another source of MG production is from protein metabolism. Aminoacetone, a protein metabolite, can be catalyzed by amine oxidases to form MG (Lyles and Chalmers, 1992). Among the amine oxidase family, semicarbazide-sensitive amine oxidase (SSAO) is the most studied enzyme. SSAO is present either as membrane-associated or soluble form in vascular tissues and adipocytes (Lyles, 1996). The activity of serum SSAO is found increased in patients with diabetic complications, vascular disorders, and heart diseases (Yu et al., 2004; Yu et al., 2003).

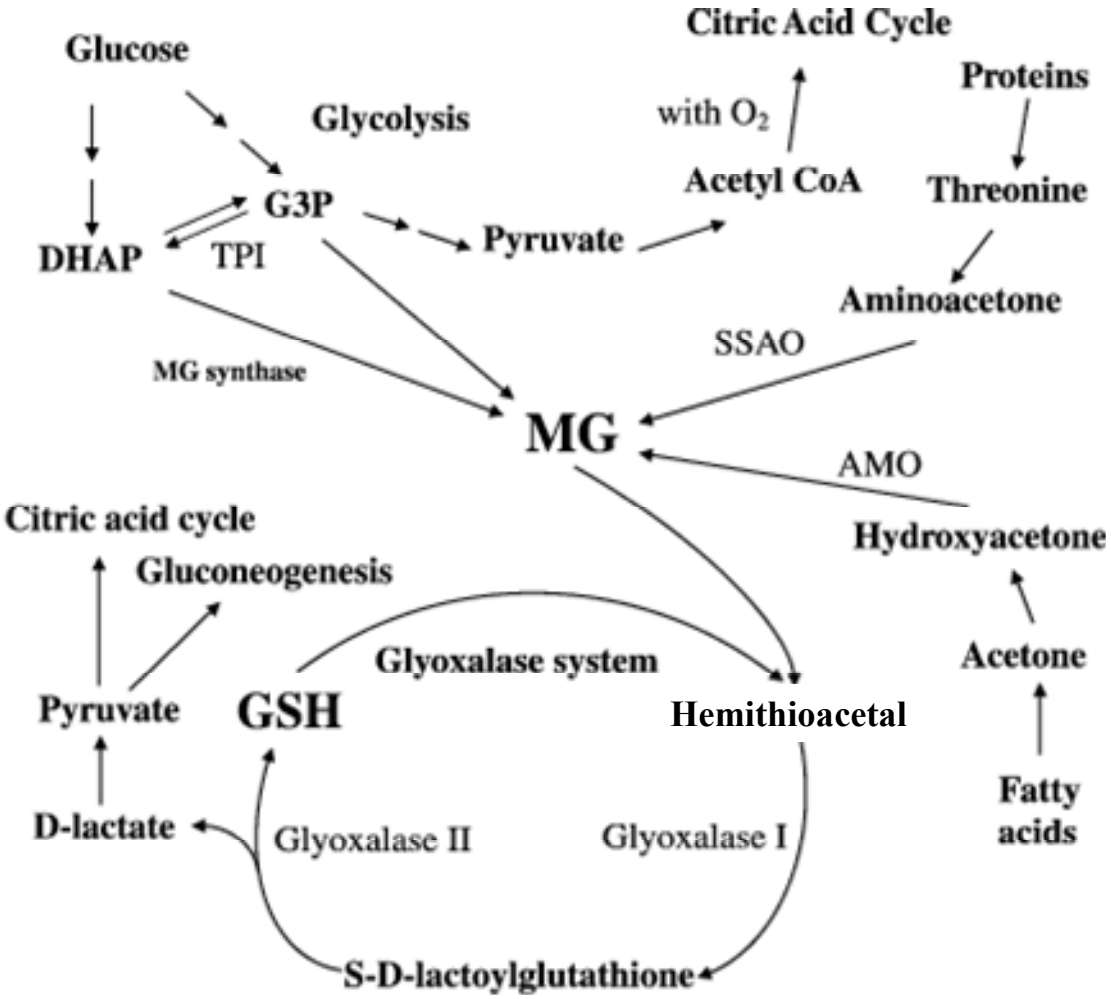


**Figure 1-6. Formation and degradation of methylglyoxal**. G3P, glyceraldehyde-3-phosphate; DHAP, dihydroxyacetone phosphate; TPI, triosephosphate isomerase; MG, methylglyoxal; SSAO, semicarbadize-sensitive amine oxidase; AMO, acetol monooxygenase; and GSH, reduced glutathione (Chang and Wu, 2006).

Under physiological conditions, the non-enzymatic fragmentation and elimination of triose-phosphate intermediates (glyceraldehyde 3-phosphate, dihydroxy-acetonephosphate) during glycolysis (Phillips and Thornalley, 1993; Richard, 1991) is disputable. However, under pathological conditions, it is well-accepted that the deprotonation of substrate to an enediolate phosphate followed by the cleavage of phosphate group from the carbon skeleton results in the formation of MG (Richard, 1993). As triose-phosphates convert to MG non-enzymatically, the formation of MG occurs in all cells and organisms. Based on previous studies (Phillips and Thornalley, 1993), the rate of MG formation under normoglycaemic conditions is 120 μM per day (Phillips and Thornalley, 1993). As the relative contribution of enzymatic and nonenzymatic pathways to total MG formation is not clear, whether nonenzymatic or enzymatic pathway is more important in MG formation awaits to be determined. Efficient gene knock-out or knock down animal/cell models might be helpful in clarifying the involvement of different pathway in MG production.

The detoxification of MG is mainly through the glyoxalase pathway and the α-ketoaldehyde dehydrogenase(s) pathway (Figure 1-6). The glyoxalase system is comprised of glyoxalase I and II using reduced glutathione (GSH) as the cofactor. MG reacts with GSH and spontaneously forms hemimercaptal which is converted into *S*-D-lactoyl-glutathione by glyoxalase I. *S*-D-lactoyl-glutathione is then metabolized into D-lactate by glyoxalase II (Racker, 1951). In mammalian system, D-lactate is further degraded to pyruvate by mitochondrial 2-hydroxyacid dehydrogenase (Thornalley, 1993). In the α-ketoaldehyde dehydrogenase pathway, MG is directly converted to pyruvate by NADPH-dependent α-ketoaldehyde dehydrogenase. Minor routes for MG degradation

have also been reported. For example, formaldehyde dehydrogenase, methylglyoxal reductase and pyruvate dehydrogenase complex can catalyze the conversion of this α-oxoaldehyde to spyruvylglutathione, L-lactaldehyde and acetyl CoA, respectively (Kalapos, 1994).

#### 1.2.5.4. Pathological effect of MG

The pathological effect of MG can occur through four major mechanisms. The initial cytotoxicity effect is induced by high concentration of MG that damages cell functions. Second, the oxidative stress due to free radical production from MG metabolism results in a further decrease of cell viability. Third, MG reacts with proteins (including enzymes) to form AGEs and alters the physiological function of these proteins (enzymes). Furthermore, the reaction between MG and DNA or RNA provides carcinogenicity potencial of MG.

Plasma MG concentration in healthy rats is approximately 5 μM (Nagaraj et al., 2002). A previous study from our lab detected plasma MG levels at 33.6 μM in 20-week-old spontaneously hypertensive rats (SHR) and 14.2 μM in age-matched Wistar–Kyoto (WKY) rats (Wang et al., 2004). An even higher MG concentration of 310 μmol/L was reported in cultured Chinese hamster ovary cells (Chaplen et al., 1998). This discrepency of MG concentration reported from different labs might due to the differences with various measurement assays and experimental settings.

#### 1.2.5.4.1. MG-induced AGE formation

MG is believed to be the most important source of AGEs (Bourajjaj et al., 2003; Shinohara et al., 1998). Studies indicate that the formation of MG-derived AGEs is increased with elevated MG levels under hyperglycemia and hypertensive conditions. MG treatment significantly increased the formation of AGEs in cultured mesenteric artery smooth muscle cells from SD rats. This MG-induced AGEs formation was significantly inhibited by pretreatment with MG scavenger N-Acetyl Cysteine (NAC) (Wu, 2005). These observations indicate a critical role of MG in the formation of AGEs. Recent studies found that MG not only reacts with long half life proteins, but also reacts with various circulating proteins, such as HSP27 (Sakamoto et al., 2002), p38MAPK (Liu et al., 2003), EGF receptor (Portero-Otin et al., 2002) and transcriptional corepressor (Yao et al., 2006). Modification of these cellular proteins leads to alteration of their physiological function and triggers diverse cellular responses such as cell activation, inflammatory response, growth arrest, and apoptosis. Modification of antithrombin III and Cl inhibitor puts forward changes in regulation of coagulation and inflammation (Aleksandrovskii, 1992). The MG-induced glycation on mSin3A, a transcription suppressor, causes increased expression of angiopoietin-2 and plays a role in the pathology of diabetic vascular diseases (Yao et al., 2007). More importantly, since arginine, lysine, and cysteine residues are usually involved in active sites of enzymes, irreversible reaction of MG with these residues would potentially alter the normal activities of these enzymes. It is found that the increased MG-induced AGEs formation dramatically inhibited the activities of antioxidant enzymes including glutathione reductase and glutathione peroxidase (Morgan et al., 2002; Wang et al., 2005). The

excessive glycation of extracellular superoxide dismutase induced by MG impaired its activity in diabetic patients (Ciechanowski et al., 2005; Kang, 2003). Moreover, the MG-induced modification of different mitochondrial membrane proteins and antioxidant enzymes results in increased oxidative stress (Rosca et al., 2005; Wang et al., 2009) and contributes to multiple forms of insulin resistance.

#### 1.2.5.4.2. MG induced oxidative stress

Oxidative stress is a state with increased production and/or decreased degeneration of reactive oxygen species (ROS). In addition to the cytotoxic effect of ROS, its role in intracellular signaling has also been recognized (Feng et al., 1995; Forman and Torres, 2002). Autooxidation and photolysis of MG result in the production of free radicals such as hydroxyl radicals and hydrogen peroxide. In cultured rat hepatocytes, a dose-dependent effect of MG on hydrogen peroxide formation was detected. The MG-induced formation of free radicals was also observed in human platelets (Leoncini and Poggi, 1996). Under in vitro conditions, , MG administration to the incubation medium resulted in a concentration dependent increase of oxidation-sensitive fluorescence of 5-(and 6)-carboxy-2',7'-dichlorodihydrofluoresceindiacetate (DCFH-DA) in different cell-types (Chang et al., 2005; Kikuchi et al., 1999; Leoncini and Poggi, 1996). As intracellular GSH plays an important role in the protection of cells against oxidative damage, a continuous and significant decrease of GSH level was observed in the presence of increasing concentrations of MG (Kalapos et al., 1992). Conversely, the oxidative stress-dependent process contributes to the generation of MG-derived AGEs. MG-induced glycation on mitochondrial membrane proteins and antioxidant enzymes result in

further increased oxidative stress. Indeed, the hyperglycaemia-induced ROS production by the mitochondrial electron-transport chain has been demonstrated to be responsible to hyperglycaemia-induced vascular damage (Nishikawa et al., 2000) in cultured endothelial cells. Moreover, free radical production and the subsequent GSH depletion lead to decrease of cell viability. The changes of plasma MG levels which parallel ROS production has also been observed in hypertension and Alzheimer disease (Wu and Juurlink, 2002; Yu, 2001).

#### 1.2.5.4.3. Effect of MG on cell proliferation

Cell proliferation involves both cell growth and cell division which leads to the increase in total cell number. Binding of growth factors to their receptor stimulates a cascade of intracellular signaling pathways include protein phosphorylation and transcription initiation (binding of transcription factors to DNA), which ultimately activates nuclear regulatory proteins that trigger cell division. Modulations of any of these cell cycle related proteins, can either stimulate or inhibit cell proliferation process.

The cell cycle consists of four distinct phases: $G_1$ phase, synthesis phase (S phase), $G_2$ phase and mitosis phase (M phase). Activation and progression of any of these cell cycle phases is subsequent to the proper completion of the previous one. Under some special physiological condition, some cells stopped dividing temporarily and reversibly enter $G_0$ phase which is a state of quiescence. Different cell cycle checkpoints are responsible for the regulation and monitoring of the cell cycle progress (Elledge, 1996). Normally, a cell does not proceed to the next cell cycle phase only when all the checkpoint requirements have been met. Temporary withdraw from cell cycle progress

allows the repair of DNA damage and thus prevent the damaged or incomplete DNA to pass on to daughter cells. The G1/S checkpoint and the G2/M checkpoint are the two main checkpoints. G1/S transition controls the rate-limiting step of cell cycle and therefore is also known as restriction point. The Cyclin-dependent kinases (Cdks) family plays a central role in initiating the cell cycle proceedings. Cdks are small serine/threonine protein kinases that catalyze the covalent attachment of phosphate groups derived from ATP to protein substrates of the cell cycle machinery. They are activated by binding to regulatory proteins called cyclins. Different types of cyclins are produced at different cell cycle phases, resulting in the periodic formation of distinct cyclin-Cdk complexes that trigger different cell cycle events. A wide range of mechanisms contribute to the regulation of cyclin levels and Cdk activity, resulting in a complicated Cdk regulatory network that forms the core of the cell cycle control system. Such regulation involves the controlled expression and destruction of cyclins and other proteins that associate with Cdks/Cdk/cyclin complexes, thus activate or inhibit the phosphorylation of Cdks. Cdk-1 and Cdk-4 act in $G_2$/M and $G_1$ phase, respectively. In contrast, Cdk2 acts subsequent to Cdk4/6 to promote $G_1$/S and S phase progression.

Cdks regulate cell cycle progression by associating with variety of small inhibitory proteins, especially p21, p27 and p57. These inhibitory proteins in mammals are also known as the "Cdk inhibitory proteins (Cip)" or "kinase inhibitor protein (Kip)" family (Sherr and Roberts, 1999), which halt the cell cycle in G1 phase by binding to and inactivating cyclin-Cdk complexes. The cyclin-Cdk complex of early G1 is Cdk2, Cdk4, or Cdk6 bound cyclin D isoform. In response to DNA damage, intracellular p53 accumulation increases and induces the p21-mediated inhibition of cyclin D/Cdk.

Another protein that plays essential role in cell cycle regulation is Mdm2. By inactivating p53, Mdm2 leads to the feedback inhibition of p21 and arrest the cells in G1 phase (Giono and Manfredi, 2007a; Giono and Manfredi, 2007b). In addition, the cyclin D/cdk complex can also be inhibited by the activation of TGF-β receptors and cyclic AMP through p15 or p27, respectively (Iavarone and Massague, 1997; Koff et al., 1991). When the cyclin D/Cdk complex is inhibited, the phosphorylation of retinoblastoma protein (Rb) reduced and therefore Rb can tightly bind to the transcription factor E2F, inhibiting its activity. Conversely, activation of the cyclin D/Cdk complex phosphorylates Rb and triggers the cells to transit the G1/S phase and initiates DNA replication by dissociating from E2F. The Cyclin/Cdk complex that controls G1/S checkpoint is Cyclin E/Cdk2 which accumulates during late G1 phase and triggers the passage into S phase.

Extensive evidences have linked MG accumulation with cell proliferation. In MG-treated mammalian cells, DNA synthesis, RNA synthesis and protein production were detected depressed. As a result, intraperitoneally or intravenously administered MG inhibits the growth of tumor cells *in vivo*. This inhibitive effect could be attributed to the competition in hydrogen bonding between nucleic acid bases to form pairs or bind to MG. Moreover, MG was found to inhibit histone acetylation in cell-free extract of rat uterus (Procaccini et al., 1971). This suggests an additional mechanism to the action of MG on DNA replication.

Increased generation of many apoptotic markers such as caspase-3 activation, DNA ladder formation and cytochrome C release were observed in cells treated with extra exogenous MG (Chan et al., 2007; Du et al., 2001b). Multiple mechanisms by which MG induce apoptosis were therefore proposed. First, p38 MAPK activation was

suggested to be an important signaling intermediate of MG-induced apoptosis in kidney epithelial cells and Schwann cells (Fukunaga et al., 2004; Liu et al., 2003). Second, ROS generated by MG-induced modification of mitochondrial glutathione reductase also triggers apoptosis (Amicarelli et al., 2003; Du et al., 2001b). Third, the JNK pathway was suggested to mediate MG-induced apoptosis (Chan et al., 2007). In addition to apoptosis, the effect of MG on cell proliferation and growth may also result from its modulation of growth factor signaling (Cantero et al., 2007). Inceased accumulation of of MG altered the PDGF-induced PDGFRβ-phosphorylation, ERK1/2-activation, and nuclear translocation, and the subsequent proliferation of mesenchymal cells (smooth muscle cells and skin fibroblasts). The formation of AGE adducts on PDGFRβ was reversed by arginine and aminoguanidine, the carbonyl scavengers. A recent study also showed that MG affects cell viability via desensitization the signaling of gp130/STAT3, a key regulator of cytokine-induced gene expressions, and thereby promotes cytotoxicity in neuroglial cells (Lee et al., 2009).

#### 1.2.5.4.4. Effect of MG/AGE on insulin signaling

The formation of AGEs/MG is increased in various pathological conditions including diabetic nephropathy (Beisswenger et al., 2005; Mostafa et al., 2007), diabetic retinopathy (Fosmark et al., 2006; Miller et al., 2006), hypertension (Wang et al., 2004), Alzheimer's disease (Kuhla et al., 2005), and atherosclerosis (Price and Knight, 2007). Most of these diseases also show dysfunction in insulin signaling. Being the most potential intermediate of AGE formation, the effect of MG is considered by modifying the key insulin signaling proteins. MG-induced modifications of these proteins alter the

function of pancreatic β cells, endothelial cells, mesangial cells and smooth muscle cells and therefore impair insulin signalling transduction pathway.

The majority of the MG-modified proteins in plasma exist as Amadori-glycated proteins rather than in the more labile Schiff base form or AGEs. These Amadori-adducts are not inert and their direct role in the pathogenesis of diabetic vascular complications has been implicated. In diabetic patients with hyperglycemia-induced microvascular complications, researchers not only found a correlation between the Amadori-glycated albumin and endothelial dysfunction, but also estabolished an independent association between the accumulation of early glycated proteins and diabetic nephropathy or retinopathy. It was reported that glycated albumin activated different signalling pathways and affected specific cellular receptors in variety of cell types. In human monocytic cells, glycated albumin induced the release of TNF-α, a factor involved in insulin resistance (Naitoh et al., 2001). More importantly, another study demonstrated that human glycated albumin selectively inhibited the PI3K/Akt pathway of the insulin signalling cascade and directly cause insulin resistance in skeletal muscle cells (Miele et al., 2003). The effect on PI3K/Akt inhibition was dependent on a PKC-mediated serine/threonine phosphorylation of IRS-1/2 proteins, but independent of ROS production. Thus, by deregulating intracellular insulin signalling, human glycated albumin may exacerbate the insulin-resistant state.

Conventionally, AGE formation is considered between a carbonyl compound and a long half-life protein, such as albumin. In contrast to long half-life proteins, insulin has an extremely short half-life, which is about 5–10 min in circulating system. Therefore, it is not expected that insulin itself can be modified in the circulating system under *in vivo*

conditions. Recently, the rapid AGE formation of short-lived proteins under *in vivo* conditions has attracted attention (Giardino et al., 1994; Giardino et al., 1996). Studies from different labs reported that MG may react with and impair the function of cellular proteins including HSP27 (Sakamoto et al., 2002), p38MAPK (Liu et al., 2003) and EGF receptor (Portero-Otin et al., 2003), insulin receptor (Riboulet-Chavey et al., 2006), and transcriptional corepressor mSin3A (Yao et al., 2006). Impaired cellular signaling may lead to inflammatory responses, growth arrest, and apoptosis (Cantero et al., 2007; Park et al., 1998; Riboulet-Chavey et al., 2006). Moreover, some previous studies indicated that a substantial proportion of insulin and proinsulin is glycated in the pancreatic ß-cells during the stages of insulin synthesis and storage. Using GlycoGel B boronate affinity chromatography, N-terminal glycated insulin has been detected in the pancreas of various animal models of Type 2 diabetes and in isolated islets (Abdel-Wahab et al., 1997c; Abdel-Wahab et al., 1996). Concentrations of glycated insulin was increased in the circulation of diabetic obese *ob/ob* mice (Abdel-Wahab et al., 1997c) and in cultured ß-cells (Abdel-Wahab et al., 1997a; Abdel-Wahab et al., 1997b). The modification of insulin has been demonstrated *in vitro* under hyperglycemic conditions in the presence of sodium cyanoborohydride whose effect is similar to glucose. An insertion of a single glucose molecule at the amino-terminus of the insulin B-chain was detected. The effects of monoglycated insulin on plasma glucose homeostasis and *in vitro* cellular glucose transport and metabolism was investigated in isolated abdominal muscle of mice. The same research group reported that the monoglycated insulin was approximately 20% less effective than native insulin in stimulating glucose uptake and both indices of metabolism (Boyd et al., 2000). Later, they detected glycated insulin in human diabetic plasma. Using

the euglycemic-hyperinsulinemic clamp technique, they found that the biological activity of human glycated insulin was also decreased (Hunter et al., 2003). An increase in glycated insulin was also identified later by radioimmunoassay in human Type 2 diabetes (Lindsay et al., 2003) .

The effect of MG in inducing insulin resistance has been conventionally attributed to the oxidative stress subsequent to MG accumulation. However, the MG-induced modification on insulin signaling proteins could be very specific. For example, a recent study demonstrated that a short exposure of L6 muscle cells to MG inhibited insulin-stimulated phosphorylation of Akt and Erk1/2 but did not affect tyrosine phosphorylation of IR (Riboulet-Chavey et al., 2006). Importantly, the deleterious effect of MG is independent of ROS. Instead, it appears to be the direct outcome of an imparied tyrosine phosphorylation on IRS-1 which is subsequent to the its binding to MG. These results strongly imply that the impaired biological function of MG-modified insulin may directly contribute to glucose intolerance seen in diabetes. The neutralization or inhibition of glycated-albumin and insulin may be a potential novel target for therapy against the development of diabetes and its complications. As the glyction reaction between reducing sugar and the N-terminal of proteins is well recognized, the glycation of insulin or proinsulin at N-terminal is not surprising. However, as maillard reaction can also occur on the amino acid residues with free amino group(s), the existence of glycated insulin on the Lys residue and/or Arg residue has not yet been detected.

Maillard products produced by food processing may incorporated into different tissues and organs of the body after intestinal absorption. Therefore, AGEs in food are potential risk factors for inflammation and vascular complications and insulin resistance.

Although only a minor part of dietary AGEs can be absorbed and deposited in tussues, it is one of the major sources of circulating AGEs and mediates significant pathological effects. In a group of diabetic subjects, dietary AGE was associated with increased levels of serum AGEs in parallel with impaired flow mediated dilation and increased serum markers of inflammation as well as markers of endothelial dysfunction (Stirban et al., 2006). The dietary AGEs/AGE precursors also modulate insulin signaling. Experiments performed in animal models have indicated a significant role for dietary AGEs in inducing insulin resistance (Hofmann et al., 2002; Sandu et al., 2005).

Although the role of MG/AGEs accumulation has been studied and some of the mechanisms are revealed, the biological consequences of glycation need to be further investigated, especially the effect of MG/AGE accumulation in the pathogenesis of insulin resistance and the pathway leading to insulin resistance.

### 1.2.6. Agents that inhibit/scavenge AGE formation

In view of wide occurrence of AGE formation and their deleterious consequences, numerous agents have been developed as potent scavengers of these reactive α-dicarbonyl products (Table 1-1). A variety of scavengers are identified as AGE inhibitors, such as aminoguanidine (Pimagedine®, AG), metformin (dimethylbiguanide), and some synthetic thiazolidine derivatives (Rahbar et al., 2000a; Ruggiero-Lopez et al., 1999; Thornalley et al., 2000). Another strategy to reduce AGE deposition might be achieved by using cross-link breakers including phenacyl thiazolium bromide (PTB) and its stable derivative alagebrium (Vasan et al., 1996; Wolffenbuttel et al., 1998). In addition, different antioxidants, by providing extra GSH, may induce the detoxification of MG and

AGEs and prevent the AGE-induced damage. Among all these AGEs inhibitors, only very few of them (i.e. metformin, pioglitazone and pentoxyfylline) are being applied in clinical practice or underclinical trials (i.e. alagebrium). The rest of them are generally used *in vitro* or *in vivo* research to study the role of AGEs or MG in the pathogenesis of different disease conditions.

#### 1.2.6.1. Inhibitors of AGE formation

To date the most promising AGE inhibitor under investigation is AG. It is a hydrazing reagent with guanidine structure. Guanidine compounds can react with and trap α-dicarbonyl compounds and prevent their further reactions with the free amine groups of protein. The effect of AG in preventing hyperglycemia-induced protein cross-linking in arterial wall was first reported in diabetic animals in 1986 (Brownlee et al., 1986). Since then, a growing body of evidence has shown the causative role of AGEs in variety of diseases and pathological states. Treatment with AG inhibited the accumulation of AGEs in capillary arterioles and thereby prevented abnormal endothelial cell proliferation and diabetic complications (Hammes et al., 1991; Soulis-Liparota et al., 1991). An *in vitro* study showed that AG can act as an antioxidant and quench hydroxyl radicals and cleave cross-links (Giardino et al., 1998). However, the biochemical side effects of AG might raise chronic toxicity problems in long-term treatment (Ou, 1993). Other amadarines, such as arnosine and pyridoxamine, also have antiglycation properties. Pyridoxamine has been shown to be more effective than AG. Unlike AG, it does not interact directly with the carbonyl moiety of the Amadori intermediate, but it interferes

**Table 1-1.** Inhibitors and breakers of advanced glycation endproducts

| Agent | Chemical Type | Mechanism of action |
|---|---|---|
| Aminoguanidine (Pimegedine®, AG) | Guanidine structure | - Traps reactive di-carbonyls impeding conversion to AGE<br>- Prevents cross-link formation<br>- Inhibits free radical formation, lipid peroxidation and oxidant induced apoptosis<br>- Large quantities can generate $H_20_2$ and so inhibit Catalase.<br>- Depletion of essential carbonyls in the body can also occur e. g. Vitamin B6 |
| Metformin (dimethylbiguanide) | | |
| Vitamin C and E Nicarnitine | Antioxidants | - Inhibit oxidative conversion involved in di-carbonyl and AGE formation |
| N-acetyl cysteine (NAC) | an altered form cysteine | - work as antioxidant, help to synthesize glutathione |
| A717 | Monoclonal antibody | - Acts on Amadori adducts containing albumin with evidence of retarding development of diabetic nephropathy |
| Pyridoxamine (Pyridorin, PM) | Vitamin B complexs | - Inhibitor of the conversion of Amadori intermediates to AGE |
| OPB-9195 | Synthetic Thiazolidine Derivative | - Trap carbonyl intermediates of advanced glycation<br>- Suppress TGFβ and VEGF expression |
| 2,3-diamino phenazine (2,3 DAP) | | - In vitro work using rat diabetic models showed AGE accumulation and mesenteric vascular hypertrophy |
| Losartan | Angiotensin II receptor inhibitor | - Reduce serum AGE in rat remnant kidney model. Mechanism unknown, but was independent of blood pressure changes |

| | | |
|---|---|---|
| Pyruvate | a-keto acid | - Prevent glycation of protein competitively by forming a Schiff base between free keto groups and free amino groups in proteins.<br>- Inhibits oxidative conversion of the initial glycation product to an AGE. |
| Phenacyl thiazolium bromide (PTB)<br>Alagebrium<br>(ALT-711) | Thiazolium Compound | - Cross-link breakers that could cleave di-ketone bridges between two adjacent carbonyl groups which could form intermolecular cross-links |

Adapted from (Singh et al., 2001)

with post-Amadori oxidative reactions by binding catalytic redox metal ions (Voziyan et al., 2003). Inhibition of the post-Amadori reactions could also decrease the production of ROS, which are known to be formed during this process (Voziyan and Hudson, 2005). Pyridoxamine is also able to bind intermediates of lipid peroxidation and prevent alteration of lysine residues and formation of CML, CEL and other derivatives during the oxidation of LDL *in vitro*.

Being an oral antihyperglycemic agent for the management of type 2 diabetes, metformin may also have an effect in inhibiting glycation reactions (Bailey and Turner, 1996). Like AG, metformin has a guanidine structure. Its inhibitory effect on protein glycation has been reported by several research groups (Rahbar et al., 2000a; Rahbar et al., 2000b; Ruggiero-Lopez et al., 1999). Glycation-induced functional and structural alterations of the diabetic myocardium were prevented by metformin. This is another possible mechanism to explain the beneficial effects of metformin on diabetic vascular complications (Beisswenger and Ruggiero-Lopez, 2003).

Some synthetic compounds with thiazolidine structure, such as OPB-9195, have recently been found to be effective inhibitors of AGE formation. OPB-9195 is known to trap carbonyl intermediates of advanced glycation and showed inhibitive effects on diabetic neuropathy and nephropathy (Tsuchida et al., 1999). Administration of OPB-9195 was found to restrain the cellular production of growth factors such as TGF-β and VEGF (Tsuchida et al., 1999). In addition, it improved motor nerve conduction velocity and suppressed the oxidative stress-induced DNA damage in diabetic rats (Wada et al., 2001).

Plenty of i*n vitro* and in *vivo* studies have verified the effectiveness of other agents to inhibit AGE accumulation. Antioxidant such as Vitamin E, C and nicarnitine inhibit oxidant activity and unspecifically increase the clearance of AGE. The monoclonal antibody A717 acts on Amadori adducts containing albumin and prevent the development of diabetic nephropathy. Interestingly, an angiotension II receptor antagonist, Losartan, was also observed to reduce serum AGE in rat kidney model. Although the mechanism is unknown, this effect was shown to be independent of blood pressure changes (Sebekova et al., 1999).

#### 1.2.6.2. AGE breakers

The abnormal accumulation of glycation-induced crosslinks between proteins increases the stiffness of tissues or organs, especially vascular wall. Immpaired biological function of related tissues thus leads to decreased elasticity of connective tissue and matrix components which is one of the major characteristics of the normal aging process of mammals. Moreorver, it is the major reason that causes thet vascular complications of diabetes. Although AG and related compound have been applied in medical practice, they demonstrate severe side effect. In addition, they cannot reverse the existing AGEs deposited in the tissues to improve the pathogenesis of aging that associated with diabetes and hypertension. In 1996, the first AGE-crosslink breaker, PTB was reported (Vasan et al., 1996). In the same study, its effect on vascular hypertrophy in streptozotocin-induced diabetic rats was investigated. Intra-peritoneal administration of PTB resulted in reduction of AGE accumulation on blood vessels and attenuated the diabetes induced mesenteric vascular hypertrophy. As PTB is unstable in physiological buffers, its analog

alagebrium (4,5-dimethyl-3-phenacylthiozolim chloride) with higher stability was developed and exclusively used in different *in vitro* and *in vivo* studies (Vasan et al., 2003; Wolffenbuttel et al., 1998).

Alagebrium is a stable 4, 5-dimethylthiazolium derivative of the prototype compound PTB. It directly targets the abnormal protein crosslinks leading to the stiffness of the cardiovascular system. Treatment of alagebrium resulted in reduced abnormal protein crosslinking bonds and leads to diminished inflammatory and sclerotic signaling which contribute to the deposition of additional amounts of matrix proteins that physically stiffen tissues. In animal study, 1–3 week treatment of alagebrium in streptozotocin-induced diabetic rats efficiently supressed the hyperglycemia-induced stiffness in vasculartur system including aortic artery and carotid artery. The systemic arterial compliance aortic impedance, carotid compliance and carotid distensibility were siginificantly improved with alagebrium treatment (Wolffenbuttel et al., 1998). As alagebrium does not disrupt the natural carbohydrate modification to proteins, natural intra-molecular crosslinking and peptide bonds and therefore normal protein structure and function are maintained while abnormal crosslinking is removed. This AGE-targeting specifity provides more potential for the application of alagebrium in the treatment of patients with hypertension/diabetes related complications and aging.

### 1.3. Hypothesis and objectives

Although the linkage between AGEs accumulation and diabetes has been extensively observed, the role of MG in the development of insulin resistance has not been well studied. In the present study, it is hypothesized that MG is a critical factor that leads to the pathogenesis of insulin resistance syndrome. To test this hypothesis, we first

tested whether MG can react with the insulin molecule and change its biological function. After that, whether and how MG impairs insulin signalling pathway was examined in normal glycemic rats. As obesity is one of the major causative factors of insulin resistance, we then explored the effect of MG in the pathogenesis of obesity.

# CHAPTER TWO

## MATERIALS AND METHODS

### 2.1. Cell preparations

3T3-L1 cells (mouse fibroblast cell line), L8 cells (rat skeletal muscle cell line), and H4-II-E cells (rat hepatocyte cell line) were purchased from American Type Culture Collection.

#### 2.1.1. Culture of 3T3-L1 cells

3T3-L1 pre-adipocytes was grown to confluence in Dulbecco's modified Eagle's medium (DMEM, Invitrogen, ON, Canada) containing 10% bovine calf serum (Invitrogen, ON, Canada). At two days postconfluence, cell differentiation was induced by adding insulin (2.5 µg/ml, Sigma, St Louis, MI, USA), dexamethasone (0.25 µM, Sigma-Aldrich, MO, USA), and isobutylethylxanthine (IBMX, 0.5 mM, Sigma-Aldrich, MO, USA) to media for 3 d according to the protocol described previously (Brady et al., 1999). The cells then were grown in postdifferentiation media (DMEM containing 10% fetal calf serum and 2.5 µg/ml insulin). After completion of the differentiation protocol, >95% of the cells exhibited an adipocyte phenotype. The post-differentiation medium containing different concentrations of MG and/or different MG inhibitor/scavenger including NAC or metformin (concentrations as indicated) was changed every day until cells were differentiated. Insulin solution (100 nM) was added into the medium 20 min before harvesting the cells. Cells were then washed with phosphate buffer saline (PBS) for three times and ready for different experiments.

### 2.1.2. Culture of L8 cells and H4-II-E cells

L8-cells were cultured in a 4:1 mixture of DMEM and Medium 199 (Invitrogen, ON, Canada), complemented with 10% horse serum and antibiotics.

H4-II-E cells were cultured in DMEM medium with 10% of fetal calf serum and grow till confluence.

### 2.1.3. Culture of INS-1E cells

Cloned INS-1E cells were derived and selected from the parental rat insulinoma (Iezzi et al., 1999). The cell line was a gift from Dr. Claes Wollheim (University Medical Center, Geneva, Switzerland). INS-1E cells were cultured in RPMI 1640 (Invitrogen, ON, Canada) containing: 11.1 mM glucose, 2 mM L-glutamine, 1 mM sodium pyruvate, 10 mM HEPES, 5% fetal calf serum (Invitrogen, ON, Canada), 50 µM ß-mercaptoethanol (Sigma-Aldrich, MO, USA), and 110 U/ml penicillin (Invitrogen, ON, Canada). The cultured cells were passaged weekly by gentle trypsinization and seeded at a density of $1.2 \times 10^4$ cells/$cm^2$, i.e., $1 \times 10^6$ cells in a 10 cm Falcon dish with 8 µl complete medium. For most experiments, INS-1E cells were seeded in Falcon 12-well plates at $2 \times 10^5$ cells/well.

## 2.2. Animal treatment

All the animals were purchased from Charles River laboratories, Inc. (MA, USA), housed in temperature-regulated animal facility and maintained at 22-23°C. The experimental animals were exposed to a 12 h light/dark cycle with free access to water and different diet recipes. Rats were treated in accordance with guidelines of the

Canadian Council on Animal Care and the experimental protocols were approved by the Animal Care Committee of the University of Saskatchewan.

### 2.2.1. Treatment of Sprague-Dawley rats

Twenty nine, 7-week-old male Sprague Dawley (SD) rats were randomly divided into control group ($n = 7$), fructose-fed group ($n = 10$), fructose–NAC co-treated group ($n = 8$), and NAC treated group ($n = 4$) with a feeding period of 9 weeks. Standard rat chow (Prolab® RMH 3000, PMI® Nutrition Intl. USA) and water were given to the control group. Fructose-enriched diet consists of 60% fructose, 22% crude proteins, 5% crude fat, 5% crude fiber, 6% ash, and 2% added minerals. Body weight, blood glucose level, and systolic blood pressure were measured weekly. Blood glucose was determined using the OneTouch® blood glucose monitoring system (LifeScan, Inc, USA). For NAC or fructose–NAC treated groups, NAC was administered with water at a dose of 10 mg/kg/day. At the end of week 9, different tissues were isolated and frozen under -80°C after anaesthetization of rats by intraperitoneal injection of sodium pentobarbital (50 mg/kg body weight).

For metformin treated experiment, rats were randomly divided into control group (n=7), fructose-fed group (n=10), fructose-metformin co-treated group (n=8) and metformin treated group (n=4) with a feeding period of 9 weeks. The fructose-enriched diet, which consists of 60% fructose (replacing the 60% starch) with the remaining components in the diet the same as in standard lab rat chow (Galipeau et al., 2001; Harada et al., 2004; Song et al., 2004), has been widely used in insulin resistance studies (Galipeau et al., 2001; Harada et al., 2004; Song et al., 2004). For the fructose-metformin

co-treated group, in addition to fructose-enriched diet, metformin was administered in water at 500 mg/day/kg body weight. Body weight, plasma glucose levels, and systolic blood pressure were measured weekly. Systolic blood pressure was measured by a standard tail cuff noninvasive BP measurement system (Model 29-SSP, Harvard Apparatus, Canada) (Wu et al., 2004).

### 2.2.2. Treatment of Zucker rats

Eight 8-week-old male Zucker fatty rats and eight age-matched lean Zucker rats were fed with standard rat chow (Prolab® RMH 3000, PMI® Nutrition Intl. USA) and water. Body weight, blood glucose level were measured weekly using a Quantichrom glucose assay kit (Bioassay Systems, CA, USA). Blood samples (0.5 ml) were obtained from tail vein at the age of 10, 12 and 14 weeks for serum MG measurement. Intraperitoneal glucose tolerance test (IPGTT) was carried out after overnight fasting at the age of 16 weeks. At the end of week 16, different tissues were isolated and frozen at -80 °C after anaesthetization of rats by intraperitoneal injection of sodium pentobarbital (50 mg/kg body weight),

## 2.3. Patients

Blood samples were obtained from 20 untreated patients with mild to moderate hypertension from the clinical research units at the Sacré-Coeur Hospital and at the Hôtel-Dieu Hospital in Montreal. Based on the BMI value (=body weight in kg/ square of the height in meter), the patients were divided into obese (BMI≥30) and non-obese (BMI<30) groups. Both groups were comprised of males and females ranging in age from

46 to 68 years. All subjects provided informed written consent approved by the ethics committees of both hospitals. Venous blood was drawn into pre-chilled tubes (BD, NJ, USA) containing EDTA ($K_3$). The samples were vortexed and centrifuged immediately at 4 °C for 20 min at 3000 rpm and the plasma samples were stored at -80 °C.

### 2.4. MG measurement

Quantitation of MG was done by the widely accepted o-phenylenediamine (o-PD)-based assay as described by Chaplen *et al.* (Chaplen et al., 1996), with some modifications. Briefly, the supernatant of tissue homogenate or serum was incubated with 100 mmol/L o-PD (derivatizing agent) for 3 h at room temperature. The quinoxaline derivative of MG (2-methylquinoxaline) and the quinoxaline internal standard (5-methylquinoxaline) were measured using a HITACHI D-7000 high-performance liquid chromatography (HPLC) system (HITACHI Ltd., Ontario, Canada). The column was a Nova-Pak® C18 column (3.9 x15 mm, and 4 um particle diameter; Waters, MA, USA). The mobile phase was composed of 80% (vol) of 10 mmol/L $NaH_2PO_4$ (pH 4.5) and 20% (vol) of HPLC grade acetonitrile. Duplicate injections of each sample were made. Samples were calibrated by comparison with a 2-MQ standard.

### 2.5. Protein extraction

The cultured cells were washed with ice-cold Krebs buffer (118 mM NaCl, 4.7 mM KCl, 1.2 mM $KH_2PO_4$, 1.2 mM $MgSO_4$, 4.2 mM $NaHCO_3$, 2 mM $CaCl_2$, 10 mM glucose, 200 μM sulphinpyrazone and 10 mM Hepes, pH 7.4) for 2 times. The cells were then scraped and collected into a centrifuge tube. After centrifugation at 1000 rpm for 10

minutes, the supernatant was discarded and the pellet was resuspended in 0.2 ml of Krebs/ RIPA buffer containing 1% protease inhibitor (Sigma-Aldrich, MO, USA). After the powdered frozen rat tissue or cells in Kreb's buffer were sonicated using a ultrasonic homogenizer, transferred the supernatant into another eppendorf tube to determine the protein concentration.

### 2.6. Determination of protein concentration

The protein concentration of samples was determined by BCA (bicinchoninate) assay (Smith et al., 1985). Briefly, 50 volumes of Reagent A (1g BCA, 2g sodium carbonate, 0.16g sodium tartrate, 0.4g NaOH, 0.95g sodium bicarbonate) and 1 volume of Reagent B (4% CuSO4.5H2O) were mixed to make the working solution. The dilution series of BSA and sample protein were then prepared. Sealed samples and incubated at 37$^{o}$C for 30 minutes. The spectrophotometric absorbance of the samples was determined using a plate reader (Thermo Labsystems, Finland) at 562 nm. The protein concentration of the unknown samples was then estimated by the machine according to the slope of the standard curve.

### 2.7. Tricine SDS-PAGE

Samples were separated on Tricine SDS-PAGE gels containing 16.5% (w/v) acrylamide, as described by Schägger and von Jagow (Schagger and von Jagow, 1987). Samples were boiled for 10 min in solubilization buffer [62.5 mM Tris-HCl, pH 6.8; 2% (w/v) SDS; 10% (v/v) glycerol; and 0.025% (w/v) bromphenol blue]. After

electrophoresis, the gels were stained with Coomassie brilliant blue G (Sigma, ON, Canada) and photographed.

### 2.8. Western blotting

The supernatants containing crude cellular proteins were boiled, run on a 10-12% SDS-PAGE gel, and then transferred to a PVDF membrane (polyvinylidene difluoride, PALL Corporation, ON, Canada). The membrane was blocked with 5% skim milk solution in PBS containing 0.05% Tween-20 (PBS-T) at room temperature for 1 h and incubated with primary antibody (1:500 for p21, p27, phosphor-p21 (p-p21) and phosphor-p27 (p-p27) antibodies, Santa Cruz, MO, USA; 1:1000 for Akt and phosphor-Akt (p-Akt) and β–actin antibodies, Cell Signaling Technology, MA, USA). After washing for 3 times with the PBST for 30 min, the membrane was incubated with the HRP-conjugated secondary antibody (1:10000) for 1 h at room temperature. The immunoreactions were visualized by ECL and exposed to X-ray film (Kodak Scientific Imaging film, X-omat Blue XB-1). β-actin was used as a housekeeping protein to normalize the data for variations in loading.

### 2.9. Protein immunoprecipitation

Protein A/G–sepharose beads (Sigma-Aldrich, MO, USA) were used for immunoprecipitation. Approximately 200 µl of beads were washed with 1.6 ml of PBST 3-4 times in a screw-capped Eppendorf tube. The beads were re-suspended in 1.6 ml of PBST containing 5 µl anti-PI3K p85 antibody (Upstate Biotechnology, NY, USA) and 50 mg BSA. The tubes were set horizontally on a gentle rocking platform to keep the beads

in motion and rocking was continued overnight at 4°C. The following day, the pre-absorbed beads were centrifuged at 2,000 g for 2 min. After removing the supernatant, 1 ml of crude protein extract was added to the Eppendorf tube. The mixture was then carefully transferred to a clean 1.5 ml Eppendorf tube, and 300 µg of crude protein extract were added. The Eppendorf tubes were placed horizontally on a gently rocking platform overnight on ice. The following day, the beads were centrifuged at 2000 xg for 2 min. The supernatant was removed, and pre-chilled PBS-T was added to wash the beads. The washing was repeated at least 8 times. To elute the protein from the beads, 100 µl of protein loading buffer with fresh 10 mM Dithiothreitol (DTT) was added and heated to 95°C for 5 min. After boiling, iodoacetimide was added to Eppendorf tubes to a concentration of 25 mM from a fresh 0.5 M stock to inhibit disulfide bonds from reforming. After gentle vortexing, the tubes were centrifuged at 16,000 g for 1 min. The supernatant was carefully collected without disturbing the beads and loaded onto a protein gel as detailed above.

### 2.10. PI3K activity assay

PI3K activity in the immunoprecipitates was analyzed with a PI3K enzyme-linked immunosorbent assay (ELISA) (from Echelon Biosciences, UT, USA) according to the manufacturer's instructions. Briefly, immunoprecipitated enzyme and $PI(4,5)P_2$ substrate were incubated for 1 h at room temperature in the reaction buffer. Kinase reaction was stopped by pelleting the beads by centrifugation and transferring the reaction mixture to the incubation plate and incubated overnight at 4°C with a $PI(3,4,5)P_3$ detector protein, then added to the $PI(3,4,5)P_3$-coated microplate for 1 h for competitive binding. A

peroxidase-linked secondary detection reagent and colorimetric detection (absorbance was measured at 450 nm) is used to detect $PI(3,4,5)P_3$ detector protein binding to the plate. The colorimetric signal is inversely proportional to the amount of $PI(3,4,5)P_3$ which produced by PI3K. The expression levels of the PI3K components p85 for each time point were detected by western blot analysis of pelleted beads.

### 2.11. Cell proliferation assay

The proliferation of 3T3-L1 cells was measured by the Celltiter 96® non-radioactive cell proliferation assay kit (Promega, WI, USA). Briefly, cells were seeded onto 96-well plates (5000 cells per well) and cultured in DMEM medium (HyClone, Ontario, Canada). When they reached ~50% confluency, the medium was removed and the cells were washed with serum-free medium and incubated in serum-free medium for 48 h. The cells were then treated with/without MG, SH-6 (10 μM) or alagebrium (50 μM) for 48 h in serum-containing DMEM medium supplemented. After that, the cells were incubated with MTT [3-(4,5-dimethylthiazol-2-yl)-2,5-diphenyltetrazolium bromide] solution (final concentration 0.5 mg/ml and stock solution 5 mg/ml MTT in PBS) for at 37°C for 4 h and then with solubilization solution at room temperature for 1 h. The spectrophotometric absorbance of the samples was determined by a plate reader (Thermo Labsystems, Finland) at 570 nm.

### 2.12. Cell cycle assay

Cell cycle analysis was performed by propidium iodide (PI) staining. Briefly, 3T3-L1 cells were firstly seeded into 10 cm dishes. When they reached ~50% of

confluence, the cells were incubated in serum-free medium for 48 h and then treated with MG, SH-6 (10 μM) or alagebrium (100 μM) for 12, 16 or 20 h. Subsequently, the cells were harvested and re-suspended in PBS at $1 \times 10^6$/ml and fixed with 70% cool ethanol for 1 h. After the cells were washed and centrifuged, the pelleted cells were re-suspended in 1 ml PBS and added with 50 ml of RNase A stock solution (10 g/ml). Followed a 3 h incubation at 4°C, the cells were then pelleted and added with 1 ml of PI staining solution (3.8 mM sodium citrate, 50 mg/ml PI in PBS) and analyzed by flow cytometry on an Beckman Coulter Epics XL flow cytometer (Beckman Coulter Canada Inc, ON, Canada). Analysis was performed after 10 000 counting events.

### 2.13. Cdk2 activity assay

Cdk2 activity was determined by measuring ATP consumption with a PKLight Assay Kit (LT07-500, Cambrex Bio Science, ME, USA). Briefly, after incubation of 200 μg of proteins with 2 μg of anti-Cdk2 antibody (Santa Cruz) in cell lysis buffer for 4 h at 4°C, protein A/G plus agarose beads (20 μl) were added and the mixture was incubated overnight at 4°C with shaking. Beads were washed 3 times and suspended in 40 μl of Cdk2 kinase assay buffer containing 20 μM ATP and 0.1 μg/μl histone H1. The above mixture was reacted at 30°C for 30 min in 96-well plate before kinase stop solution and ATP detection reagent were added according to the manufacture's protocol. Bioluminescent signal in each well was detected using a microplate spectrofluorometer (NovoStar, BMG LABTECH Inc., NC, USA). Cdk2 activity was expressed as ATP consumption from 3 experiments.

## 2.14. MG-insulin adduct preparations

For mass spectrometric analysis, the adducts formed between MG and insulin (MG-insulin) were prepared by incubating human insulin (0.01–1 μg/μl) with MG (10 μM–1 mM) for 2 to 72 h *in vitro* in phosphate buffer (pH 7.4) at 37°C under sterile conditions (Lo et al., 1994). For other studies, MG-insulin adducts were prepared by incubating human insulin (0.01–1 μg/μl) with MG (1–100 μM) for 3 d *in vitro* in phosphate buffer (pH 7.4) at 37°C under sterile condition (Lo et al., 1994). To separate free MG molecules from the MG-insulin, the reaction mixture was centrifuged on a Microcon® YM-3 centrifugal filter tube [nominal MW cut-off 3000 dalton (Da), Millipore Corporation, MA, USA] at 12000 rpm for 30 min. After the first centrifugation, an equal vol of $ddH_2O$ was added and the reaction mixture was centrifuged again. This process was repeated three times at room temperature. The retained molecules on the membrane were then recovered in $ddH_2O$, and the MG concentration was measured using HPLC. Quantitation of MG was done by o-PD based assay as described previously (Chaplen et al., 1998; Lo et al., 1994; Wang et al., 2004).

## 2.15. Mass Spectrometry

Samples containing human insulin, and insulin incubated with MG, were reduced with 10 mM DTT (pH 8.0) at 55°C for 1 h and alkylated with 55 mM iodoacetamide (pH 8.0) in dark to separate the A- and B-chains of (modified) insulin. This technique ensured that the site(s) of modification could be determined by using mass spectrometry (MS). Insulin samples and MG-insulin incubates were first analyzed by matrix-assisted laser desorption/ionization-time of flight (MALDI-TOF) MS, before and after

reduction/alkylation. Samples and incubates were purified by solid-phase extraction using packed disposable pipette tips ($ZipTip_{C18}$, Millipore, Billerica, MA, USA), according to the manufacturer's instructions. Extracted samples (0.75 µl) were then combined with an equal vol of dihydroxybenzoic acid (DHB) matrix solution (20 mg/mL in 75% acetonitrile containing 0.1% TFA) and applied to a 96-well MALDI target plate. Mass spectra were acquired on a Voyager-DE STR instrument (Applied Biosystems, MA, USA), operating in the positive ion and linear modes, with delayed ion extraction. Typical operating conditions were: accelerating voltage 25,000 V, grid voltage 95.5%, guide wire voltage 0.05%, extraction delay time 400 ns, and laser power 1790. Spectra were generated by combining the scans from 200 laser shots. Mass-to-charge (*m/z*) ratios for the observed protonated peptide ion peaks were determined using bovine insulin (*m/z* 5734.65) for close eternal calibration.

Reduced and alkylated MG-insulin incubates were further analyzed by liquid chromatography-mass spectrometry (LC-MS) and tandem mass spectrometry (MS/MS) to locate the site(s) of MG attachment. Samples were diluted 50-fold in 0.1% aqueous TFA. A 5 µl aliquot was then analyzed by LC-MS using a capLC ternary HPLC system interfaced to a Q-Tof Ultima Global hybrid tandem mass spectrometer fitted with a Z-spray nanoelectrospray (nanoES) ion source (Waters). Typical operating conditions were: nanoES capillary 3.50 kV, lens 1 100 V, cone 100 V, source temperature 80°C, desolvation temperature 150°C, cone gas flow 143 L/h, collision energy 10 eV (MS), and 32 eV (MS/MS). Solvents A and C comprised 0.2% formic acid in water, while solvent B consisted of 0.2% formic acid in acetonitrile. Reduced-insulin and MG-insulin peptides were captured on a C18 trapping column (Symmetry 300, 0.35x5 mM Opti-pak; Waters

Milford, MA, USA) and washed for 3 min using solvent C at a flow rate of 30 µl/min. The flow path was then switched using a 10-port rotary valve, and the peptides eluted onto a C18 analytical column (PepMap, 75 µm x 15 cm, 3 µm particle size; LC Packings). Separations were performed using a linear gradient of 0:100 to 60:40% B:A over 43 min. The composition was then changed to 80:20% B:A and held for 10 min to flush the column before re-equilibrating for 7 min at 0:100% B:A. Mass calibration of the Q-Tof instrument was performed using a product ion spectrum of Glu-fibrinopeptide B acquired over the *m/z* range 50 to 1900. Predicted *m/z* ratios for possible A- and B-chain MG-insulin were based on the known molecular masses of human insulin and MG and the formation of multiple adducts with and without concomitant loss of water (vide infra). Multiply protonated (4+) ions corresponding to the insulin B-chain and various MG-insulin adducts were detected by LC-MS (*m/z* 400 to 1900). These were selected for LC-MS/MS analysis (*m/z* 100 to 1900), and the resulting product ion spectra deconvoluted using the instrument software (MaxEnt 3) to identify N-terminal (b-type), C-terminal (y-type), immonium, and internal fragment ions.

To study the reaction between metformin and MG, a solution containing 25 µM MG and 25 µM metformin in 0.2 M sodium phosphate buffer (pH 7.4) was prepared and incubated at 37 ºC for 24 h. The resulting incubate was diluted 1000-fold in 50:50 v/v water/acetonitrile containing 0.1% formic acid and analyzed by flow injection electrospray ionization mass spectrometry (FI-ESI-MS), using a HP1100 binary solvent pump and autosampler (Hewlett-Packard, Palo Alto, USA) coupled to a Quattro LC quadrupole tandem mass spectrometer via a Z-spray$^{TM}$ interface (Micromass, Manchester, UK). The samples were introduced at a flow rate of 20 µl/min and ionized by positive-ion

electrospray using a capillary potential of 3 kV, a cone voltage of 30 V, and a source and drying gas temperature of 120 ºC and 350 ºC, respectively. MS data were acquired in the *m/z* range 110 – 400 at the rate of 0.8 s/scan, with an interscan delay of 0.1 s, and MS spectra generated using the MassLynx™ instrument software. Structural analysis of selected precursor ions was subsequently performed by collision-induced dissociated (CID) and product-ion tandem mass spectrometry (MS/MS), using a collision gas (Ar) pressure of 2 x $10^{-3}$ mbar and a collision energy ($E_{LAB}$) of 20 eV. MS/MS data were acquired in the *m/z* range 50 – 280, and product-ion spectra generated using MassLynx™.

### 2.16. Real-time quantitative polymerase chain reaction (PCR)

For total-RNA preparation, 3T3-L1 cells were homogenized in TRIzol® reagent (Invitrogen, ON, Canada) and RNA was isolated according to the manufacturer's instructions. Total RNA was reverse-transcribed in triplicate using RevertAid™ H Minus M-MuLV reverse transcriptase (MBI, Fermentas Burlington, ON, Canada) in the presence of 5x RT buffer (MBI, Fermentas, MD, USA), random primer (Invitrogen, Burlington, ON, Canada), dNTP mixture (Amersham Pittsburgh, PA, USA) at 42°C for 50 min, followed by 72°C for 10 min. The primers used in this study for real-time PCR are summarized in Table 2-1. The real-time PCR was carried out in an iCycler iQ apparatus (Bio-Rad, CA, USA) associated with the ICYCLER OPTICAL SYSTEM software (version 3.1) using SYBR Green PCR Master Mix (Bio-Rad). All PCRs were triplicated and performed in 96-well optical-grade PCR plates and run for 45 cycles at 95°C for 20 s, 62°C for 1 min, and 72°C for 30s. After cycling, melting curves of the PCR products were acquired by stepwise increase of the temperature from 62° to 95°C.

**Table 2-1. The primers used for real-time PCR**

| Primer | Sequence |
|---|---|
| INSULIN RECEPTOR-1 | 5’- CGGCCCGATGCTGAGAACAAC-3' |
| INSULIN RECEPTOR-2 | 5’- CAGCACATGCGCATCAGGTCAGT-3' |
| IRS-1 | 5’- AGGGGCTGCTTCCATTTGTAG-3' |
| IRS-2 | 5’- ACCACCGCTGCCCC CTCCTG-3' |
| PI3K-1 | 5’- GCCACAGCA GCCTTCAACAAA-3' |
| PI3K-2 | 5’- CAACATCAGCGCAAACAGGGTAAT-3' |
| LEPTIN-1 | 5'- CGGGGCGCTGGTGTAGGGAGATT -3' |
| LEPTIN-2 | 5'- ACACCGCATGGAGAGTCGCAGGAG -3' |
| ADIPONECTIN-1 | 5'- ATGGGTAGTTGCAGTCAGTTGGTA -3' |
| ADIPONECTIN-2 | 5'- GCCGCTTATGTGTATCGCTCAG -3' |
| PPARγ-1 | 5'- AGGGCTTCCGCAGGTTTTTGA -3' |
| PPARγ-2 | 5'- CACAGGCCGAGAAGGAGAAGC -3' |
| C/EBPα | 5’- CTTGCGCAGGCGGTCATTGTCACT -3' |
| C/EBPα | 5’- GGCCGGCCTCTTCCCCTACCAG -3' |

## 2.17. Measurement of [$^3$H]-2-Deoxyglucose uptake

[$^3$H]-2-deoxyglucose ([$^3$H]-2-DOG, PerkinElmer) was used for glucose uptake experiments in different insulin-sensitive cells as described previously (Brady et al., 1999). Briefly, confluent cells in 24-well plates were washed with serum-free DMEM and incubated in the same medium for 3 h. The cells were then washed twice with glucose-free and serum-free DMEM, followed by incubation in the same medium for 30 min. Thereafter, the cells were exposed to insulin, MG-insulin, or MG at different concentrations for 30 min and continuously incubated for another 20 min after the addition of [$^3$H]-2-DOG (0.1 µCi/500 µl) with glucose (50 µM) to the medium. All incubations were performed at 37°C. The incubation was stopped by washing cells three times with ice-cold glucose-free phosphate buffer. The cells were lysed in 0.1% SDS and then transferred into scintillation vials for counting (Beckman LS 3801 scintillation counter).

## 2.18. Determination of C-peptide secretion from INS-1E cells

C-peptide is stoichiometrically related to insulin on a one-to-one basis and is coreleased with insulin (Polonsky, 1995). By measuring C-peptide concentration, the amount of insulin secreted can be deduced. In our study, C-peptide was determined by a rat C-peptide ELISA kit (WAKO, Osaka, Japan) using rat C-peptide as a standard. The insulin secreting INS-1E cells were plated into 24-well plates at a density of $2 \times 10^4$ cells/well. After 2-days culture, the cells were maintained at 37°C for 2 h in glucose-free RPMI 1640, washed, and preincubated in a glucose-free Krebs-Ringer-bicarbonate medium (pH 7.4) containing (in mM): 135 NaCl, 3.6 KCl, 5 $NaHCO_3$, 0.5 $NaH_2PO_4$, 0.5

$MgCl_2$, 1.5 $CaCl_2$, 10 HEPES (KRBH buffer), and 0.1% BSA. After a 30-min preincubation, insulin or MG-insulin was added into the medium, respectively. Cells were incubated for another 90 min at 37°C in the presence of 16.7 mM of glucose. At the end of incubation, medium was collected and centrifuged for 10 min at 2500 *g* and 4°C to remove cell debris. The supernatant was used immediately or stored at –20°C until C-peptide measurement.

**2.19. Adipogenesis assay**

3T3-L1 cells were treated with/without MG, SH-6 (10 μM) or alagebrium (50 μM) for 48 h and then continue cultured in fresh medium. When the cells reached 80% confluence, differentiation was induced by adding 2.5 μg/ml insulin, 0.25 μM dexamethasone (Sigma-Aldrich, MO, USA), and 0.5 mM isobutylmethylxanthine (Sigma-Aldrich, MO, USA) to media for 2 days according to the protocol described previously (Brady et al., 1999; Jia et al., 2006). The cells were then grown in post-differentiation medium (DMEM containing 10% fetal calf serum and 2.5 μg/ml insulin). On the fifth day of post-differentiation, cells were fixed with 4% (v/v) formaldehyde in PBS, and then stained with Oil Red solution for 15 min. A stock solution of oil red O (0.5 g in 100 ml of isopropanol) was prepared and filtered through a 0.2 μm filter. The working solution was prepared by diluting the stock solution by distilled water (3:2), left for 1 h at room temperature, and filtered through a 0.2 μm filter before use. Cells in 12-well plate were stained with 200 μl oil red O working solution for 15 min at room temperature. The cells were rinsed five times with water and pictures were photographed under microscope. Cells were considered as being lipid-positive when droplets were

stained red. The dye retained by the cells was eluted by incubation with 500 µl of isopropanol and quantified by measuring absorbance at 500 nm by a plate reader (Thermo Labsystems, Finland).

### 2.20. Determination of insulin degradation through liver cells

The H4-II-E cells were cultured in 12-well plates to confluence ($2x10^5$ cells/well) and were treated with insulin or MG-insulin at 37°C for 15 min. Thereafter, the cultured medium was collected and insulin concentration was measured with a rat-specific insulin ELISA kit (Mercodia, Uppsala, Sweden).

### 2.21. Intraperitoneal glucose tolerance test

The intraperitoneal glucose tolerance test (IPGTT) was carried out after 12–14 h fasting. After the basal glucose level was measured, conscious rats were injected intraperitoneally with 1.5 g/kg body weight of 50% (w/v) glucose solution in 0.9% (w/v) saline. A blood sample was then collected from the tail vein and blood glucose level was measured using OneTouch® blood glucose monitoring system (LifeScan, Canada) at 0, 10, 15, 30, 60, and 120 min after the glucose injection.

### 2.22. Immunohistochemistry study

Cells were cultured on glycine coated cover glasses in DMEM medium. Formaldehyde solution (40%) was added directly into the culture medium to a final concentration of 4% and incubated at room temperature for 30 min. After rinsing the cover glass with PBS-T for 4 times over 30 min, cells were permeabilize with 0.5%

Triton X-100 in PBS-T for 5 min, and then blocked with 5% horse serum in PBS-T for 30 min. Anti-CEL antibody(1:200) was added and incubated for 60 min. After rinsing the the cells with PBS-T for 4 times over 30 min, the Alexa-546 fluorescence labed anti-mouse second antibody (1: 10000; Molecular Probes, OR, USA) was applied and incubated for 30 min in the dark. The cells were rinsed with PBS-T for 4 times and mounted with cover slips. The excess PBS-T was blotted away and the edges were sealed with nail polish. A second coat was applied after the polish had dried, the slides were then covered with foil and stored under -80°C

### 2.23. Biochemical examination of blood samples

Blood samples were collected from the aorta of rats. Insulin level in serum (μg/l) was determined with a rat-specific insulin ELISA kit (Mercodia AB, Sweden). The levels of triglyceride, total cholesterol, and high-density lipoprotein (HDL)-cholesterol were assayed in the Laboratory of Biochemistry and Hematology, Royal University Hospital, University of Saskatchewan, Saskatoon, Canada.

### 2.24. Statistical analysis

Data are expressed as mean ±SEM and analyzed using one way ANNOVA in conjunction with *t* test where applicable. Difference between groups was considered statistically significant when $P < 0.05$.

# CHAPTER THREE

## STRUCTURAL AND FUNCTIONAL CHANGES IN HUMAN INSULIN INDUCED BY METHYLGLYOXAL

### 3.1. Introduction

Insulin resistance is a state in which increased concentrations of insulin are required to produce a given biological response (Rett, 1999). Because the major effect of insulin is to promote overall glucose utilization, insulin resistance is also defined as reduced insulin mediated whole-body glucose uptake (DeFronzo and Beckles, 1979; Rett, 1999). Altered insulin action can lead to a number of important pathophysiological states, such as Type 2 diabetes mellitus and hypertension. All of these clinical manifestations are associated with an increased cardiovascular risk. Currently, the causes and mechanisms of insulin resistance remain poorly understood, although they could be tightly linked to both genetic and environmental factors (Alzaid, 1996; Permutt et al., 2005).

MG readily interacts with certain arginine or lysine residues in selected proteins to form irreversible AGEs. MG is the most reactive AGEs precursor (Kalapos, 1999). The reaction of MG with arginine residues of proteins forms hydroimidazolone Nε-(5-hydro-5-methyl-4-imidazolon-2-yl)-ornithine (MG-H1), as well as argpyrimidine (Ahmed et al., 2002). MG can also react with lysine residues of proteins to form CML and CEL. The physiological concentrations of plasma MG are from 0.2 to 14.2 μM in rats (Babaei-Jadidi et al., 2003; Nagaraj et al., 2002; Wang et al., 2004) and 1.4 μM (Thornalley et al., 1989) in healthy humans. Increased MG levels have been reported in different insulin resistance states. The serum concentration of MG increases 5–6 fold in patients with type

1 diabetes mellitus and 2–3 fold in patients with type 2 diabetes. The characteristic protein modification induced by MG has been found in the aorta of stroke-prone spontaneously hypertensive rats (Mizutani et al., 1999). Our previous results showed increased levels of MG and AGEs in vascular smooth muscle cells from SHR rats (Wu, 2005; Wu and Juurlink, 2002). Plasma MG concentration was significantly elevated at 8, 13, and 20 wk of age in parallel with increased blood pressure increase in SHR, whereas the MG levels remained unchanged in age-matched normotensive WKY rats (Kalapos, 1999; Wang et al., 2005).

MG and related AGEs such as CEL have been recognized as indicators of carbonyl overload burden *in vivo* (Singh et al., 2001) and are correlated with age (Li et al., 1996). It has been reported that MG decreased the activity of glutathione reductase (Vander Jagt et al., 1997; Wu and Juurlink, 2002), which might be due to MG-induced glycation of arginine residues. Whether MG induces functional and structural changes in the insulin molecule, which may in turn play an important role in the development of insulin resistance, is unknown. To investigate whether MG causes structural modification of insulin molecule, we have used MALDI-TOF mass spectrometry to study MG-induced mass changes in insulin molecules. We have also used MS/MS to identify the amino acid residue(s) at which the insulin molecule is modified by MG. Whether MG-modified insulin decreased insulin-mediated glucose uptake was examined in insulin-sensitive cells. To further determine the change of biological functions of insulin, the effects of insulin and MG-modified insulin on C-peptide secretion, an indicator for insulin release from pancreatic ß-cells, were examined and compared. The degradation of insulin and MG-

insulin through hepatocytes was also compared. Finally, both the effect of MG on the insulin-induced glucose uptake and the expression of insulin receptor were explored.

## 3.2. Results

### 3.2.1. MG induced mass changes of insulin

To determine whether MG can modify on insulin molecules, we subjected human insulin to electrophoresis in Tricine SDS-PAGE gels after incubation with MG and/or phosphate buffer for 3 d. As shown in Figure 3-1, incubation of insulin (1 μg/μl) with MG (100 μM) resulted in additional bands with lower electrophoretic mobility than native insulin on SDS-PAGE. Several new bands appeared when insulin was incubated with higher concentration of MG (1 mM) was carried out. However, with the same MG concentrations and incubation conditions, no new band was observed for glucagon (data not shown).

As the accuracy of molecular mass determination by SDS-PAGE is limited, we turned to mass spectrometry for a more accurate and sensitive determination of MG-induced mass changes. The MALDI-TOF mass spectrum of intact human insulin (Figure 3-2*A*) contained peaks at *m/z* 5808 and 2905, which corresponded to the singly (1+) and doubly (2+) protonated molecular ions of insulin. However, incubation of 1 μg/μl (170 μM) insulin with 10 μM MG for 3 d resulted in additional peaks that provided evidence for the formation of MG-insulin (Figure 3-2*B*). The peak at *m/z* 5880, for example, corresponded to the addition of one MG molecule (72 Da), while a peak at around *m/z* 5934 corresponded to the addition of two MG molecules with concomitant loss of a single water molecule (72+54). The same results were observed from three other independent

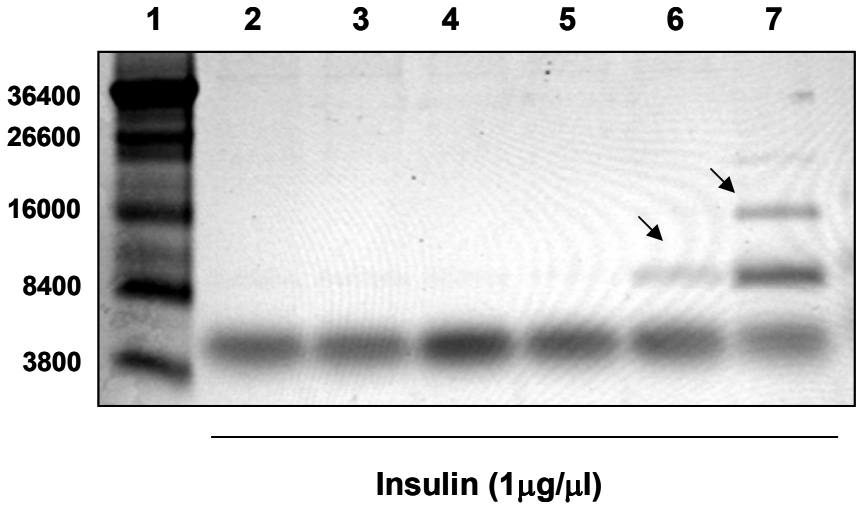


**Figure 3-1. MG-induced mass changes of insulin.** Human insulin was incubated with or without MG for 3 days. The molecular masses of different sample components were determined by Tricine SDS-PAGE. Line 1: molecular standard (kDa); Line 2: freshly prepared insulin control; Line 3: insulin incubated with phosphate buffer; Line 4: insulin incubated with MG (1 μM); Line 5: insulin incubated with MG (10 μM); Line 6: insulin incubated with MG (100 μM); Line 7: insulin incubated with MG (1 mM). The arrows point to new bands with lower electrophoretic mobility than insulin.

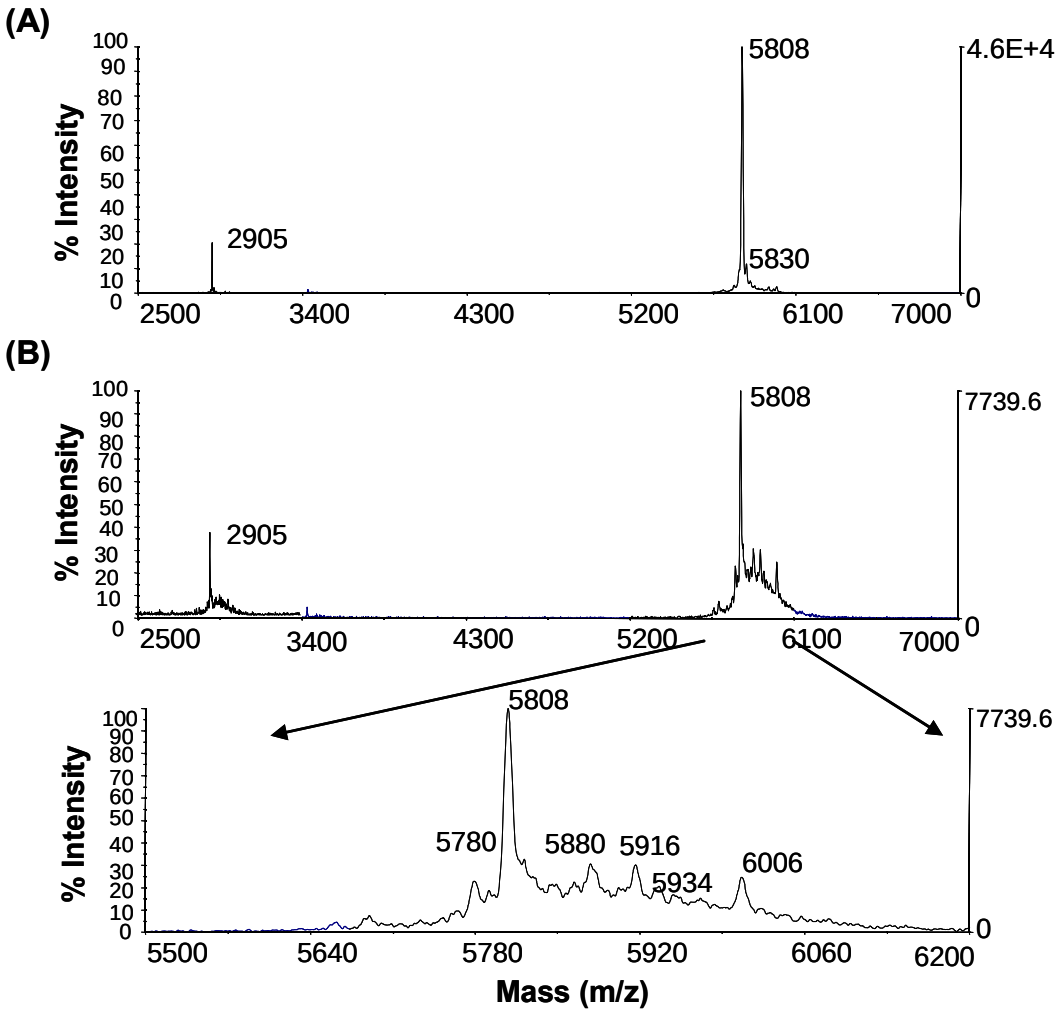
(A)
% Intensity
100
90
80
70
60
50
40
30
20
10
0
2905
5808
5830
4.6E+4
0
2500
3400
4300
5200
6100
7000
(B)
% Intensity
2905
5808
7739.6
0
5780
5880
5916
5934
6006
5500
5640
5780
5920
6060
6200
Mass (m/z)

**Figure 3-2. MALDI-TOF MS analysis of MG-induced mass changes in human insulin.** ***A)*** In the absence of MG, human insulin gives rise to singly and doubly protonated molecular ions at *m/z* 5808 and 2905, respectively. ***B***) Incubation of human insulin (1 μg/μl) with MG (10 μM) for 3 d gives rise to additional peaks, indicating the formation of MG-insulin adducts. Closer inspection reveals peaks that correspond to the addition of one or more MG molecules with (+54 Da) and without (+72 Da) concomitant loss of water.

experiments. Different incubation times were also tested. Interestingly, 24 and 48 h incubations gave similar MS profiles for the resulting MG-insulin adducts (data not shown), whereas incubation times of less than 2 h did not give rise to additional peaks, even when the concentration of MG was increased to 10 mM.

### 3.2.2. Amino acid target(s) for MG modification of insulin

To determine the position(s) of MG attachment, we treated human insulin and MG-insulin incubates each with dithiothreitol to reduce intramolecular disulfide bonds. The resulting free thiol groups were then blocked by carbamidomethylation with iodoacetamide to separate permanently the A- and B-chains, and the reaction products were analyzed by MALDI-TOF MS. The mass spectrum of reduced insulin alone contained major peaks at *m/z* 2611 and 3543 (Figure. 3-3*A*), corresponding to the reduced and alkylated A- and B-chains, respectively. However, incubation with MG produces additional peaks that showed progressive enlargement of the B-chain with increasing MG concentrations (Figure 3-3*B*–*D*).

The most prominent B-chain adducts appearing at the final concentrations of MG above 15 μM corresponded to a mass increase of 54 Da (*m/z* 3597). MS/MS analysis of the corresponding 4+ ion (*m/z* 900.2), generated by nanoES, produced a spectrum in which all the observed b-ions were shifted by + 54 Da (Figure 3-4*A*-*b*) relative to the corresponding spectrum for the unmodified insulin B-chain (*m/z* 886.7) (Figure 3-4*A*-*a*). In contrast, all the observed y-ions remained unchanged (Figure 3-4*B*-*b*), a result consistent with attachment of MG (as R-*Nn*=CH-C ($CH_3$)O) to the N terminus of the insulin B-chain. MS/MS analysis of the + 108 Da adduct (*m/z* 913.7) also showed a b-ion

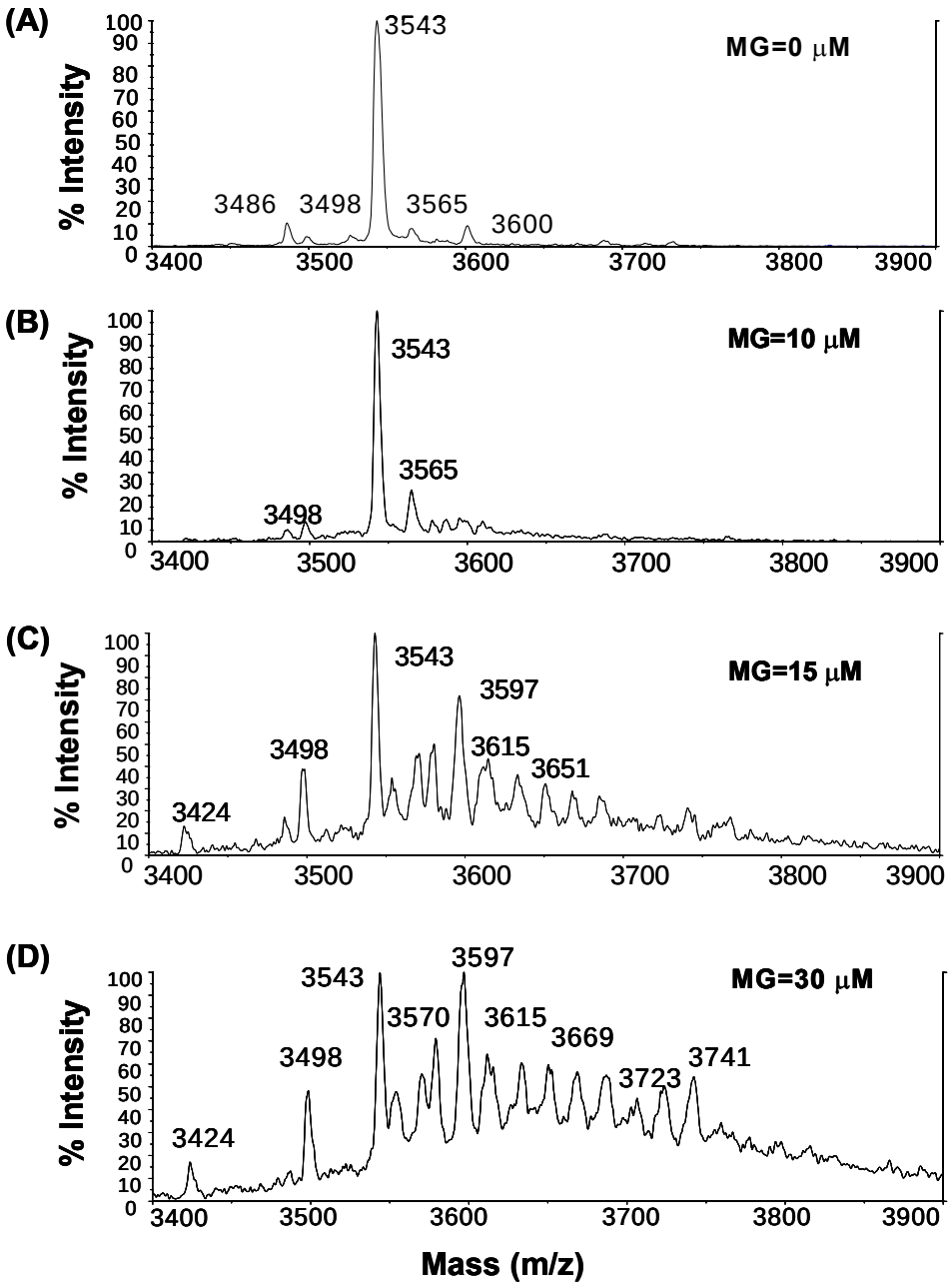


**Figure 3-3. MALDI-TOF MS analysis of MG-induced mass changes of the B-chain of human insulin.** ***A***) In the absence of MG, the predominant peak is that of the reduced and alkylated B-chain, with small additional peaks corresponding to attachment of sodium (+22 Da) and a third carbamidomethyl (+57 Da) group. Incubation with increasing concentrations of MG (10, 15, and 30 μM) results in the progressive formation of a dehydrated (+54 Da) MG adduct at *m/z* 3597, along with other putative B-chain derivatives (***B–D***).

shift of + 54 Da (Figure 3-4*A*-*c*). However, a shift of + 54 Da was also seen in the larger observable y-ions ($y'_{15}$ and above; Figure 3-4*B*-*c*) whereas the smaller observable y-ions ($y'_4$ and below; not shown) remained unchanged. The intervening region contained arginine as the only basic residue, the side chain of which would increase in mass by 54 Da on reaction with MG (*vide infra*). These observations indicated that MG adduction can occur both at the N terminus of the insulin B-chain and at an internal, arginine residue. Furthermore, low abundance peaks marked * (Figure 3-4*A*-*c* and 3-4*B*-*c*) provided evidence for a shift of + 108 Da in certain b-ions ($b_{16}^+$ and below) relative to the unmodified B-chain. This suggested that sites other than arginine might be modified, and that the spectrum observed for *m/z* 913.7 was actually a superimposition of MS/MS spectra for several isobaric B-chain adducts modified with two MG molecules. This also explained why the shifted and unshifted y- and b-ions were sometimes observed together in the MS/MS spectra of MG adducts. In such cases (e.g., Figure 3-4*B*-*C*) the relatively high abundance of the unshifted y-ions suggested that internal MG modifications were less stable than the N-terminal modification.

### 3.2.3. MG-insulin impaired glucose uptake by different insulin-sensitive cells

[$^3$H]-2-DOG uptake by 3T3-L1 adipocytes was determined after the cells were treated with insulin (1, 10, and 100 nM) or MG-insulin, which was generated by incubating insulin at the same concentrations as for native insulin with 1, 10, or 100 μM MG, respectively. As shown in Figure 3-5*A*, 3T3-L1 cells showed a significant increase of [$^3$H]-2-DOG uptake induced by insulin in a concentration-dependent manner. However,

**(A)**

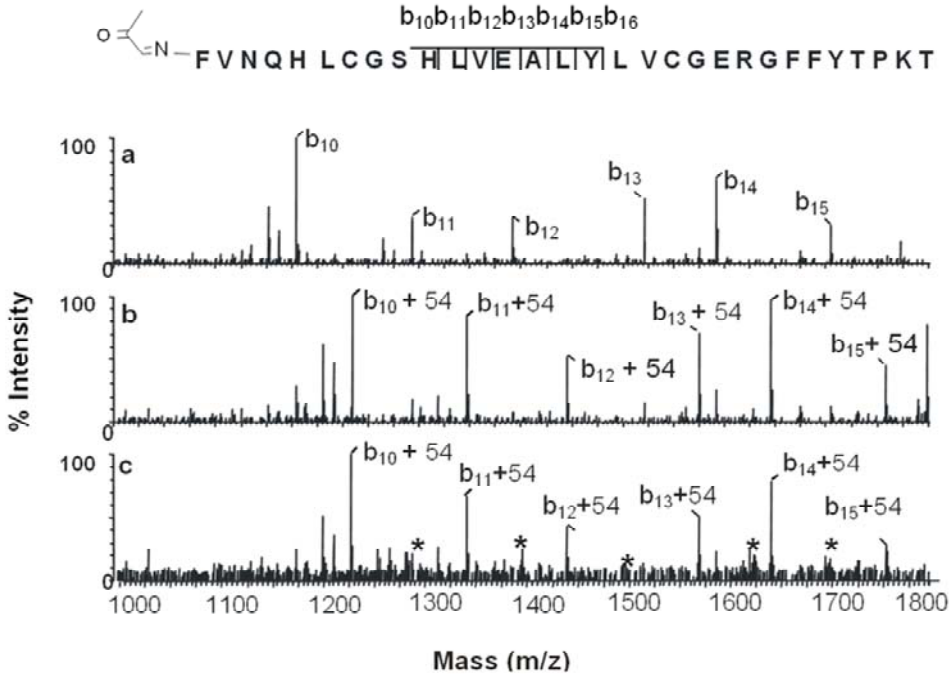
b10b11b12b13b14b15b16
FVNQH LCGS HLVEALY LVCGERGFFYTPKT
a
b
c
b10
b11
b12
b13
b14
b15
b10 + 54
b11+54
b12 + 54
b13 + 54
b14+ 54
b15+ 54
b12+54
b13+54
b14+54
b15+54
100
0
% Intensity
1000
1100
1200
1300
1400
1500
1600
1700
1800
Mass (m/z)

**(B)**

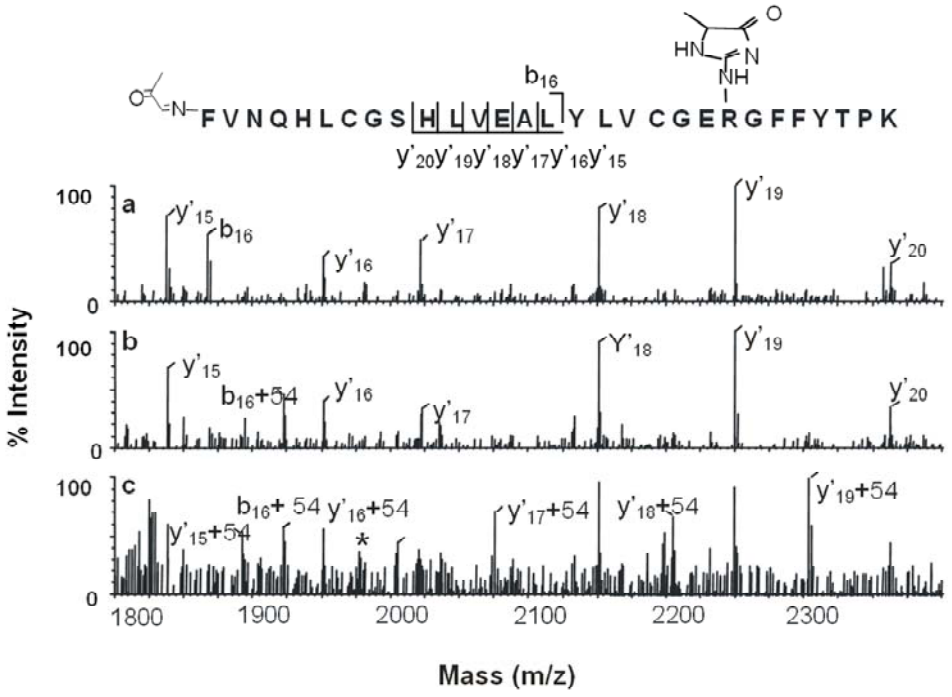
b16
FVNQHLCGS HLVEALY LV CGERGFFYTPK
y'20y'19y'18y'17y'16y'15
a
b
c
y'15
b16
y'16
y'17
y'18
y'19
y'20
b16+54
Y'18
b16+ 54
y'16+54
y'15+54
y'17+54
y'18+54
y'19+54
100
0
% Intensity
1800
1900
2000
2100
2200
2300
Mass (m/z)

**Figure 3-4. Deconvoluted MS/MS spectra of insulin B-chain.** (***A***–*a*) The b-ions observed for the quadruply protonated ion at *m/z* 886.7 correspond exactly to those predicted for the reduced, alkylated B-chain; (***A***–*b*) a shift of + 54 Da in the b-ion series for *m/z* 900.3 is consistent with attachment of MG at the N terminus; (***A***-*c*) evidence of a further b-ion shift (*) for *m/z* 913.5 suggests that a second MG moiety can attach near the N terminus and/or elsewhere on the insulin B-chain. (***B***–*a*) MG-insulin adducts were generated by the incubation of insulin (1 μg/μl) with MG (30 μM). The y-ions observed for the quadruply protonated ion at *m/z* 886.7 correspond exactly to those predicted for the reduced, alkylated B-chain; (***B***–*b*) the *y*-ions and internal fragments observed for *m/z* 900.3 are identical to those observed for *m/z* 886.7, confirming that MG is attached to the N terminus; (***B***–*c*) for *m/z* 913.5, a shift of + 54 Da in larger y-ions is consistent with further modification of insulin B-chain at the arginine residue.

a significantly lower uptake of [$^3$H]-2-DOG was observed after the cells were treated with MG-insulin, compared with the cells treated with the concentration-matched native insulin (Figure 3-5*A*). Similar result was also observed in L8 skeletal muscle cells (Figure 3-5*B*).

To clarify whether the lower glucose uptake in MG-insulin treated group had resulted from free unattached MG in the solution, the effect of MG on the expression of insulin receptor at mRNA concentration was also explored in 3T3-L1 cells using real-time PCR. After treatment of 3T3-L1 cells with MG (3 or 30 μM) for 24 h, mRNA expression levels (computed tomography) of insulin receptor were 12.3 ± 0.2 or 12.1 ± 0.15, which was not significantly different from that of MG-untreated group (11.9 ±0.2) ($P$ >0.05 $n$=4 in each group, data not shown).

### 3.2.4. Effects of MG-insulin on C-peptide secretion from INS-1E cells

Whether MG-insulin impairs the insulin-induced feedback inhibition of insulin release from pancreatic ß-cells was investigated. As shown in Figure 3-6*A*, when INS-1E cells were co-exposed to native insulin (100 nM) and glucose (16.7 mM) for 2 h, the C-peptide release dropped to 76.5% of the C-peptide release from cells treated only with glucose at the same concentration ($P$ <0.05, $n$=4 for each group). When INS-1E cells were co-treated with MG-insulin and glucose, the insulin-induced inhibition of C-peptide secretion disappeared, in comparison with cells treated with native insulin and glucose ($P$ <0.05, $n$=4 for each group). Without the formation of MG-insulin adducts, an acute application of MG and insulin did not alter the insulin-induced inhibition of C-peptide release ($P$ >0.05, $n$=4 for each group).

(A)

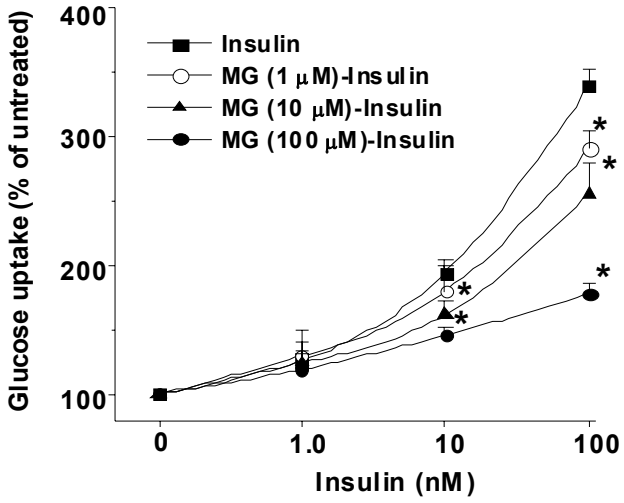
Glucose uptake (% of untreated)
400
300
200
100
Insulin
MG (1 μM)-Insulin
MG (10 μM)-Insulin
MG (100 μM)-Insulin
*
0
1.0
10
100
Insulin (nM)

(B)

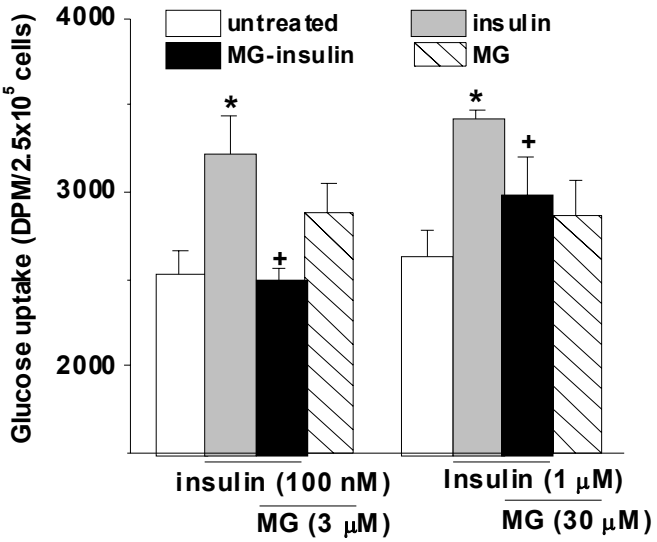
Glucose uptake (DPM/2.5x10^5 cells)
4000
3000
2000
untreated
MG-insulin
insulin
MG
*
+
insulin (100 nM)
MG (3 μM)
Insulin (1 μM)
MG (30 μM)

**Figure 3-5. MG-insulin induced lower glucose uptake in adipocytes 3T3-L1 (*A*) and L8 cells (*B*).** MG-insulin adducts (MG-insulin) were prepared by incubation of human insulin with MG for 3 d. [$^3$H]-2-DOG uptake was determined after the cells were treated with insulin or MG-insulin for 30 min. $^*P < 0.05$ *vs.* insulin group, $^+P < 0.05$ *vs*. insulin group, $n = 5–6$ for each group. DPM: disintegrations per minute.

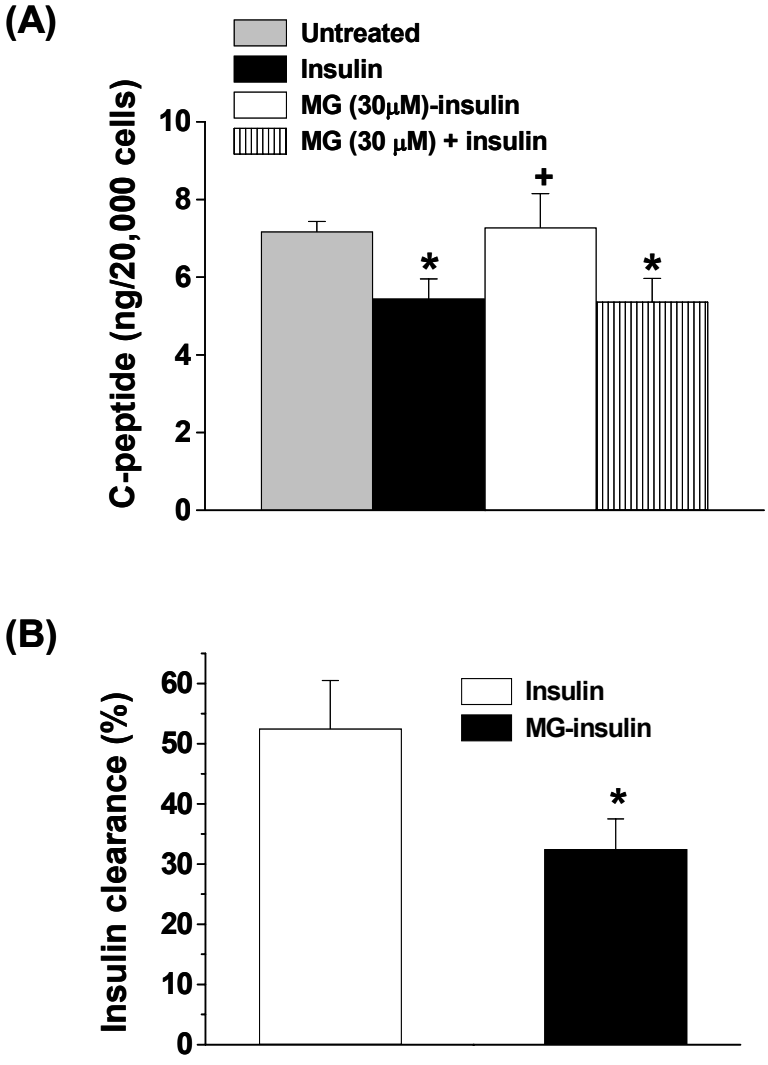
(A)
Untreated
Insulin
MG (30μM)-insulin
MG (30 μM) + insulin
C-peptide (ng/20,000 cells)
0
2
4
6
8
10
*
+
*
(B)
Insulin
MG-insulin
Insulin clearance (%)
0
10
20
30
40
50
60
*

**Figure 3-6. The modification on insulin molecule decreased its biological functions.** ***A***) MG-insulin has lower feedback inhibition on C-peptide secretion from INS-1E cells. C-peptide in the medium was measured after INS-1E cells were treated 2 h with insulin (100 nM), MG-insulin adducts (MG-insulin), or MG + insulin (coapplication) in the presence of glucose (16.7 mM). MG-insulin was generated from incubating insulin (1 μg/μl) with MG (30 μM) for 3 d as described in Materials and Methods. $^{*}P < 0.05$ *vs*. control, $^{+}P < 0.05$ *vs*. insulin group, $n = 4$ for each group. ***B***) Insulin was measured after H4-II-E cells were treated with insulin (200 nM) or MG-insulin (200 nM) for 15 min. MG-insulin was generated from incubating insulin (1 μg/μl) with MG (30 μM) for 3 d as described in Materials and Methods. Clearance rate = (200 nM – measured insulin concentration in cultured medium)/200 nM. $^{*}P < 0.05$ *vs*. insulin group, $n = 6$ for each group.

### 3.2.5. Decreased degradation of MG-insulin through hepatocytes

Liver is the main site for insulin clearance, removing ~50% of the circulating insulin through a receptor-mediated endocytosis process (Gorden et al., 1978; Li Calzi et al., 1997). To investigate whether MG-insulin could still be removed by hepatocytes properly, we treated H4-II-E cells with insulin (200 nM) or same concentration of MG-insulin for 15 min and then determined insulin clearance in culture medium. As shown in Figure 6*B*, we found a significantly higher insulin clearance rate (51.5% ± 5.6) in the cells treated with native insulin, compared with that from cells treated with MG-insulin (32.0% ± 3.6).

## 3.3. Discussion

Increased plasma MG concentration and MG-induced irreversible advanced glycated endproducts have been observed in different insulin resistant states, including diabetes and hypertension (Singh et al., 2001; Thornalley et al., 1989; Wang et al., 2005). The abnormal MG concentration in patients paralleled the development of insulin-resistance syndrome, which involves complex etiological factors. Previous studies have suggested that MG may render certain types of cells resistant to hormones and growth factors (Du et al., 2003; Portero-Otin et al., 2002). However, the underlying mechanisms for this MG effect have not been further investigated. To clarify the correlation between abnormal MG metabolism and insulin resistance, we explored in this study whether MG causes structural and functional changes the insulin molecule.

Insulin travels from pancreatic β-cells through the circulation to its target tissues. Events at any one of these loci can influence the ultimate action of the hormone. If

arginine or lysine residue of insulin had been glycated by MG, the biological function of insulin in the regulation of glucose homeostasis would be significantly changed. Our results showed that incubation of insulin with MG for 3 d resulted in new bands with lower electrophoretic mobility, in addition to native insulin, on Tricine SDS-PAGE gels (Figure 3-1). Importantly, this was not observed when glucagon was incubated with MG at the same concentrations (data not shown). Both insulin and glucagon are involved in glucose regulation, and they have common pancreatic origin. Glucagon, a 29-amino acid single-chain polypeptide, contains two arginines at position 17 and 18 and one lysine at position 13, while insulin consists of a 21-amino acid A-chain and a 30-amino acid B-chain with one arginine at position 22 and one lysine at 29 on its B-chain. Our results suggest that the generation of MG-insulin adducts may depend on a special molecular recognition between MG and insulin. In support of this scheme, recent studies on human peripheral blood lymphocytes as well as many plasma proteins from different animals (rat, mouse, and monkey) show that only a limited number of proteins undergo glycation (Jana et al., 2002; Poggioli et al., 2002). However, the selectivity of glycation of proteins, as assessed by measurement of extent of glycation in cells, may depend on the reactivity of individual proteins to glycation and the rate of degradation and/or repair of the glycated protein.

Mass spectrometry gives an accurate and sensitive measure of MG-induced mass changes in the insulin molecule and provides strong evidence for the formation of MG-insulin adducts. The peak at *m/z* 5880 (Figure 3-2) corresponds to the addition of one MG molecule (72 Da) to insulin, while the peak at *m/z* 5934 corresponds to the addition of two MG molecules with concomitant loss of a single water molecule (72+54 Da). It

has been reported that MG derivatizes lysine or arginine residues of human serum albumin *in vitro* (Ahmed et al., 2002). These findings are consistent with our observations. For example, addition of MG to lysine forms the monolysyl adduct CEL, resulting in a mass increase of 72 Da. In contrast, MG undergoes a condensation reaction with arginine to form one of three hydroimidazolone isomers (MG-H1, H2, and H3), resulting in a net mass increase of 54 Da. However, other peaks observed during MS analysis suggest that multiple additions of MG occur both with and without concomitant loss of water, despite the fact that insulin contains a single lysine and arginine residue. For example, the peak at *m/z* 5916 corresponds to a mass increase of 108 Da (54 + 54), which implies two condensation reactions involving addition of MG. Glyoxal, another metabolite of glucose, can react with free amine groups ($R\text{-}NH_2$) to give a reaction product ($R\text{–}N\text{=}CH\text{–}CHO$) that results in concomitant loss of water (Glomb and Monnier, 1995). Similar reactions between MG and side-chain or N-terminal amino groups would result in multiple mass increases of 54 Da, as observed for intact insulin. MG adduction at both the N terminus of the insulin B-chain and at internal residues (predominantly arginine) was subsequently confirmed by tandem MS analysis of insulin B-chain adducts (*vide supra*).

Our study shows that MG-insulin adducts induce a significant and concentration-dependent decrease in glucose uptake in insulin-sensitive adipocytes and skeletal muscle cells (Figure 3-5). Normally, insulin is promptly released from pancreatic islet ß-cells in response to increased plasma glucose concentration and interacts with its specific receptors on different target cells. Fat and muscle cells express a particular GLUT protein isoform, GLUT-4, which is also known as the insulin-regulated GLUT (Klip et al., 1994). Therefore, these two types of cells exhibit an extraordinary glucose uptake response to

insulin stimulation. Insulin receptors locate on the membrane of insulin-sensitive cells. An unchanged transcriptional expression of insulin receptor was observed after the cells were treated with or without MG. It is, therefore, unlikely that MG has a direct effect on the binding affinity or expression levels of insulin receptors. Apparently, the formation of MG-insulin adducts reduced the capability of native insulin to stimulate glucose uptake.

The autocrine control of insulin release by the extracellular insulin concentration has attracted great attention since the discovery of insulin receptors and insulin receptor substrates in pancreatic ß-cells. Insulin is produced in pancreatic ß-cells as proinsulin, an 86-amino acid single-chain polypeptide (MW 9000 kDa), and then cleaved into insulin (MW 5800 kDa) and C peptide (27-amino acids). C-peptide is coreleased with insulin on a one-to-one basis (Polonsky, 1995). By measuring the secretion of C-peptide, the amount of insulin released from ß-cells could be estimated, especially for the determination of insulin or MG-insulin on the autocrine regulation mechanism. Our result confirmed that insulin inhibited insulin secretion, as reflected by the decreased C-peptide release, from INS-1E cells. Once MG-insulin adducts are formed, the glycated insulin can no longer inhibit insulin (C-peptide) secretion (Figure 3-6*A*). It is worth noting that, in addition to impaired glucose uptake, hyperinsulinemia is another common phenomenon in insulin-resistance syndrome such as T2DM or human obesity (Olefsky and Kolterman, 1981). Under physiological conditions, pancreatic ß-cells sense the change of blood glucose levels and adjust insulin output accordingly. Circulating insulin in turn further modulates insulin release to provide a fine-tuned control of insulin metabolism. The formation of MG-insulin adducts can result in an abnormal autocrine control of insulin release.

In addition to the increased insulin secretion from pancreatic ß-cells, hyperinsulinemia might be also partially due to the disturbance of a normal receptor-mediated insulin clearance induced by MG-insulin adducts. The circulating insulin levels are not only determined by its secretion from pancreatic ß-cells but also depend on insulin clearance from the circulation. As for other peptide hormones, endocytosis is the major mechanism for removal of insulin. In this process, the insulin receptor with bound hormone is internalized. Endocytosis of this complex in insulin-targeted cells leads to insulin degradation and recycling of receptors back to the plasma membrane (White and Kahn, 1994). Degradation of insulin occurs mainly in liver (50%) and muscles (Polonsky, 1995). Recently, it has been noticed in obese patients that insulin resistance is associated with reduced clearance of insulin from plasma (Jones et al., 2000), despite no clear mechanism. We observed a significantly high insulin clearance rate (or lower concentration of insulin) in the culture medium from the cells treated with native insulin, compared with that from cells treated with MG-insulin (Figure 3-6*B*). This finding indicated that MG-insulin adducts cannot go through endocytosis properly, or there is an aggregation of MG-insulin. However, further experiments will be needed to clarify the mechanism behind this phenomenon.

The physiological concentration of plasma MG in rats is between 0.2 and 5 μM *in vivo* (Babaei-Jadidi et al., 2003; Nagaraj et al., 2002). Our previous study detected the plasma MG levels of 33.6 μM in 20-week-old SHR and 14.2 μM in age-matched WKY rats (Wang et al., 2004). It has been reported that the plasma concentration of MG is 1.4 μM in healthy humans (Thorburn et al., 1989) and 26.6 μM in normal Chinese hamster ovary (Chaplen et al., 1998). Differences in these reported endogenous MG levels could

be explained by different species, and different MG assays used in different laboratories. Normal human plasma insulin concentrations are 0–0.5 nM with a 5–10 fold increase following ingestion of food. In the present *in vitro* study, MG at 1–30 μM was used to interact with insulin at 1–100 nM to determine the glucose uptake. Obviously, the concentrations used for insulin are close to those plasma concentrations observed after food intake, while the concentrations chosen for MG also fall into physiological and pathophysiological range according to different reports. Moreover, higher concentrations of MG may prove necessary for detection of its *in vitro* interaction with insulin molecule. *In vivo* conditions with physiological pH, temperature as well as intact biochemical and enzymatic reactions may facilitate the interaction of MG and insulin at a much lower MG concentration.

In summary, our results show that MG modifies the B-chain of human insulin *in vitro*, and that modification occurs predominantly at the N terminus and arginine residue via Schiff base formation. The extent of modification increases with the relative concentration of MG. The formation of MG-insulin adducts leads to the reduction of insulin-mediated glucose uptake by its target cells or tissues, impaired autocrine control of insulin release from pancreatic ß-cells, and decreased hepatic clearance of insulin from liver cells. A chronic increase in the circulating MG concentration, with enhanced formation of MG-insulin adducts, might play an important role in the development of insulin resistance. Therefore, clarification of the role of MG in the development of insulin resistance may lead to a discovery of new mechanisms and methods for the management and prevention of insulin-resistance syndromes, including diabetes and hypertension.

# CHAPTER FOUR

## ACCUMULATION OF ENDOGENOUS METHYLGLYOXAL IMPAIRED INSULIN SIGNALING IN ADIPOSE TISSUE OF FRUCTOSE-FED RATS

### 4.1. Introduction

MG interacts readily with certain free amino acid residues in proteins and forms AGEs (Monnier and Cerami, 1981). Increased accumulation of MG was observed in different insulin resistance states including diabetes patients (Beisswenger et al., 2005; Wells-Knecht et al., 1996) and hypertensive animals (Wang et al., 2005; Wang et al., 2004). These findings suggest that MG accumulation may play an important role in the development of insulin resistance.

Insulin resistance may occur through different mechanisms including defects in insulin signaling (Sechi and Bartoli, 1997). When insulin binds to insulin receptor (IR), the intrinsic tyrosine kinase activity of IR is activated. The activated receptor then phosphorylates selected tyrosine residues of substrate proteins such as IRS1-4, Shc proteins, and SHP-2. Following insulin stimulation, tyrosine and serine phosphorylation of IRS-1 is increased. IRS proteins provide docking sites for PI3K. PI3K plays a critical role in stimulating GLUT4 translocation by catalyzing the phosphorylation of $PIP_2$ to $PIP_3$. As a consequence, PI3K activation results in an enhanced glucose uptake (Cheatham and Kahn, 1995; Yamauchi et al., 1996). Recent studies reported that MG inhibited the insulin signaling in cultured skeletal muscle cells (Riboulet-Chavey et al., 2006). However, the effect of MG accumulation on insulin signaling in whole animal, particularly in adipose tissue, remains unclear. In the present study, fructose, the MG

precursor, was administered to SD rats to increase the endogenous levels of MG and the expression of insulin signaling molecules were examined. To further explore the direct effect of MG on insulin signaling, cultured 3T3-L1 adipocytes were treated with MG and its scavenger, NAC (Wu and Juurlink, 2002). The effect of MG on the phosphorylation of IRS-1 and PI3K activity were then investigated.

## 4.2. Results

### 4.2.1. MG accumulation in rats correlated with the development of insulin resistance

As shown in Figure 4-1*A*, 9 weeks of fructose feeding increased plasma triglyceride dramatically ($P < 0.05$ vs. untreated control rats) while NAC co-treatment significantly reversed this increase. Although plasma HDL-cholesterol level did not differ between control and fructose-fed rats, it was increased by NAC treatment (Figure 4-1*A*). An increased blood pressure was also observed in fructose-fed rats (data not shown). However, neither fructose ($n = 10$) nor NAC ($n = 4$) treatment changed plasma levels of total cholesterol and blood hemoglobin A1c ($P > 0.05$, data not shown). In all treatment groups of rats, fasting blood glucose level was 5–6 mM. At the end of 9-week of treatment, the intraperitoneal glucose tolerance test was performed and no difference was found among these four groups except a higher glucose level at the 90 min point in the fructose-fed rats (data not shown). As shown in Figure 4-1*B*, serum insulin level was increased significantly to 178% in fructose-fed group ($n = 10$) in comparison with that from untreated control group ($P < 0.05$, $n = 7$). NAC co-treatment lowered the fructose-induced increase in insulin. The insulin-induced [$^3$H]-2-DOG uptake by visceral adipose

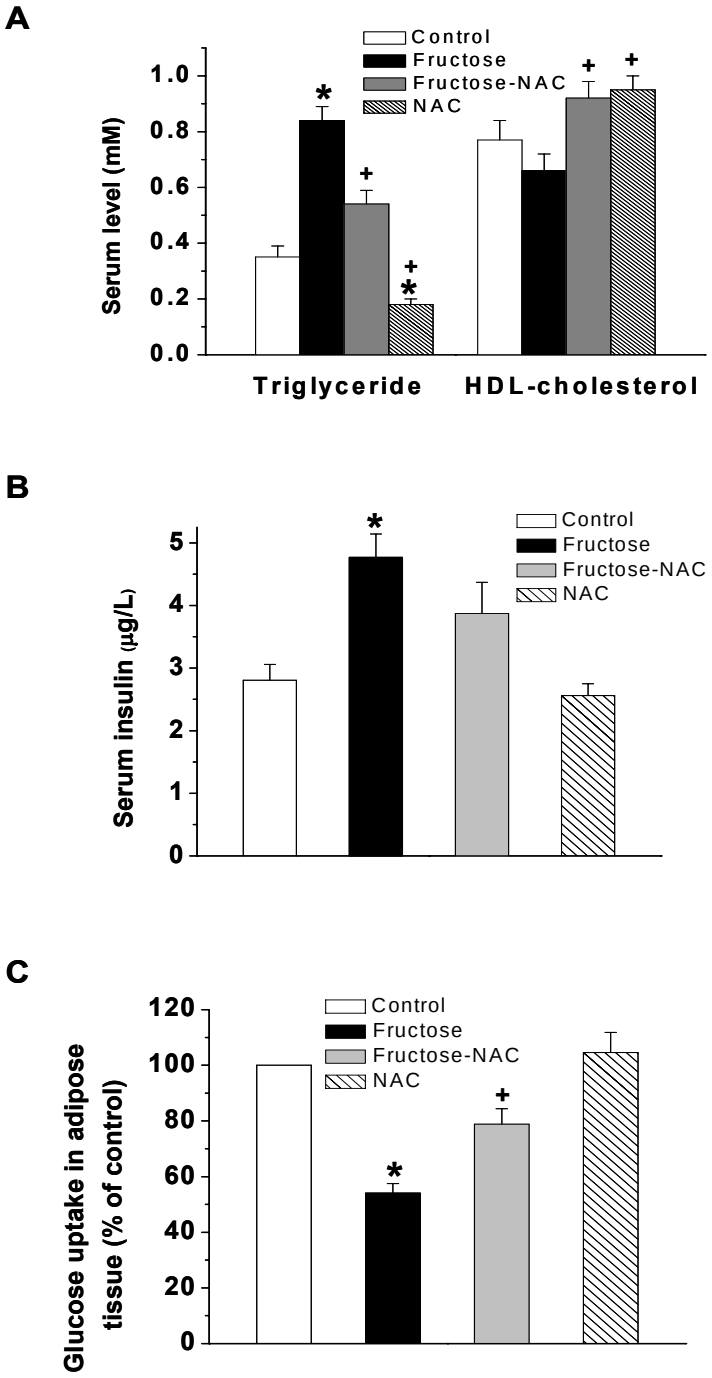
A
Control
Fructose
Fructose-NAC
NAC
Serum level (mM)
1.0
0.8
0.6
0.4
0.2
0.0
Triglyceride
HDL-cholesterol
B
Serum insulin (μg/L)
5
4
3
2
1
0
C
Glucose uptake in adipose tissue (% of control)
120
100
80
60
40
20
0

**Figure 4-1. Effects of fructose and/or NAC treatment on the development of insulin resistance in SD rats.** Fructose and/or NAC feeding induced changes in serum triglyceride and HDL-cholesterol (***A***), serum insulin level (***B***), and insulin-stimulated glucose uptake in adipose tissue (***C***). *$P < 0.05$ vs. untreated control rats; $^{+}$ $P < 0.05$ vs. fructose-fed rats, $n = 7–10$ for control, fructose-fed and fructose–NAC treated group, $n = 4$ for NAC treated group.

tissue dropped dramatically in fructose-fed rats ($P < 0.05$, $n = 7–10$ in each group) (Figure 4-1*C*). Glucose uptake stimulated by 100 nM insulin in fructose-fed rats was only 55% of that observed for control rats. With NAC co-treatment, however, this value was enhanced by 38.2% ($P < 0.05$ vs. fructose-fed rats, $n = 4$ in NAC treated group; $n = 8$ in fructose-fed group).

As shown in Figure 4-2*A*, 9 weeks of fructose feeding significantly increased MG content by more than 2-fold in adipose tissue from 1.5 ± 0.05 μmol/g protein in untreated group to 4.37 ± 0.25 μmol/g protein in treated group ($P < 0.05$, $n = 4$). A significant increase in MG level was also observed in blood serum from 1.81 ± 0.41 μM in control rats to 3.29 ± 0.30 in fructose-fed rats ($P < 0.05$, $n = 4$, Figure 4-2*B*). The increased MG levels in adipose tissue and serum were both lowered by co-administration of NAC (Figure 4-2*A, B*). In serum samples, it was even returned to control level. However, NAC treatment alone did not show significant effect on MG accumulation.

### 4.2.2. Alteration of PI3K expression in the adipose tissue of fructose-treated rats

Using Western blotting analysis, we compared protein levels of key insulin signaling genes in adipose tissue from the rats treated with or without fructose. The protein level of PI3K was increased significantly by 29% in fructose-fed rats compared to the untreated control group ($P < 0.05$, $n = 4$ for each group; Figure 4-3*A, B*). The increased PI3K protein expression at protein level was counteracted by NAC co-treatment. On the other hand, neither IR nor IRS-1 expression was changed significantly by the treatment with fructose, NAC, or fructose–NAC (Figure 4-3*A, B*).

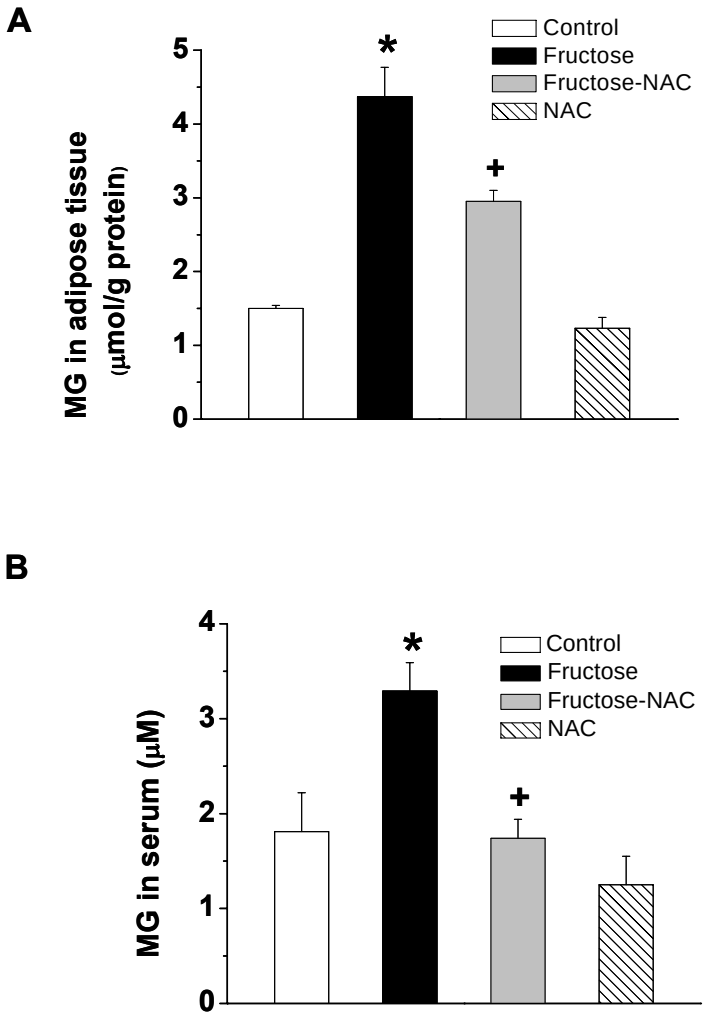


**Figure 4-2. Effects of fructose and/or NAC treatment on the MG levels in SD rats.** MG levels were measured in adipose tissue (***A***) and serum (***B***) of untreated rats, fructose-treated rats, fructose–NAC co-treated, and NAC-treated rats, respectively. **P* < 0.05 vs. control rats; $^{+}$ *P* < 0.05 vs. fructose-fed rats. *n* = 4 for each group

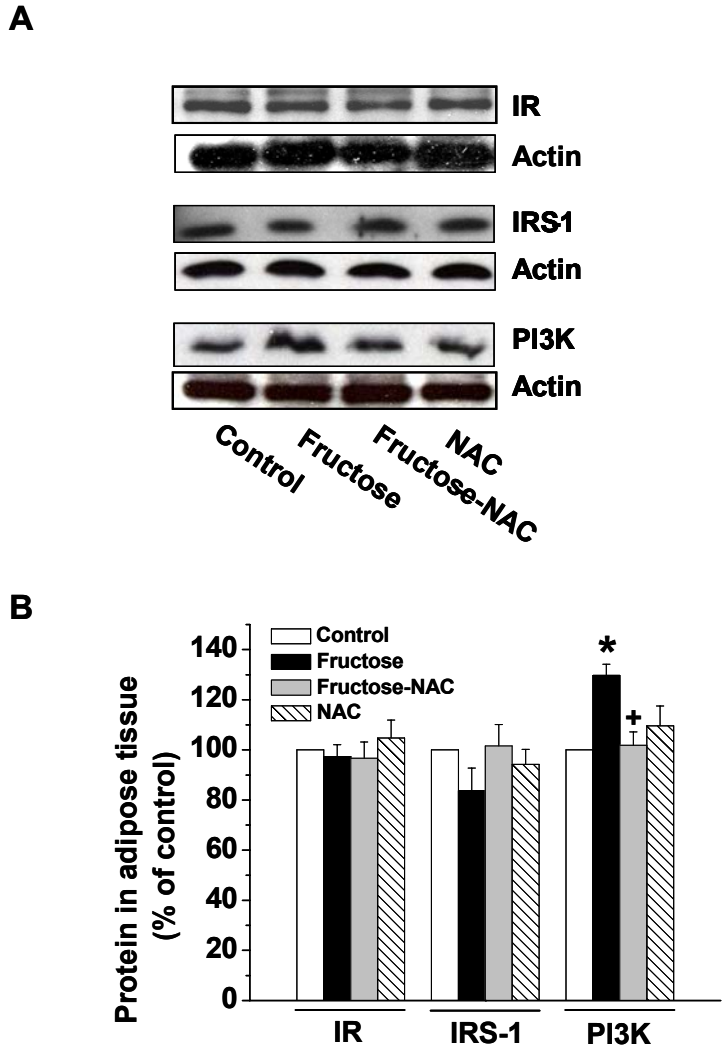


**Figure 4-3. Effects of fructose or fructose–NAC co-treatment on the expression of IR, IRS-1, and PI3K.** Western blotting showed the expression of IR, IRS-1, and PI3K in adipose tissue from differently treated groups of rats (***A***) and the expression was presented as % of that from untreated rats (***B***). $^{*}P < 0.05$ vs. control rats, $^{+}P < 0.05$ vs. fructose-fed rats, $n = 4$ for each group.

### 4.2.3. Decreased association between PI3K and IRS-1 in fructose-fed rats

Generally, the tyrosine phosphorylated IRS-1 binds to various effector molecules including the regulatory subunit of PI3K and recruits PI3K catalytic subunit to its regulatory subunit then results in its activation. We therefore, evaluated the tyrosine phosphorylation of IRS-1 and the recruitment of PI3K to IRS-1 in adipose tissue. In fructose-fed rats, the tyrosine phosphorylation of IRS-1 was not changed significantly compared to the control level, although a declining tendency was shown ($P > 0.05$, $n = 4$ for each group; Figure 4-4*A*). However, the amount of PI3K recruited to the phosphorylated IRS-1 was reduced to 70.9% of the control level from untreated rats ($P < 0.05$, $n = 4$ for each group). The reduced IRS-1/PI3K association was restored by NAC co-administration (Figure 4-4*B*).

### 4.2.4. Effects of MG on the insulin-signaling pathway of 3T3-L1 cells

In order to further confirm whether the alteration of PI3K in fructose-fed rats was caused by the enhanced MG accumulation, we directly treated 3T3-L1 adipocytes with MG and examined the expression and phosphorylation of IR, IRS-1, and PI3K. As shown in Figure 4-5*A*, when the cells were treated with MG (20 μM), glucose uptake significantly decreased compared to the untreated cells ($n = 6$, $P < 0.05$). This MG-reduced glucose uptake in 3T3-L1 adipocytes was counteracted by NAC co-administration. No significant change in the protein expression of IR, IRS-1, or PI3K was observed in 3T3-L1 adipocytes after exposure to MG, MG-NAC, or NAC (600 μM) (data not shown).

However, the insulin-induced tyrosine phosphorylation of IRS-1 (Figure 4-5*B*)

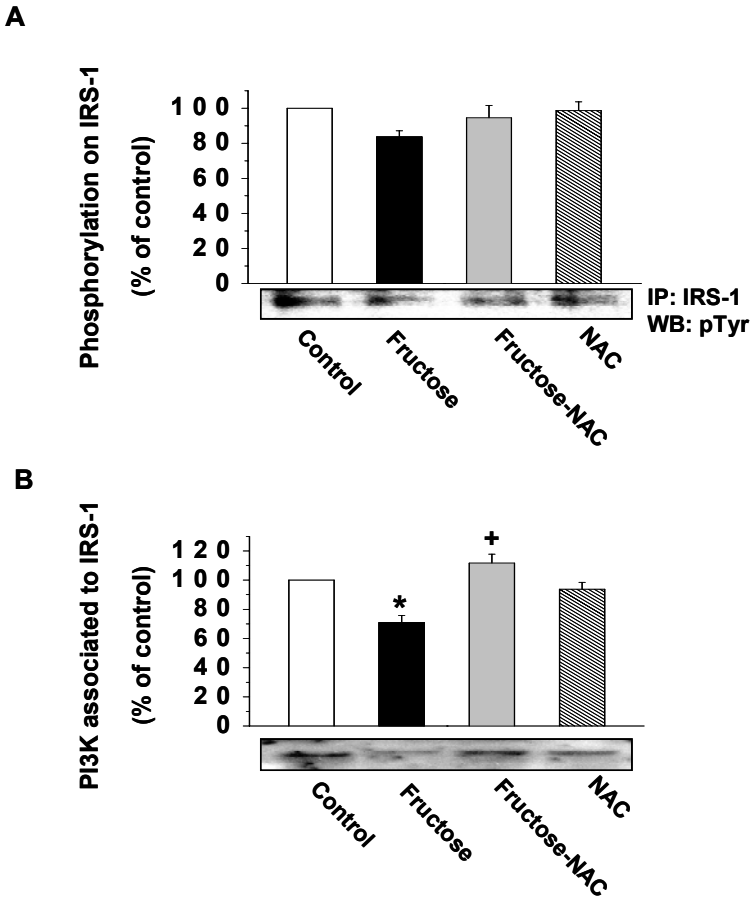


**Figure 4-4. The tyrosine phosphorylation of IRS-1 (*A*) and PI3K associated to IRS-1 (*B*) in adipose tissue of control, fructose, fructose–NAC or NAC treated rats.** Tissue lysates were subjected to immunoprecipitation (IP) with IRS-1 antibody. The immunoprecipitates were then subjected to Western blotting (WB) using anti-pTyr (***A***) or PI3K p85 antibody (***B***). The immunoreactivity levels were compared to the control levels of IRS-1 phosphorylation (***A***) or IRS-1 associated PI3K (***B***), respectively. *$P < 0.05$ vs. control rats, $^{+}$ $P < 0.05$ vs. fructose-fed rats, $n = 4$ for each group.

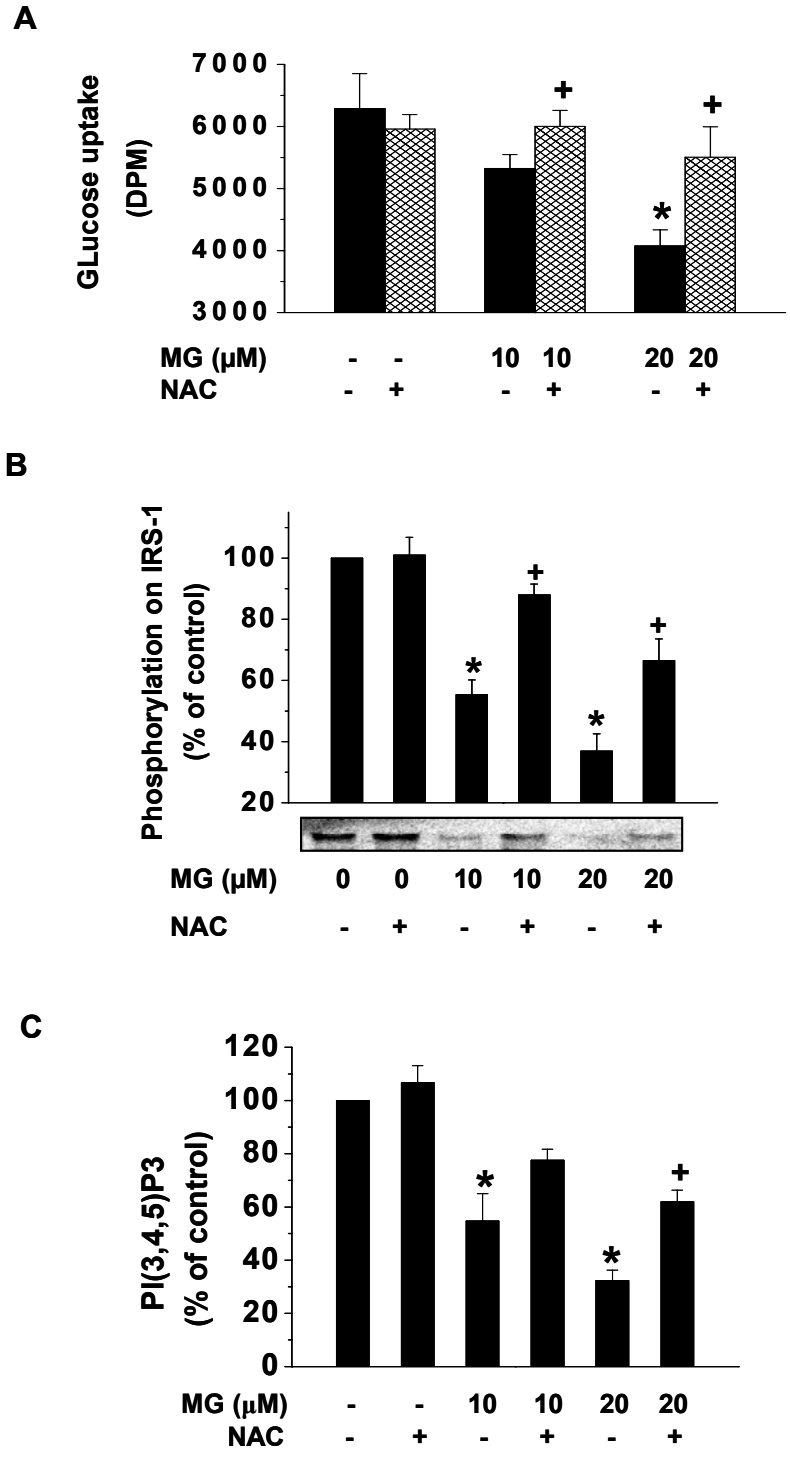
A
GLucose uptake (DPM)
7000
6000
5000
4000
3000
MG (μM) - - 10 10 20 20
NAC - + - + - +
B
Phosphorylation on IRS-1 (% of control)
100
80
60
40
20
MG (μM) 0 0 10 10 20 20
NAC - + - + - +
C
PI(3,4,5)P3 (% of control)
120
100
80
60
40
20
0
MG (μM) - - 10 10 20 20
NAC - + - + - +

**Figure 4-5. Effects of MG and/or NAC on insulin-induced glucose uptake (A), IRS-1 phosphorylation (B), and PI3K activity (C) in cultured 3T3-L1 adipocytes.** (***A***) The insulin-stimulated glucose uptake in cultured 3T3-L1 adipocytes after different treatments. The differentiated 3T3-L1 adipocytes were exposed to 100 nM insulin for 30 min and continuously incubated for another 20 min after the addition of [$^3$H]-2-DOG (0.1 μCi/500 μl) with glucose (50 μM) to the medium. The cell lysate was then transferred into scintillation vials for scintillation counting. (***B***) The cells were treated with or without MG, NAC, or MG plus NAC at the concentrations indicated. After IRS-1 protein was immunoprecipitated (IP), Western blotting (WB) was carried out using anti-phosphotyrosine (pTyr) as 1st antibody. (***C***) PI3K activity was measured by a competitive ELISA kit and presented as % of that from control rats. $^*P < 0.05$ vs. control cells, $^+P < 0.05$ vs. cells treated with same concentration of MG, $n = 6$ in A; $n = 3$ in B and C each group.

and PI3K activity (Figure 4-5*C*) were both impaired by MG treatment. The phosphorylation level on tyrosine residue of IRS-1 was inhibited significantly to 55.3 ± 4.9% or 36.9 ± 5.6% of the control levels by 10 or 20 μM MG treatments (Figure 4-5*B*) ($P < 0.05$, $n = 3$). As shown in Figure 4-5*C*, MG markedly decreased PI3K activity in 10 and 20 μM MG treated groups, which were also restored by NAC co-treatment ($P < 0.05$, $n = 3$).

## 4.3. Discussion

The increased level of MG observed in different insulin resistance states including diabetes and hypertension (McLellan et al., 1994; Wang et al., 2004) suggests an important role of MG in the development of insulin resistance. The main source of MG in mammals is anaerobic glycolysis. MG is also formed during the metabolism of acetone or aminoacetone from lipolysis or protein catabolism (Kalapos, 1999; Wu, 2006). Fructose, a precursor of MG, is metabolized by hexokinase or ketohexokinase to glyceraldehyde-3-phosphate and dihydroxyacetone phosphate, which can directly form MG. Recently, we reported that fructose significantly increased MG generation in cultured vascular smooth muscle cells in a concentration and time dependent manner (Wang et al., 2006). However, whether increased accumulation of endogenous MG induced by fructose treatment directly contributes to the development of insulin resistance is still unsettled.

In the present study, we observed increased MG accumulation in serum and in adipose tissue, as well as the development of insulin resistance in fructose-fed rats (Figures 4-1 and 4-2). In addition, we found a significant reduction of IRS-1/PI3K association in adipose tissue (Figure 4-4). To clarify the role of MG in the development

of insulin resistance, we directly treated 3T3-L1 adipocytes with MG and investigated the effect of MG on insulin signaling in these cells. Although the expression level of IR, IRS-1, and PI3K were not changed by MG treatment, reduced IRS-1 tyrosine phosphorylation and kinase activity of PI3K were observed in MG treated cells. Furthermore, MG treatment significantly reduced the insulin-stimulated glucose uptake by 3T3-L1 adipocytes (Figure 5-5*A*). These results indicated the direct inhibition of MG on insulin signaling in these cultured adipocytes. The inhibition of PI3K activity by MG was consistent with the decreased tyrosine phosphorylation on IRS-1. Moreover, MG-induced alterations in IRS-1 phosphorylation and PI3K activity were reversed by NAC, which further supports the role of MG in the impaired insulin-mediated glucose uptake in fructose-fed rats.

Since PI3K plays a pivotal role in the metabolic and mitogenic actions of insulin by specifically phosphorylating phosphatidylinositol substrates and producing second messengers to regulate glucose transport, the insulin induced tyrosine phosphorylation of IRS-1 and the activated PI3K are necessary for insulin signaling in different insulin sensitive tissues. Therefore, the impaired insulin-mediated glucose uptake in adipose tissue of fructose-fed rats is likely caused by the reduced IRS-1 phosphorylation and impaired IRS-1/PI3K association. Interestingly, enhanced PI3K expression was observed in fructose-fed rats (Figure 4-3), which seems inconsistent with the development of insulin resistance. However, this increased PI3K expression likely reflected the compensative response to the inhibited PI3K recruitment to IRS-1 in fructose-fed rats. The discrepancy between *in vivo* and *in vitro* studies on PI3K expression and IRS-1 phosphorylation observed in the present study suggests that other metabolic factors in

addition to MG accumulation, for instance, the autocrine control of insulin release may also play a role in the development of insulin resistance *in vivo*.

Given that MG and MG-derived AGEs can induce non-enzymatic modifications of various amino acid residues (e.g., Lys and Arg) that are generally present in the active sites of different insulin signaling proteins, MG-induced structural modifications of these proteins might also impair insulin signal transduction. Recently, a study suggested that MG might increase serine phosphorylation on IRS-1 in rat L6 myoblast cells (Riboulet-Chavey et al., 2006). However, direct interaction of MG with the IRS-1 and PI3K proteins needs to be further explored in future. Previous studies from our as well as other laboratories suggest that fructose or MG induces the formation ROS and reactive nitrogen species (Chang et al., 2005; Fukunaga et al., 2005; Wang et al., 2006) in cultured smooth muscle cells or rats, which may also play a role in the MG-impaired insulin signaling pathway.

In summary, our study demonstrated that elevation of endogenous MG level in fructose-fed rats reduced IRS-1/PI3K association and altered PI3K activity, which may lead to the decreased insulin-stimulated glucose uptake in adipose tissue and contribute to insulin resistance. Unraveling this new MG-mediated mechanism will help to better understand the pathogenic development of insulin resistance and related diseases.

# CHAPTER FIVE

## SCAVENGING METHYLGLYOXAL BY METFORMIN IMPROVED INSULIN RESISTANCE IN FRUCTOSE-TREATED RATS

### 5.1. Introduction

The three most important tissues that are involved in the pathogenesis of insulin resistance are skeletal muscle, liver and adipose tissues. Skeletal muscle constitutes the largest insulin-sensitive tissue in the body and is the primary site for insulin-stimulated glucose utilization. Due to their different physiological function in metabolism, these tissues showed different expression profile of insulin signaling genes/proteins under insulin resistance condition. In the previous chapter, effect of MG on the insulin signaling pathway in adipose tissue from fructose-treated rats was studied. Our earlier study also suggested that MG causes structural modification of the insulin molecule, reducing the biological function of insulin in cultured adipose cells. However, the question of whether or not an increase in endogenous MG accumulation induces a direct change in the insulin signaling pathway in insulin-target skeletal muscle remains largely unresolved. In the present study, the consequence of MG accumulation on insulin transduction in skeletal muscle was investigated.

In the present study, insulin resistance was induced in rats fed chronically with fructose, a precursor of MG. An increase in the formation of endogenous MG was observed in these fructose-treated rats, a condition associated with impairment of the insulin signaling pathway and the development of insulin resistance. When co-treated with metformin, a well known oral biguanide insulin sensitizer used for the management of type II diabetes, the alterations in these fructose-fed rats, including increased MG level,

decreased glucose uptake, and decreased or impaired IRS-1 and PI3K expression or activity, were markedly reversed. To further explore the mechanism for the action of MG, cultured skeletal muscle cells (L8 cells) were directly treated with MG in the absence or presence of metformin. The expression of IRS-1, PI3K and PKC at both mRNA and protein levels, along with IRS-1 phosphorylation status and PI3K activity, were investigated in the treated cells. Metformin is a well-known insulin sensitizer used for the management of type II diabetes. With a guanidine structure, it has a potential inhibitive effect on protein glycation. Finally, whether the metformin-induced insulin-sensitizing effect, as observed in fructose-fed rats or MG-treated cells, is due to antagonism of MG or to MG sequestration was explored *in vitro* using mass spectrometry.

## 5.2. Results

### 5.2.1. The development of insulin resistance in fructose-fed rats

After 9 weeks' treatment with fructose, the rats showed a significant increase in plasma triglyceride levels (Table 5-1), serum insulin (Figure 5-1*A*), and enhanced blood pressure (data not shown). As shown in Figure 5-1*A*, the serum insulin level was enhanced significantly from 2.80±0.12 μg/L in the control group to 4.87±0.18 μg/L in fructose-fed group. Likewise, plasma triglyceride increased from 0.35 ± 0.04 mM to 0.84 ± 0.05 mM by fructose feeding (Table 5-1). However, total cholesterol, HDL-cholesterol and blood hemoglobin A1C in plasma were not changed (Table 5-1). In all groups of rats treated with or without MG and/or metformin, the fasting blood glucose level was maintained at 5-6 mM. At the end of the 9 week treatment, IPGTT was performed and a notable difference was observed in metformin-treated rats, compared with the control rats

**Table 5-1. Biochemical parameters of control or fructose/metformin treated rats.**

| **Tests** | **Control** (n=7) | **Fructose** (n=10) | **Fructose-metformin** (n=8) | **Metformin** (n=4) |
|---|---|---|---|---|
| Total cholesterol (mM) | 0.85 ± 0.09 | 0.88 ± 0.07 | 0.77 ± 0.1 | 0.70 ±0.07 |
| Triglyceride (mM) | 0.35 ± 0.04 | 0.84 ± 0.05* | 0.72 ± 0.06 | 0.16 ±0.03*+ |
| HDL-cholesterol (mM) | 0.77 ± 0.07 | 0.66 ± 0.06 | 0.63 ± 0.04 | 0.61 ± 0.08 |
| Hemoglobin A1C (mM) | 4.3 ± 0.21 | 4.4 ± 0.07 | 4.41 ±0.16 | 4.6 ±0.16 |

* $P<0.05$ vs. control, $^{+}P<0.05$ vs. fructose-treated group

($p<0.05$, n=4 for metformin treated group, n=7 for other groups; Figure 5-1*B*).

A decreased insulin-stimulated glucose uptake in insulin targeted tissues has been identified as being a key indicator of insulin resistance (Matthaei et al., 2000). We observed that the insulin-induced glucose uptake by abdominal adipose tissue dropped dramatically in fructose-fed rats, in comparison with that from untreated control rats ($P<0.05$). With insulin (100 nM) stimulation, as shown in Figure 5-1*C*, glucose uptake by adipose tissue is 198% in the control group (n=6), and 117% in fructose-fed rats (n=6, $p<0.05$), of the basal glucose uptake without insulin stimulation. Similarly, insulin-stimulated glucose uptake was reduced significantly in cultured L8 cells after a 48 h treatment with MG (30 μM), in comparison with control cells ($P<0.05$, n=6 for each group, Figure 5-1*D*). The lowered glucose uptake in adipose tissue induced by fructose feeding, or in MG-treated L8 cells, was restored significantly by co-treatment with metformin (Figures 5-1*C* and 1*D*).

### 5.2.2. Increased endogenous accumulation of MG or related AGEs in fructose-fed rats or MG-treated cells

A 9-week fructose feeding caused a significant increase in MG concentration in SD rats. A dramatic increase in MG formation of more than 2-fold was observed in skeletal muscle, from 2.32 μmol/g protein in the untreated group to 6.98 μmol/g protein in the fructose-treated group ($p<0.01$, n=4, Figure 5-2*A*). In comparison with untreated rats, MG levels were also increased from 1.8 to 3.29 μM in serum ($p<0.01$, n=4, Figure 5-2*B*). The increased endogenous MG accumulation was abolished by metformin co-treatment in skeletal muscle as well as in serum (Figure 5-2*A* and *B*).

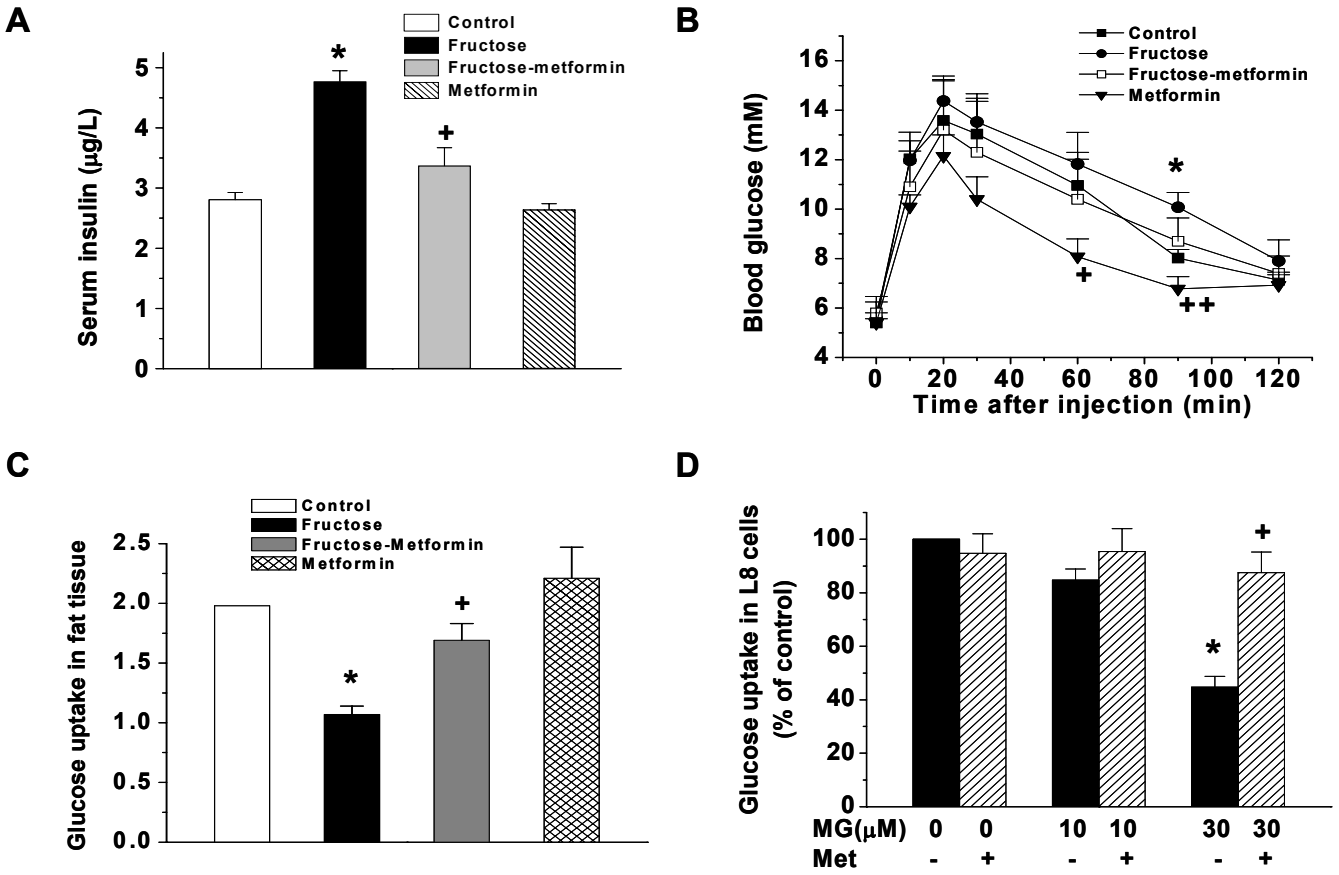
A
Control
Fructose
Fructose-metformin
Metformin
Serum insulin (μg/L)
0
1
2
3
4
5
*
+
B
Control
Fructose
Fructose-metformin
Metformin
Blood glucose (mM)
4
6
8
10
12
14
16
0
20
40
60
80
100
120
Time after injection (min)
*
+
++
C
Control
Fructose
Fructose-Metformin
Metformin
Glucose uptake in fat tissue
0.0
0.5
1.0
1.5
2.0
2.5
*
+
D
Glucose uptake in L8 cells
(% of control)
0
20
40
60
80
100
*
+
MG(μM) 0 0 10 10 30 30
Met - + - + - +

**Figure 5-1. Effects of fructose, MG, and metformin on the development of insulin resistance.** ***A.*** Serum insulin levels in rats treated with fructose (n=10), fructose plus metformin (n=8), or metformin (n=4), respectively. *P<0.05 vs. control rats (n=7); $^{+}$P<0.05 vs. fructose-fed rats. ***B***. Glucose tolerance test. *P<0.05 vs. control rats; $^{+}$P<0.05 or $^{++}$P<0.01 vs. fructose-fed rats. ***C***. Insulin-stimulated glucose uptake by adipose tissues from different treated rats. *P<0.05 vs. control rats; $^{+}$P<0.05 vs. fructose-fed rats. ***D***. Insulin stimulated glucose uptake in cultured skeletal muscle cells (L8) treated with or without MG, metformin (100 μM) or MG plus metformin (100 μM). *P<0.05 vs. control cells; $^{+}$P<0.05 vs. MG-treated cells. n=6 in each group.

Using immunohistochemical staining and Western blotting analysis, we further investigated whether or not MG-induced changes in AGEs vary in skeletal muscle cells from different treated groups. Figure 5-2*C* indicated enhanced AGE formation in L8 cells after 48 h treatment with MG (10 or 30 μM), as shown by a significant increase in the levels of CEL. Co-treatment with metformin reduced MG-induced AGE formation, compared with that in cells treated with MG alone (Figure 2*C*).

### 5.2.3. Effects of fructose and metformin on the expression of insulin signaling molecules in skeletal muscle

To investigate the effects of fructose and metformin on the insulin signaling pathway, mRNA expression of IR, IRS-1, and PI3K in skeletal muscle from different treated groups of rats was examined using quantitative real time-PCR. As shown in Figure 5-3, the mRNA levels for IRS-1 and PI3K were decreased, to 78.6±3.1% (n=7, $P<0.05$) and 61.6± 3.1% (n=7, $P<0.05$), respectively, in skeletal muscle from fructose-fed rats when compared with untreated control rats (n=4). The reduction in IRS-1 and PI3K expression was significantly reversed when the rats were co-treated with metformin (Figure 5-3). There were no significant changes in mRNA levels of IR observed among untreated, fructose-fed, and fructose-metformin co-treated rats. The 9 week treatment with metformin alone increased mRNA level of PI3K but had no effect on IR and IRS-1 mRNA levels in skeletal muscle.

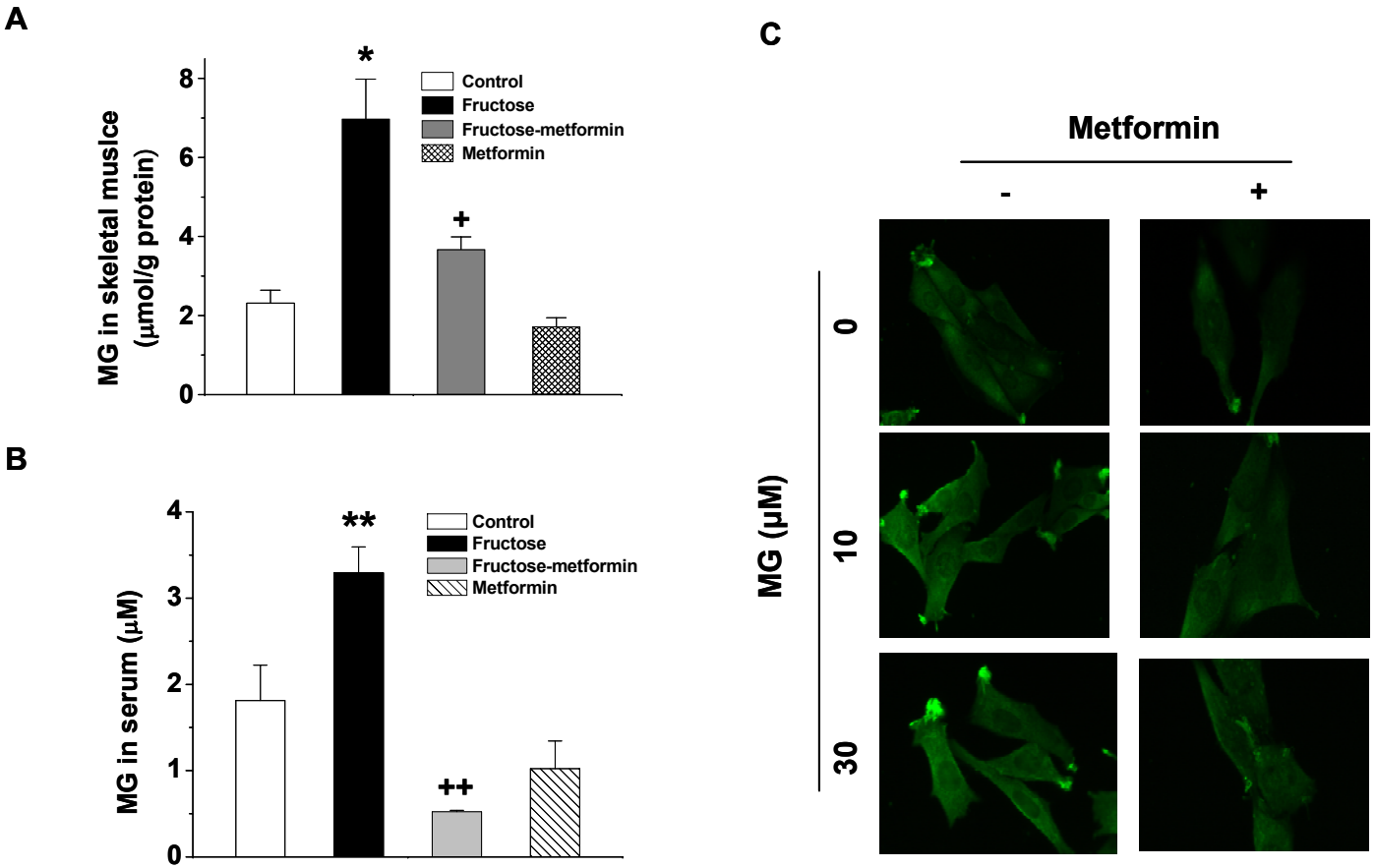
A
MG in skeletal muslce (μmol/g protein)
0
2
4
6
8
*
+
Control
Fructose
Fructose-metformin
Metformin
B
MG in serum (μM)
0
1
2
3
4
**
++
Control
Fructose
Fructose-metformin
Metformin
C
Metformin
-
+
MG (μM)
0
10
30

**Figure 5-2. Formation of MG/AGEs in different treated rats or L8 cells.** MG levels in skeletal muscle (***A***) and serum (***B***) of control, fructose treated, metformin treated and fructose-metformin co-treated rats. **P<0.01 vs. control rats; **P*<0.05 vs. control rats; $^{++}P$<0.01 vs. fructose-fed rats; $^{+}P$ <0.05 vs. fructose-fed rats. n=4 for each group. ***C.*** L8 cells seeded on cover glass slips were treated with MG (10-30 μM) for 48 h and stained with mouse anti-CEL antibody. More positive staining appeared in MG-treated cells and MG-induced CEL formation was inhibited by co-applying metformin (100 μM).

### 5.2.4. Effects of MG and metformin on IRS-1 phosphorylation and PI3K activity in skeletal muscle cells

To investigate whether the MG treatment impaired insulin resitance by changing the function of IRS-1, the insulin-dependent tyrosine phosphorylation of IRS-1 was examined after MG/metformin treatment. Tyrosine phosphorylation in IRS-1 decreased to 76.6% of the control level with 30 μM MG treatment (Figure 5-4*A*), but it was restored by co-administration of metformin. However, it appears that metformin alone does not alter IRS-1 phosphorylation in L8 cells. In addition, we found a reduction in the kinase activity of PI3K (Figure 5-4*B*). The activity of PI3K (indicated as the concentration of PI(3,4,5)P3 was decreased after 48 h treatment with MG at both 10 and 30 μM concentrations. Co-treatment with metformin improved PI3K activity in the (10 μM) MG-treated group.

### 5.2.5. Identification of metformin-MG adducts

We used mass spectrometry to investigate the formation of guanidine-MG adducts following incubation of metformin with MG for 24 h. The positive-ion ESI-MS spectrum of an unreacted metformin (25 μM) solution contains only one significant peak (*m/z* 130) corresponding to the $[M+H]^+$ or protonated molecular ion of metformin (Figure 5-5*A*-a). In contrast, the ESI mass spectrum of the incubate (25 μM MG + 25 μM metformin) contains several peaks (Figure 5-5*A*-b), the most abundant of which (*m/z* 202) corresponds to the $[M+H]^+$ ion resulting from direct addition of MG (72 Da) to metformin (Figure 5-6). This reaction is analogous to the formation of CEL upon reaction

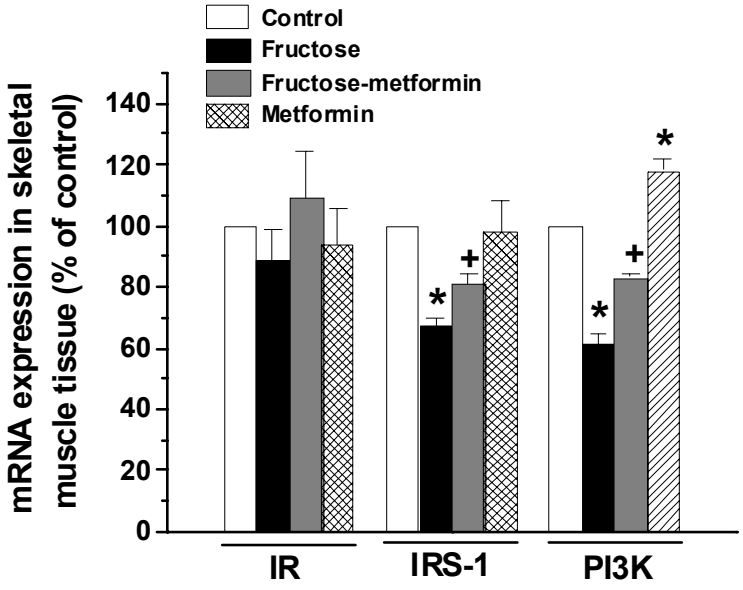


**Figure 5-3. Expression of IR, IRS-1, and PI3K in in skeletal muscle from different treated rats.** After 9 weeks treatment of fructose or/and metformin, skeletal muscle was frozen and total RNA was extracted. The mRNA expression of IR, IRS-1 and PI3K was determined using real-time PCR. *$P$<0.05 vs. control rats, $^{+}P$<0.05 vs. fructose-fed rats. n=4 for control group, and n=7 for fructose or fructose-metformin treated group, n=3 for metformin treated group.

A

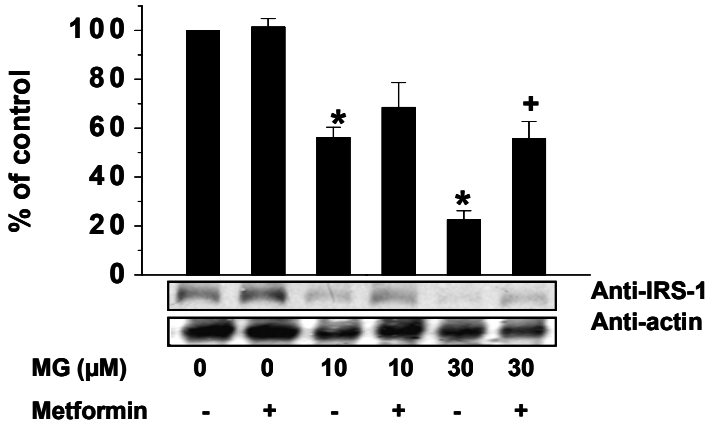
100
80
60
40
20
0
% of control
*
*
+
Anti-IRS-1
Anti-actin
MG (μM) 0 0 10 10 30 30
Metformin - + - + - +

B

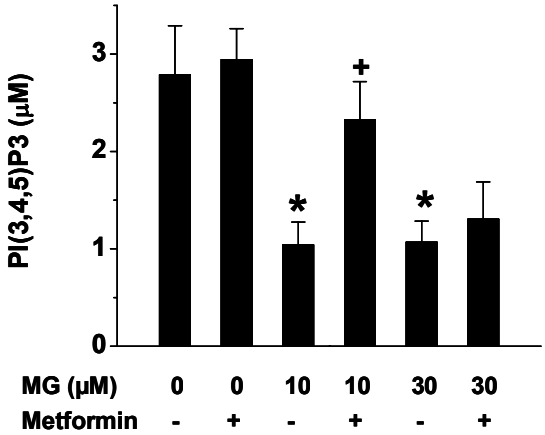
3
2
1
0
PI(3,4,5)P3 (μM)
*
+
*
MG (μM) 0 0 10 10 30 30
Metformin - + - + - +

**Figure 5-4. Effects of MG and/or metformin on IRS-1 and PI3K in L8 cells.** After treatment with or without MG (10 or 30 μM) in the absence or presence of metformin (100 μM) for 48 h, the L8 skeletal muscle cells were exposed to 100 nM insulin for 10 min. IRS-1 phosphorylation (***A***) was investigated by immunoblotting (WB) experiment using rabbit a anti-IRS-1 antibody as the primary antibody. **P*<0.05 vs. control cells, $^{+}$*P*<0.05 vs. MG-treated cells. ***B.*** The PI3K activity was evaluated using a competitive ELISA kit. The activity of PI3K was proportional to the production of $PI(3,4,5)P_3$. **P*<0.05 vs. control cells, $^{+}$*P*<0.05 vs. MG-treated cells. n=3-4 for each group.

of MG with the primary amino group of a lysine side chain (Ahmed et al., 2002). The product ion MS/MS spectrum of this compound (Figure 5-5*B*-b) contains fragments corresponding to metformin (*m/z* 130) and to the neutral loss of water (*m/z* 184) and of MG bound to an amino group (*m/z* 113), confirming its identity as a 1:1 metformin:MG adduct.

However, the heaviest ion observed in the incubate ESI-MS spectrum (Figure 5-5A-b) corresponds to the addition of two MG molecules to a single molecule of metformin (*m/z* 274). This is consistent with the ability of metformin to form tautomeric structures (Figure 5-6) that contain two primary amino groups capable of forming adducts with MG, and which are stabilized by conjugation of the rearranged C=C bonds. The identity of this 1:2 metformin:MG adduct is again confirmed by the product ion MS/MS spectrum (Figure 5-5*B*-c), which contains fragments corresponding to loss of water and $CO_2$ (*m/z* 256 and 230, respectively) from either or both of the attached MG moieties, and to sequential loss of MG (*m/z* 202) and water (*m/z* 184) from the molecular ion, as well as metformin itself (*m/z* 130). Other ions observed in the incubate ESI-MS spectrum (Figure 5-5*A*-b) arise from the reaction of MG with certain metformin tautomers to form the cyclic condensation product triazepinone (*m/z* 184), a reaction analogous to that between MG and the side chain of arginine (Ahmed and Thornalley, 2002). Subsequent addition of a second MG molecule to the terminal primary amino group gives rise to a triazepinone : MG adduct (*m/z* 256). MS/MS spectra serve to differentiate between incubation products based upon metformin and triazepinone, the former (Figure 5-5*B*-b and c) containing metformin (*m/z* 130) as a significant product ion, whereas the latter (Figure 5-5*B*-a) contain characteristic product ions, such as those corresponding to

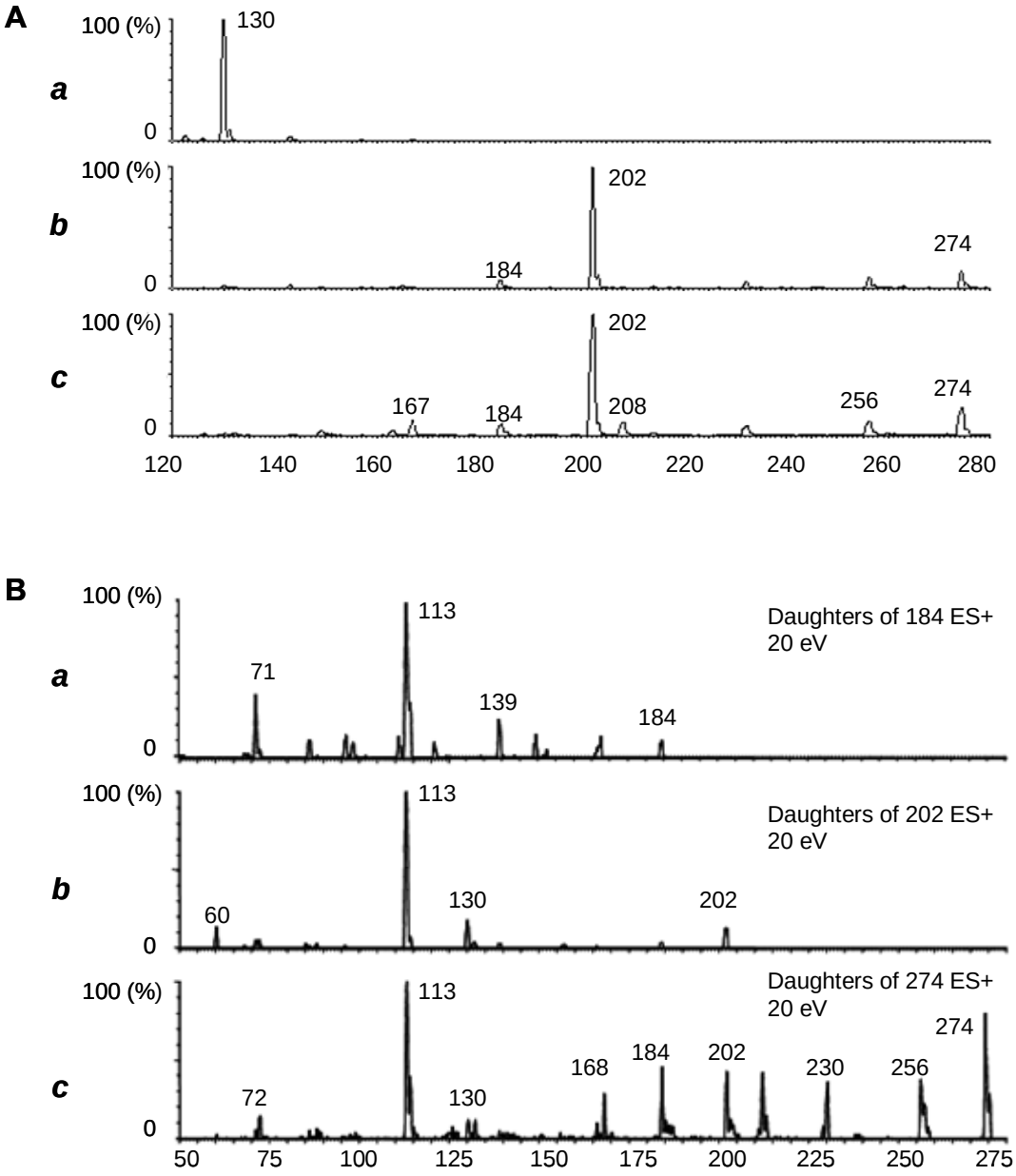
A
100 (%)
a
130
0
100 (%)
b
202
184
274
0
100 (%)
c
202
167
184
208
256
274
0
120 140 160 180 200 220 240 260 280
B
100 (%)
a
113
71
139
184
Daughters of 184 ES+
20 eV
0
100 (%)
b
113
60
130
202
Daughters of 202 ES+
20 eV
0
100 (%)
c
113
72
130
168
184
202
230
256
274
Daughters of 274 ES+
20 eV
0
50 75 100 125 150 175 200 225 250 275

**Figure 5-5. Identification of metformin-MG adducts by ESI-MS. *A.*** Normalized positive ion ESI mass spectra of (**a**) 25 μM metformin solution, (**b**) incubate of 25 μM metformin with 25 μM methylglyoxal (MG) in 0.2 M sodium phosphate buffer, and (**c**) 42-fold dilution of incubation products in 50:50 v/v water/acetonitrile containing 0.1% formic acid. ***B.*** Product-ion tandem mass (MS/MS) spectra obtained by collision-induced dissociation (CID) of the incubation products (**a**) triazepinone (*m/z* 184), (**b**) the 1:1 metformin: MG adduct (*m/z* 202), and (**c**) the 1:2 metformin:MG adduct (*m/z* 274). The "daughter ions" in ***B*** refer to the fragment ions produced by collision-induced dissociation of MG-metformin ions in ***A***.

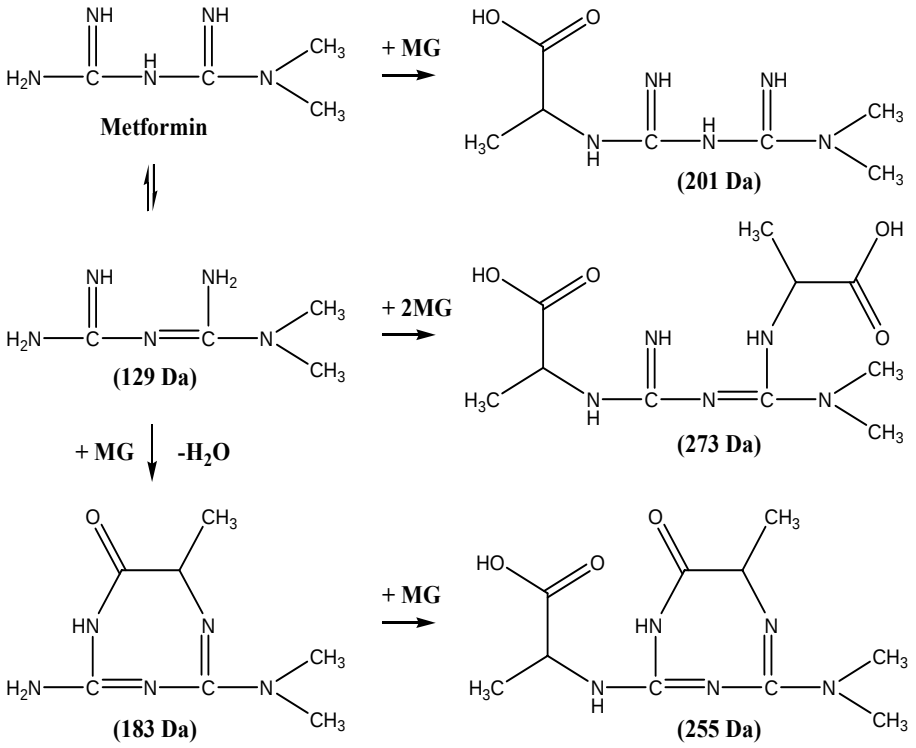


**Figure 5-6.** Incubation products of metformin and MG.

neutral loss of ammonia (*m/z* 167) and dimethylamine (*m/z* 139), that are consistent with a stabilized cyclic triazepinone structure (Figure 5-6).

## 5.3. Discussion

The results of our present study suggest that the endogenous accumulation of MG is associated with impaired insulin signaling and the development of insulin resistance in fructose-fed rats. The altered mRNA expression of IRS-1 and PI3K in skeletal muscle of fructose-fed rats, combined with a reduction in the levels, activities and phosphorylation of IRS-1 and PI3K proteins in MG-treated skeletal muscle cells, supports the hypothesis that MG plays an important role in the development of insulin resistance. Our data show that metformin not only reduced MG levels but also prevented the formation of MG-induced AGEs, while protecting insulin signaling molecules against MG-induced damage in both fructose-fed rats and MG-treated skeletal muscle cells. Using mass spectrometry, we also confirmed that metformin combines readily with MG to form stable products that effectively sequester MG, preventing it from reacting with insulin signaling molecules that may be present *in vivo*.

It has been shown that a diet high in fructose or sucrose can induce insulin resistance, although the mechanism is not yet fully understood (Hallfrisch et al., 1983; Reiser et al., 1989). The main source of MG in mammals is anaerobic glycolysis (Koop and Casazza, 1985; Lyles and Chalmers, 1992). MG is also formed during lipolysis and protein catabolism (Lyles and Chalmers, 1992; Yu et al., 2003). Like glucose, fructose is a monosaccharide and a precursor of MG. In the present study, after 9 weeks of fructose treatment, SD rats developed insulin resistance with decreased glucose uptake,

hyperinsulinemia, high blood pressure, and high triglyceride, which is consistent with previous reports. However, we observed a significant increase in MG accumulation in skeletal muscle from the rats fed with fructose as well as other tissues, including plasma and adipose (Figure 2*A*, 2*B*). This increased MG level coincides with the suppression of IRS-1 and PI3K mRNA levels in skeletal muscles from fructose-treated rats (Figure 3). The direct inhibitive effect of MG on the insulin signaling molecules was further confirmed in cultured skeletal muscle cells. Consistent with our animal study, when the cells were treated with MG concentrations of 10 or 30 μM for 48 h, significant reduction in IRS-1 phosphorylation and in the kinase activity of PI3K were observed in these MG-treated L8 cells (Figure 5-4). Our results suggest that increased MG accumulation in fructose-fed rats might not be just a concurrent phenomenon, but likely a causative factor for the development of insulin resistance. It was reported recently that insulin signaling was induced by MG treatment in cultured skeletal muscle cells (Riboulet-Chavey et al., 2006). In that study, 2.5 mM MG treatment reduced insulin-stimulated glucose transport by decreasing phosphorylation on IRS-1 and Erk proteins. Given that MG concentrations of 500 μM have been used to study MG-induced apoptosis in Jurkat cells (Du et al., 2001a; Du et al., 2000), however, one should not exclude the possibility that, with concentrations in the milimolar range, MG-induced apoptosis may be involved in the decreased phosphorylation of IRS-1 and ERK proteins. Indeed, we have observed that the percentage of cells undergoing apoptosis is significantly higher in cells treated with 100 μM MG, though not with 10 μM MG (unpublished data). According to our observations, and previous reports (Nagaraj et al., 2002), the plasma concentration of MG is less then 5

μM in normal adult SD rats. Hence, the concentrations of MG (10-30 μM) used to treat cultured cells in our present study may be considered pathophysiologically relevant.

It has been found that MG modifies proteins by reacting with arginine or lysine residue. Since these reactions usually occur as a time-dependent chronic reaction, it was believed that MG only modifies proteins with long half lives, such as albumin or certain structural proteins. However, our previous study indicated that MG can also modify the insulin molecule and impair its biological function (Jia et al., 2006). The recent discovery that MG modifies transcriptional co-repressor protein mSin3A also suggests a potential role for MG in modifying key transcription-related proteins and hence, regulating gene expression (Yao et al., 2006). It is not clear, however, which particular molecule(s) in the insulin signaling pathway have been modified by MG. Theoretically, MG could interact with insulin signaling molecules at many potential steps, modifying IR, IRS-1, PI3K and/or other downstream molecules. Although arginine and lysine residues are considered the main targets for MG, and are widely distributed in many proteins, modification by MG appears to be quite specific (Jana et al., 2002; Poggioli et al., 2002; Yao et al., 2006), depending, at least in part, on the conformation of the protein.

In this study, we used metformin to treat fructose-fed rats or MG-treated L8 cells, since decreased plasma levels of MG have been reported in type 2 diabetes patients following treatment with metformin (Beisswenger et al., 1999; Ruggiero-Lopez et al., 1999; Tanaka et al., 1999). A similar inhibitive effect of metformin on the MG levels in serum and skeletal muscle was observed in our fructose-fed rats. In addition, we observed that the administration of metformin inhibited the formation of MG-induced AGEs, including MG-glycated lysine and MG-glycated arginine residues (Figure 5-2C), while

greatly improving insulin-stimulated glucose uptake (Figure 5-1). Moreover, the altered expression of IRS-1 and PI3K, and decreased IRS-1 phosphorylation and PI3K activity induced by MG were markedly reversed by metformin treatment in fructose-treated rats or MG-treated cells (Figure 5-3 and 5-4). Although the mechanism of metformin action remains somewhat controversial, different studies have shown it to be an insulin sensitizer (Bailey and Turner, 1996; Cleasby et al., 2004; Lord et al., 2003; Santos et al., 1997; Stith et al., 1996), whether or not this activity depends upon its MG-reducing capabilities is unclear. One *in vitro* study suggests that metformin acts as a scavenger of MG, due to its reaction with MG to form guanidine-dicarbonyl adducts (Brownlee et al., 1986). A 1:1 metformin-MG adduct (202 Da) was also observed in our MS experiments, confirming the existence of the guanidine-dicarbonyl adduct reported previously (Brownlee et al., 1986). In addition, our ESI-MS and MS/MS experiments (Figure 5-5) identified a stable 1:2 metformin:MG adduct (274 Da), with additional peaks (256 and 230 Da) corresponding to loss of water and $CO_2$ respectively, from either or both of the attached MG moieties. These results clearly demonstrate the MG-scavenging capabilities of metformin, under experimental conditions. Indeed, the almost complete disappearance of metformin from the full scan MS spectrum upon addition of MG (Figure 5-5*A*) suggests that most of the metformin is converted to various incubation products. Furthermore, all of the ions observed in the undiluted incubate are present in the ESI-MS spectrum of a (42-fold) diluted incubate (Figure 5-5*A*-c), showing that these reaction products can be formed at physiologically relevant concentrations. Taken together, our results show that metformin combines readily with 1 or 2 mole equivalents of MG to form stable products that effectively sequester MG, preventing it from reacting with

proteins and other molecules that may be present *in vivo*. The propensity of metformin to form stable adducts with MG is consistent with this drug's effectiveness in treating insulin resistance and type 2 diabetes.

In conclusion, the MG-induced impairment of insulin signaling observed in this study may help us to better understand the pathogenic development of insulin resistance and diabetes. Furthermore, the simultaneous attenuation of insulin resistance and MG levels by metformin indicates that the MG-sequestrating capability of metformin could directly contribute to its insulin sensitizing effect.

# CHAPTER SIX

## METHYLGLYOXAL MEDIATES ADIPOCYTE PROLIFERATION AND CONTRIBUTES TO THE DEVELOPMENT OF OBESITY

### 6.1. Introduction

MG, a reactive dicarbonyl compound, is mainly created by glycolysis and lipolysis (Kalapos, 1999; Kalapos, 2007a; Kalapos, 2007b). It interacts readily with certain free amino acid residues in proteins and forms AGEs (Monnier and Cerami, 1981). MG-induced ROS (Chang et al., 2005; Chang and Wu, 2006; Pi et al., 2007) and MG-derived protein modifications (Riboulet-Chavey et al., 2006; Shamsi et al., 1998) have been addressed as possible cause factors for insulin resistance *in vitro* or *in vivo*. Moreover, increased accumulation of MG and AGEs were observed in diabetic (Beisswenger et al., 2005; Wang et al., 2007a; Wang et al., 2004) and hypertensive (Vasdev et al., 1998; Wang et al., 2004; Wu and Juurlink, 2002) animals and patients. For this reason, alagebrium, an AGE breaker, has been clinically tested to treat hypertension and cardiovascular diseases by reversing this mechanism of aging (Coughlan et al., 2007).

As the most common cause of hypertension and diabetes, obesity is well recognized as a result of excessive consumption of dietary fat and carbohydrates, which are both precursors of MG and AGEs. The association between obesity and diabetes and hypertension led us to postulate a possible role of MG in the development of obesity. The development of obesity involves both adipocyte hypertrophy (increased size of adipocyte) and hyperplasia (increased adipocyte number) (Gregoire, 2001; Hausman et al., 2001). While imbalanced energy intake-induced adipocyte hypertrophy contributes to the

typically adult-onset obesity, the development of hyperplastic adipose tissue is thought to be mainly associated with the obesity in children (Ebbeling et al., 2002; Hager et al., 1977). However, proliferation of adipocytes is also observed in adult obesity. Recently, the role of PI3K/Akt pathway and its downstream effectors in adipogenesis especially the proliferation of pre-adipocytes (Chuang et al., 2007; Fajas et al., 1998; Graff et al., 2000; Menghini et al., 2005; Rosen et al., 2000; Zhou et al., 2001), has been recognized. It has been found that Akt phosphorylates p27 and p21(Cdk inhibitors), prevents the localization of these proteins to nucleus, and thus attenuates their inhibitory effect on Cdk2 and the cell cycle progression from $G_1$ to S phase (Bhattacharya and Ullrich, 2006; Naaz et al., 2004; Peng et al., 2003). Loss of Cdk inhibitors produces adipocyte hyperplasia and obesity (Naaz et al., 2004). In addition, the degradation of Akt is also required for the cellular transition from quiescence to the proliferative state.

Inhibitory effect of MG on cell growth has been extensively reported (Cantero et al., 2007; Kani et al., 2007; Ota et al., 2007). In the present study, we hypothesized that MG stimulates adipocyte proliferation through the PI3K/Akt pathway. To investigate this hypothesis, we first compared the MG levels in obese and normal patients and rats. The effects of MG on Akt signaling and cell proliferation were further examined in cultured adipocytes (3T3-L1 cells). Our results suggest that increased MG accumulation may induce adipocyte proliferation and differentiation by stimulating Akt activity, and thus contributes to the development of obesity.

## 6.2. Results

### 6.2.1. Increased MG accumulation in obese patients

There was no difference between the age and sex distribution in the obese and non-obese patient groups. The body weight of non-obese and obese group was 73.78±2.70 kg and 98.31±7.38 kg, respectively. The mean BMI value for non-obese group and obese group was 25.23±1.05 and 33.5±3.0, respectively. The mean plasma MG level in obese patients was 3.5 ±0.4 μM, which was significantly higher than that of the non-obese group (2.1 ±0.1 μM). Correlation analysis indicated a strong correlation between plasma MG level and BMI value ($r$=0.606, $P$=0.0046, Figure 6-1).

### 6.2.2. MG stimulated proliferation of cultured adipose cells

To investigate whether MG induces the proliferation of adipose cells, we carried out cell proliferation assay with or without MG treatment. The result showed that 5, 10 and 20 μM MG significantly increased the proliferation rate of 3T3-L1 cells to 115±2.1%, 126±3.6% and 119±3.3% of the untreated cells ($P$<0.05 *vs.* Control; n=48 in each group, Figure 6-2*A*). The co-treatment with Akt inhibitor SH-6 (10 μM) or the AGE breaker alagebrium (50 μM) alleviated the cell proliferation induced by MG (10 μM) to the control level (Figure 6-2*B*).

The effect of MG on cell proliferation was further confirmed by the cell cycle phase distribution after MG treatment (Figure 6-3). Comparing the cell number in $G_1$, S and $G_2$ cell phase at different time points, we found that the MG-treatment lead to a faster cell cycle progression (Figure 6-3*A*), which represented as increased cell number in S phase after 16 or 20 h of MG (10 μM) treatment (Figure 6-3*A*-*b*) and increased cell number in $G_2$ phase after exposure of cells to MG (10 μM) for 20 h (Figure 6-3*A*-*c*). The

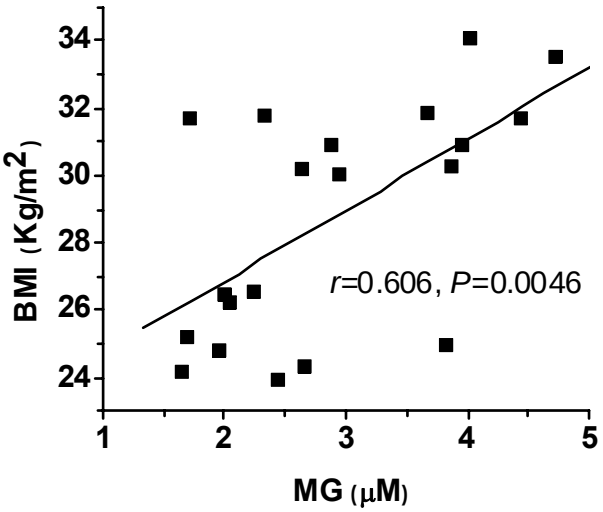


**Figure 6-1. Plasma MG concentration is closely correlated to BMI value of patients**

Blood samples were obtained from 20 untreated patients with mild to moderate hypertension from the clinical research units at Sacré-Coeur Hospital and at Hôtel-Dieu Hospital in Montreal. The body mass index (BMI) =body weight in kg/ square of the height in meter, $r$=0.606, $P$=0.0046.

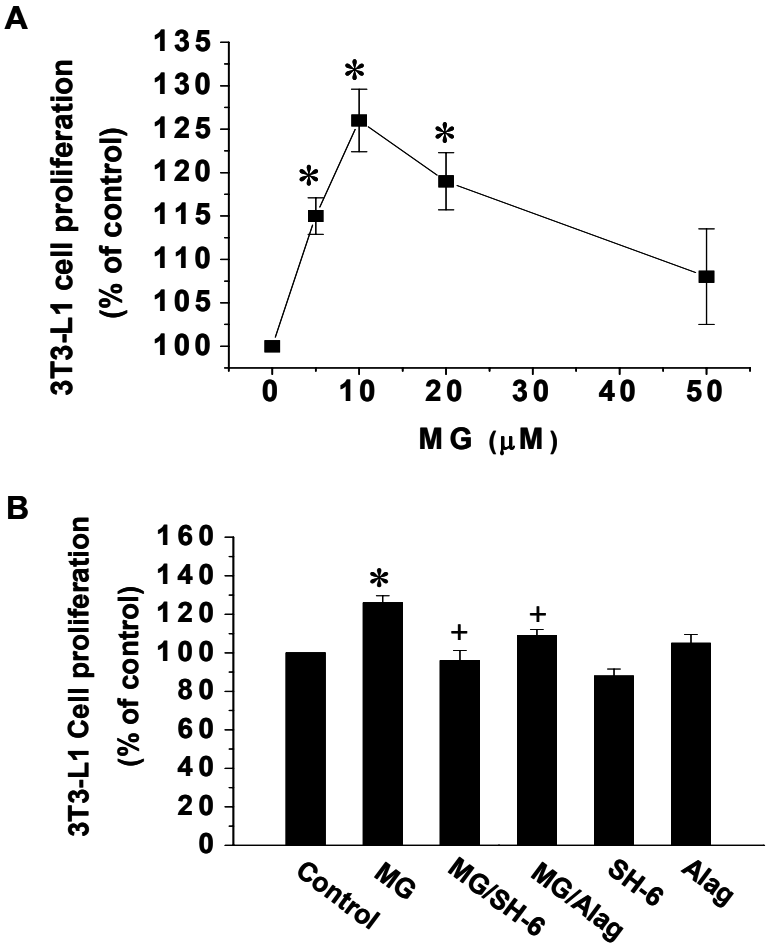
A
3T3-L1 cell proliferation
(% of control)
135
130
125
120
115
110
105
100
0
10
20
30
40
50
MG (μM)
*
*
*
B
3T3-L1 Cell proliferation
(% of control)
160
140
120
100
80
60
40
20
0
*
+
+
Control
MG
MG/SH-6
MG/Alag
SH-6
Alag

**Figure 6-2. The effect of MG, SH-6 or alagebrium on 3T3-L1 cell proliferation.** The proliferation of 3T3-L1 cells was determined by using a Celltiter 96® non-radioactive cell proliferation assay kit. The relative cell proliferation of each group was presented as the ratio between arbitrary absorbance on 570 nm of each group and that from the control group without treatment. The effect of different MG concentrations on cell proliferation was shown in (***A)*** and the effect of 10 μM MG with/without SH-6 and alagebrium was shown in (***B)***. **P*<0.05 *vs* control cells; $^{+}$*P*<0.05 *vs* MG treated cells; n=48 in each group.

co-administration of SH-6 (10 μM) significantly reversed the effect of MG on cell cycle progression in S and $G_2$ phases (Figure 6-3*B-b, c*).

### 6.2.3. Effect of MG on the expression and activity of Akt and its downstream effectors

As Akt plays an important role in regulating cell growth by phosphorylating p21 and p27 (Zhou et al., 2001), we further examined the effect of MG on phosphorylation and expression of Akt and its targeted effectors p21 and p27 (Figure 6-4). After treating 3T3-L1 cells with MG (10 μM) and/or SH-6 (10 μM)/alagebrium (50 μM) for 24 h, increased levels of phospho-Akt (p-Akt) as well as phospho-p21 (p-p21) and phospho-p27 (p-p27) were observed (Figure 6-4-*A*, *B*). The co-administration of SH-6 or alagebrium significantly prevented the phosphorylation of Akt, p21 and p27 induced by MG. Furthermore, the expression of p21 protein was attenuated in cells co-treated with SH-6 or alagebrium ($P<0.05$ *vs* MG-treated cells, n=3). However, the expression of p27 protein was not affected by MG treatment.

In another group of experiments, we examined the effect of MG on Cdk2 activity in 3T3-L1 cells. As shown in Figure 6-6*C*, after the cells were treated with MG (10 μM) for 24 h, the activity of Cdk2 was increased to 4 fold of the control level. The increased Cdk2 activity was reversed by co-administration of either SH-6 or alagebrium. However, there was no significant change in the protein levels of Cdk2 in the cells treated with or without MG (10 μM) for 24 h (data not shown).

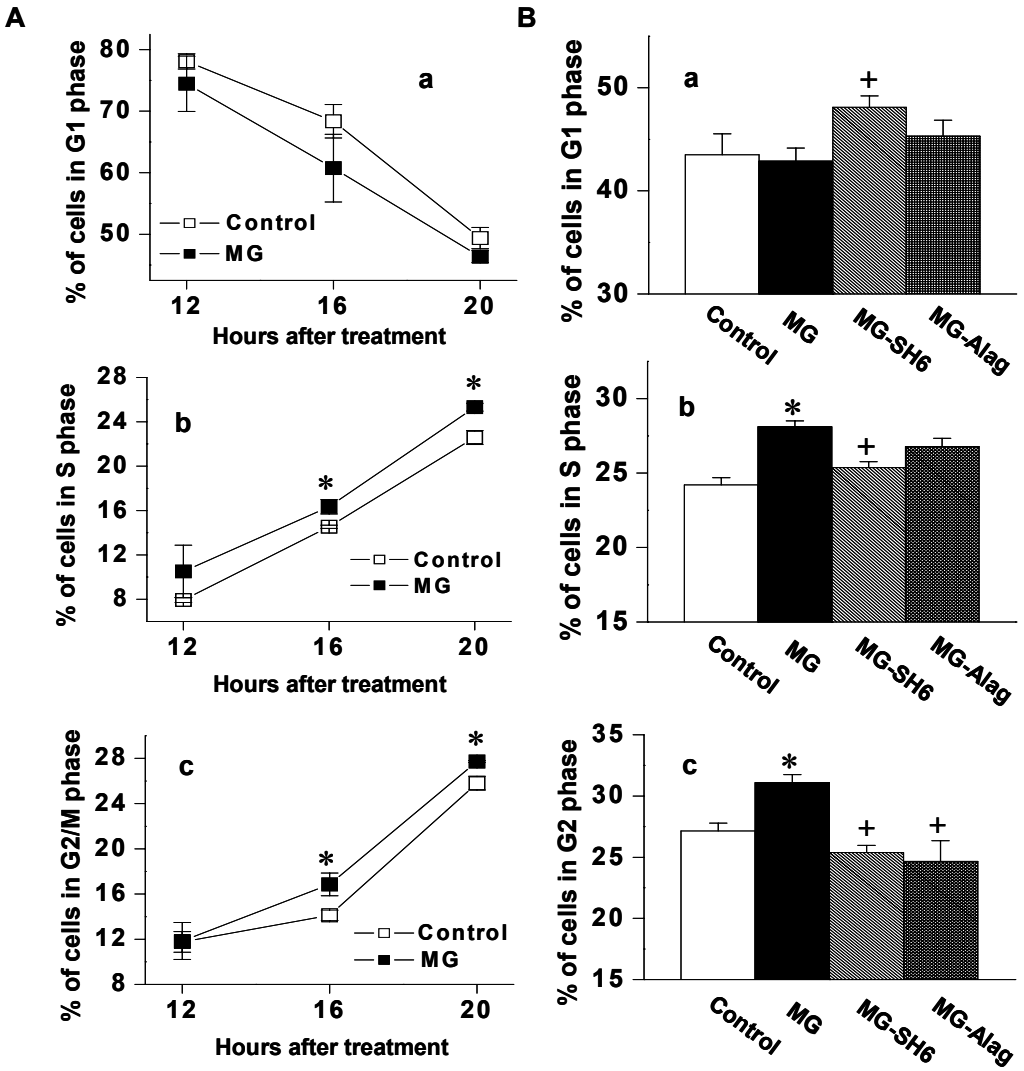


**Figure 6-3. Effect of MG on cell cycle progression of 3T3-L1 cells.** After 12, 16, 20 and 24 h of MG (10 μM) treatment, cellular DNA content was determined by a flow cytometer (***A***). The effect of MG with/without SH6 (10 μM) or alagebrium (50 μM) on cellular DNA content is shown in (***B)***. **P*<0.05 *vs* control group; $^{+}$*P*<0.05 *vs* MG treated group; n=6 in each group. The indicated percentage of the cell number is average of three experiments.

### 6.2.4. MG-stimulated proliferation resulted in more lipid accumulation in 3T3-L1 cells

We have observed that incubation of 3T3-L1 cells with MG (10 μM) caused increased cell proliferation. To investigate whether the increased pre-adipocyte number could cause more differentiated adipocytes, we treated the 3T3-L1 cells with MG, SH-6 or ALT711, respectively, for 48 h. On the fifth day of post-differentiation, the triglyceride deposition in 3T3-L1 cells was measured using the Oil Red O staining. Results showed that MG treatment for 48 h increased the lipid content in differentiated 3T3-L1 cells to 115.7±1.6% of the control level (Figure 6-5*A, B*). The increased lipid content in MG-treated cells was attenuated by SH-6 or alagebrium co-administration. More importantly, the enhanced mRNA expression of adiponectin and leptin, two important adipogenic markers, further confirmed the increased adipogenesis in MG (10-30 μM)-treated 3T3-L1 cells (Figure 6-5*C*).

## 6.3. Discussion

Increased MG levels and MG-related advanced glycation endproducts have been reported in different insulin resistance states, which is associated with various clinical manifestations such as hypertension and diabetes (Chang et al., 2002; McLellan et al., 1994; Riboulet-Chavey et al., 2006; Wang et al., 2004). As one of the major factors of insulin resistance, the correlation between endogenous MG accumulation and the development of obesity remains unidentified.

In the present study, we for the first time indicated an association between an increased MG level with the development of obesity. Our data showed an increased MG

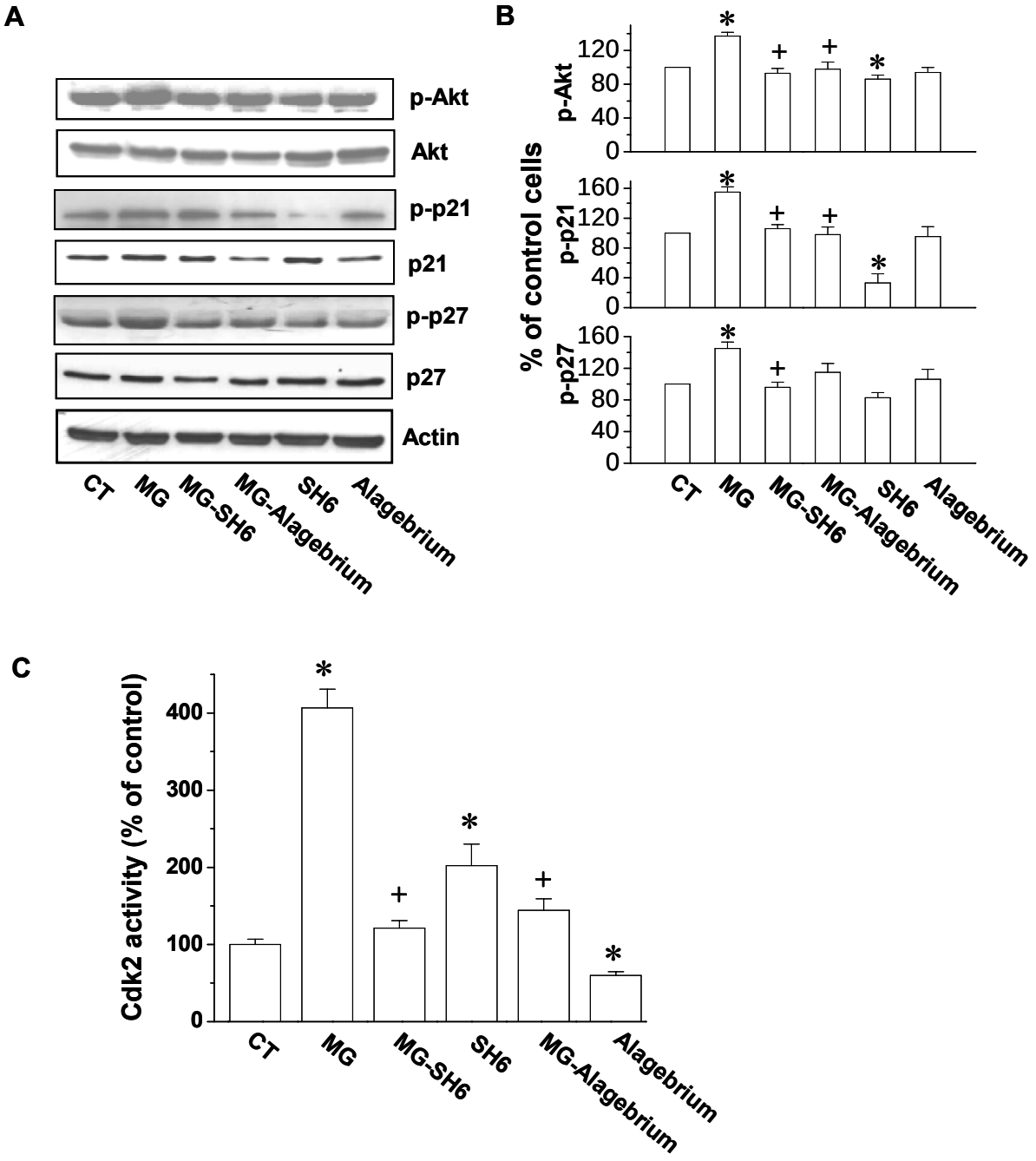
A
p-Akt
Akt
p-p21
p21
p-p27
p27
Actin
CT
MG
MG-SH6
MG-Alagebrium
SH6
Alagebrium
B
% of control cells
p-Akt
p-p21
p-p27
0
40
80
120
160
C
Cdk2 activity (% of control)
0
100
200
300
400

**Figure 6-4. Effect of MG on Akt and its target effectors in 3T3-L1 cells.** After 24 h treatment with or without MG (10 μM) in the presence or absence of SH-6 (10 μM)/alagebrium (50 μM), the protein levels of Akt, p21 and p27 (***A***), the levels of phospho-Akt (p-Akt), phosphor-p21 (p-p21) and phosphor-p27 (p-p27) (***B***), and the activity of Cdk2 (***C***) were determined and compared. The results of Western blotting were quantified by Chemigenus$^2$ Bio imaging system and presented as the percentage of that from control cells. The activity of Cdk2 in 3T3-L1 adipocytes treated with 10 μM MG was determined by measuring ATP consumption with a PKLight Assay Kit. **P*<0.05 *vs* control (CT) cells; $^+$*P*<0.05 *vs* MG treated cells. The results were based on data from three experiments.

A

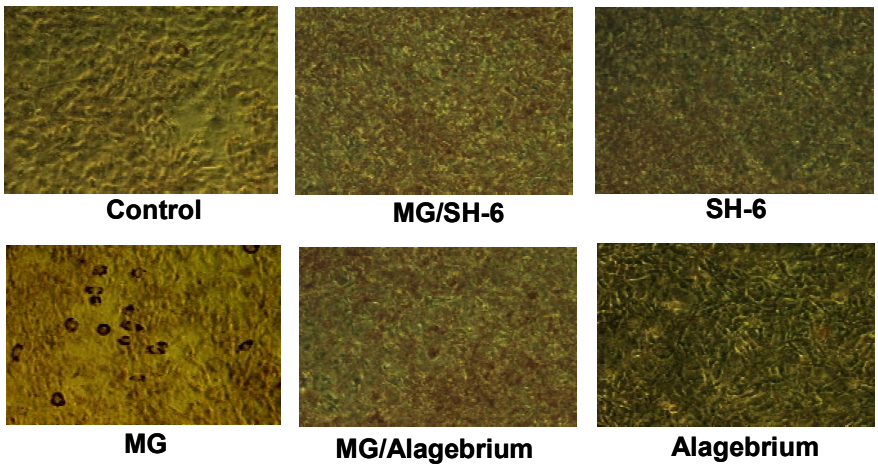
Control
MG/SH-6
SH-6
MG
MG/Alagebrium
Alagebrium

B

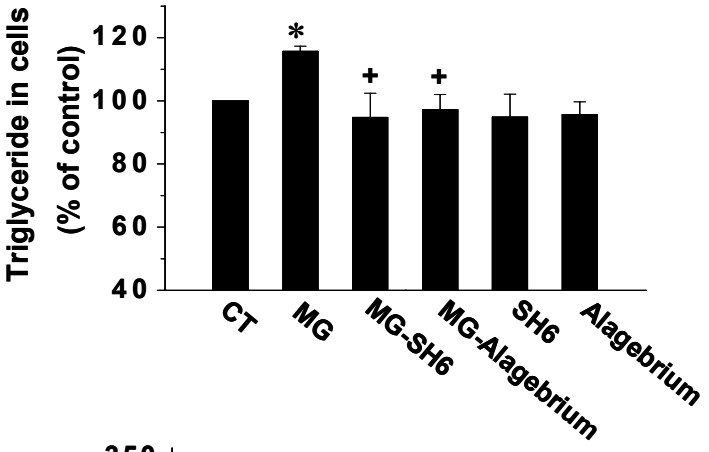
Triglyceride in cells
(% of control)
120
100
80
60
40
*
+
+
CT
MG
MG-SH6
MG-Alagebrium
SH6
Alagebrium

C

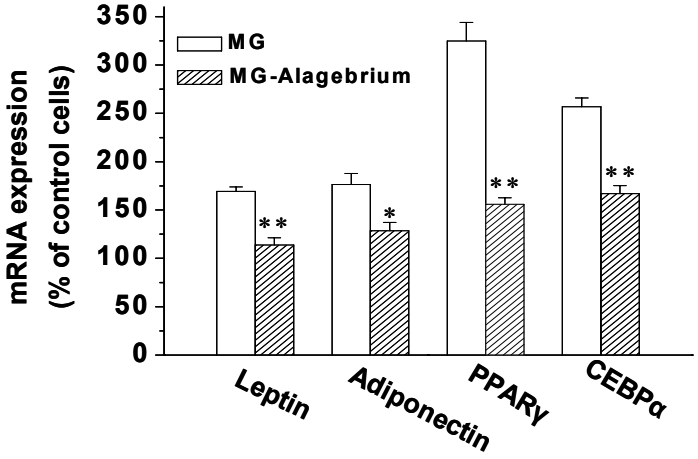
mRNA expression
(% of control cells)
350
300
250
200
150
100
50
0
MG
MG-Alagebrium
**
*
**
**
Leptin
Adiponectin
PPARγ
CEBPα

**Figure 6-5**. **MG induced adipogenesis in 3T3-L1 adipocytes.** After treating the cells with MG, SH-6 or alagebrium for 48 h, the cells were cultured till confluence and differentiation was then induced by adding 2.5 μg/ml insulin, 0.25 μM dexamethasone and 0.5 mM isobutylmethylxanthine for 48 h. When 70% of the cells became differentiated (after about 5 days culture) in post-differentiation medium, the Oil Red O staining or the RNA extraction was carried out. The lipid staining in adipocytes was shown in (***A***). The lipid content in adipocytes from different groups was quantified and presented as the percentage of that from control cells (***B***). The mRNA expression of adiponectin, PPARγ, C/EBPα and leptin in differentiated cells treated with MG alone or with MG and alagebrium were determined by real-time PCR (***C***). *P<0.05; **P<0.01; n=3 in each group.

level in obese patients (Figure 6-1). With cultured 3T3-L1 cells, we futher confirmed that MG induced an increase in p-Akt, p-p21 and p-p27, enhanced the activity of Cdk2, accelerates the cell cycle progression and proliferation of pre-adipocytes, thus contributing to the development of obesity.

Obesity is an enlargement of adipose tissue. Obesity in children involves both adipocyte hyperplasia and hypertrophy while adult-onset obesity was generally considered due to adipocyte hypertrophy. However, various lines of evidence indicate that adipocyte hyperplasia is also an important factor in the development of adult-onset obesity, especially morbid obese patients whose BMI value are greater than 39 (Drolet et al., 2008; Hirsch and Batchelor, 1976; Jo et al., 2009; Naaz et al., 2004). In the present study, we demonstrated that MG increased the fat cell number by promoting growth and proliferation of pre-adipocytes (3T3-L1 cells). After 16 to 20 h of treatment, MG (10 μM) increased the cell numbers in S and G2 cell cycle phase (Figure 6-5*A*) which indicated a stimulated progression of cell cycle. As a result, treatment with 10-20 μM MG for 48 h increased the number of 3T3 –L1 cells as measured by a cell proliferation assay (Figure 6-4). To our knowledge, this is the first report about the stimulating effect of MG on cell proliferation. The increased proliferation was also observed when vascular smooth muscle cells were treated with MG (unpublished data). On the contrary, the effect of MG on apoptosis has been extensively studied (Cantero et al., 2007; Kani et al., 2007; Ota et al., 2007). A previous study reported an increased apoptotic cell number when mouse Schwann cells were treated with 500-1000 μM MG (Ota et al., 2007). The major difference in our study is that the 3T3-L1 cells were treated with 5-20 μM MG instead of 500-1000 μM. The dose we used is much more relevant to the physiological

concentration of MG, which is around 0.2-5 μM in human/rats based on previous studies (Babaei-Jadidi et al., 2003; Nagaraj et al., 2002; Wang et al., 2008) and the present study. We did observe a decreased proliferative effect when the MG concentration increased to 100 μM. This might indicate a biphasic effect of MG on cell proliferation. Most probably, the inhibitory effect of MG might be due to the acute effect of high MG concentration, but not the effect of MG at the physiological level.

Our observation on MG-treated 3T3-L1 cells not only showed the effects of MG on cell proliferation and cell cycle regulation, but also implied a possible underlying mechanism. The PI3K/Akt signal cascade plays an important role in regulating cell proliferation. Based on our results, the effect of MG on cell proliferation was at least to some extent due to the MG-increased activity of Akt and its related signaling pathway. In our study, 10μM of MG in cultured 3T3-L1 cells increased the phosphorylation of Akt. Furthermore, MG treatment increased the phosphorylation of p21 and p27 (Figure 6-6*A*, *B*), major regulators that arrest the cells at the $G_1$/S checkpoint. The increased phosphorylation of p21 and p27 activates their degradation and leads to the entry of cells into S phase from G1 phase. This explains the MG-activated cell proliferation detected in our experiment. Further observation of the increased activity of CDK2 in MG-treated cells supported this hypothesis (Figure 6-4*C*). Increased Akt activity was observed in MG-treated 3T3-L1 cells suggesting that change in Akt, especially its activity, is critical in adipocyte proliferation in these obese rats.

Alagebrium, also known as ALT-711, is the first drug to be clinically tested for the purpose of breaking the crosslinks caused by AGEs (Coughlan et al., 2007). It is designed to reverse the stiffening of blood vessel walls that contributes to hypertension

and cardiovascular disease, as well as many other forms of degradation associated with protein cross linking. In our study, alagebrium was used as a specific inhibitor to block the effects of MG (Wang et al., 2009). A similar role of alagebrium in reversing the MG-induced cell proliferation and attenuating the activity of Akt and its downstream effectors (Figures 6-3, 4) confirmed our observation that MG mediates adipocyte proliferation by stimulating Akt activity. In the cell cycle assay, however, alagebrium showed a less potent effect in reversing MG's effect compared with SH-6. This seems reasonable because SH-6 directly targets Akt whereas alagebrium does not.

In summary, our study revealed the effect of MG in stimulating adipogenesis by up-regulating the signaling of Akt and its downstream pathway. This stimulates cell cycle progression and proliferation of the pre-adipocyte, which eventually leads to increased number of adipocytes and contributes to the development of obesity. The study of MG might offer a new approach to explain the development of obesity especially the adult-onset mobid obesity.

# CHAPTER SEVEN

# DISCUSSION AND CONCLUSIONS

## 7.1. General discussion

MG and related AGEs have been recognized as indicator of carbonyl overload burden. Increased MG accumulation have been reported in diabetes and hypertensive patients and animals (Kalapos, 1999; Mizutani et al., 1999; Wu and Juurlink, 2002). In the present study, increased MG levels in different tissues were observed in SD rats with insulin resistance (Figure 4-2 and Figure 5-2). In adipose tissue, the MG content increased from 1.5 μmol/g protein in normal rats to 4.37 μmol/g protein in rats with insulin resistance. Similarly, a dramatic increase in MG formation of more than 2-fold was observed in skeletal muscle, from 2.32 to 6.98 μmol/g protein. In addition, the MG level also elevated in blood serum from 1.81 μM to 3.29 μM after 9 weeks treatment of fructose. MG inhibitor, NAC and metformin efficiently reversed the MG accumulation and the progress of insulin resistance. Increased accumation of MG was detected in both obese patients and Zucker fatty rats (Figure 6-1). With the BMI value changed from 25 to 33, the plasma MG in obese patients increased from 2.1 μM to 3.5 μM. Correlation analysis indicated a strong correlation between plasma MG and BMI value/body weight in the tested human/animal samples.

At the cellular level, the mechanism responsible for the development of insulin resistance can be categorized as three levels: 1) pre-receptor defect (defective insulin production and function); 2) receptor defect (decreased number of receptors, reduced

binding of insulin, mutations of IR); or 3) post-receptor defect (defective insulin signal transduction and abnormal GLUT4 molecules).

In chapter three, the MG-induced structural modification on insulin molecule was investigated. The mass spectrometry study provided strong evidence for the formation of MG-insulin adducts. MG additions at both the N-terminus of the insulin B chain and at internal arginine residue were subsequently confirmed by tandem MS analysis of insulin B-chain adducts. The MG-insulin adducts induced a significant and concentration-dependent decrease in glucose uptake in insulin-sensitive adipocytes and skeletal muscle cells as compared to intact insulin. The autocrine control of insulin release by the extracellular insulin level was also altered by the glycation of insulin. Our results suggested that the formation of MG-insulin could no longer inhibit insulin (C-peptide) secretion. In addition, a significant lower MG-insulin clearance rate was observed through hepotocytes, which indicated that MG-insulin adducts could not go through endocytosis properly, or there was an aggregation of MG-insulin. The reduced glucose uptake by insulin sensitive cells leads to an increased glucose level in the circulation system. Together with the over accumulation of insulin/MG-insulin, the MG-induced glyation on insulin molecules resulted in the development of insulin resistance.

Skeletal muscle and adipose tissue, which, account for two-third of all cells in a typical human body, are most strongly influenced by insulin. The former plays a central role in movement, breathing, circulation, etc, and the latter accumulates excess food energy against future needs. In Chapter four and five, the effects of MG on insulin signaling transduction in these tissues/cells were investigated, respectively. In adipose tissue of fructose-treated rats, the elevation of endogenous MG level reduced IRS-1/PI3K

association and PI3K activity (Figure 4-3, 4). Fructose treatment also decreased the expression of IRS-1 and PI3K in skeletal muscle tissue (Figure 5-3). In cultured fat cells and skeletal muscle cells, MG treatment mimicked the impaired insulin signaling under *in vivo* condition, with reduction on IRS-1 phosphorylation and PI3K activity. The impaired insulin signaling observed in cultured cells, to some extend, explains the development of insulin resistance in fructose-fed SD rats.

One major factor in the development of insulin resistance syndrome is obesity, especially abdominal obesity or belly fat. In Chapter six, we examined the link between MG accumulation to the increased number of white adipose cells. Treatment of MG during the pre-adipocyte stage induced a increased proliferation of 3T3-L1 cells, which were shown by cell proliferation assay and cell cycle assay (Figure 6-3, 4). When the function of Akt and its downstream effectors were examined, a more active Cdk2 and lower activity of Cdk inhibitive protein (p21, p27) were detected (Figure 6-4) in MG treated cells. Furthermore, it was found that MG treatment during the pre-adipocyte stage caused more lipid accumulation later on in the differentiation stage. These results indicated that by stimulating Akt signaling pathway, MG might mediate adipocyte proliferation and increase the cell number in adipose tissue, thus, contribute to the occurrence of obesity, especially obesity in children and serious adult-onset obesity.

## 7.2. Conclusions

Based on this study, we clarified the effect of MG in the pathogenesis of insulin resistance syndrome. MG, as the most potent precursor of AGEs, impairs the activity of insulin signaling pathway by glycating insulin molecule and possibly other proteins in the

insulin signaling pathway Moreover, this study revealed a previously unrecognized effect of MG in adipogenesis by up-regulating Akt activity. In summary, this study elucidates 1) the correlation of increased MG accumulation and insulin resistance syndrome; 2) the causative effects of MG on the development of insulin resistance syndrome through modifying the structure and biological function of insulin, impairing insulin signaling and inducing obesity as summarized in Figure 7-1.

## 7.3. Significance of the study

Insulin resistance or metabolic syndrome is a group of phenotyles including hypertension, obesity, dyslipidemia and hyperinsulinemia. It promotes the development of coronary artery disease, stroke and type 2 diabetes, which contribute significantly to the spiraling cost of health care in the world, especially in western countries. Our study found that MG may contribute to the pathogenesis of insulin resistance syndrome through its effects on insulin signaling and adipogenesis. The results from this study might offer new mechanisms to explain the development of insulin resistance and to prevent the related diseases.

## 7.4. Future direction

A number of future considerations were brought up in each study of this thesis. The future directions of immediate interest are discussed below:

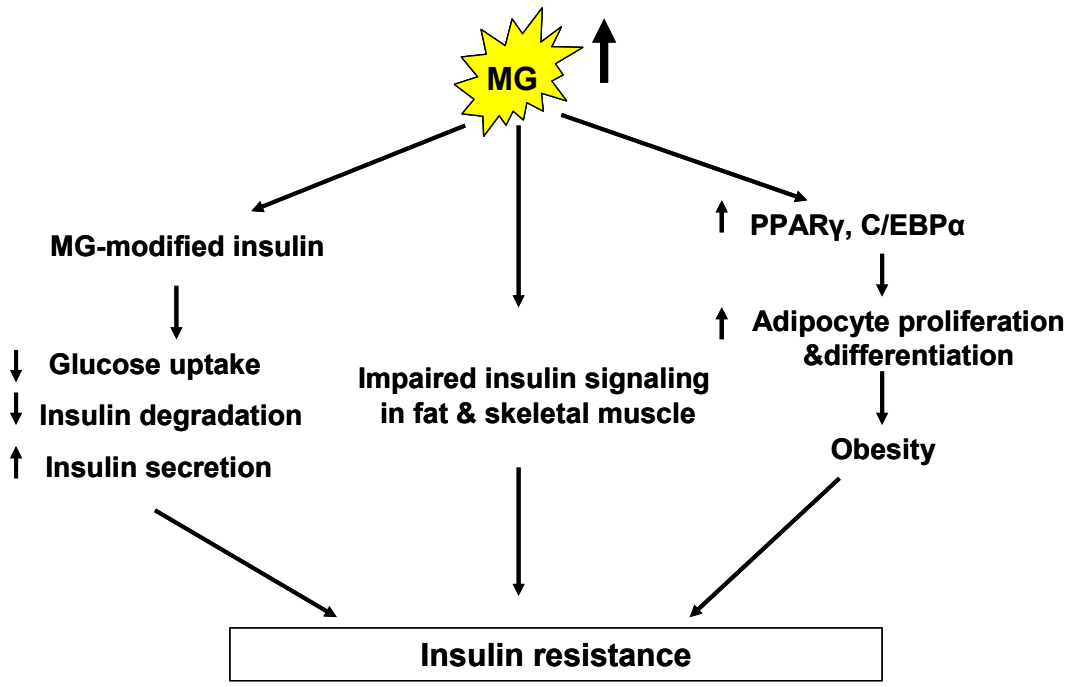


**Figure 7-1. The role of methylglyoxal in the pathogenesis of insulin resistance.** Increased MG accumulation induces insulin resistant state through three mechanisms. First, MG can modify the structure of insulin and alter its biological function. Second, MG accumulation in animals result impaired insulin signaling in adipose tissue and skeletal muscle tissue. Furthermore, increased MG accumulation induces proliferation and differentiation of adipocytes and causes obesity which is the major cause of insulin resistance.

### 7.4.1. To study whether MG alters the structure of insulin signaling proteins

A previous study reported the modification of MG on IRS protein (Riboulet-Chavey et al., 2006). In Chapter three, we also observed that MG glycates the insulin molecule *in vitro* on the Arg residue and N-terminus. In chapter four and five, while we found MG treatment impaired the insulin signaling in adipose cells and skeletal muscle cells, the further mechanism that causing this effect was not elucidated. Although we detected that MG could modify insulin on Arg residue, this specific MG-insulin adduct has not been detected *in vivo*. To this purpose, we have collected plasma samples from patients with obesity, hypertension or/and diabetes, for further examination. Preliminary MS study will be carried out to detect the existence of MG-inulin adduct in these samples. In future studies, how MG change the structure and function of insulin signaling proteins, such as IR, IRS and PI3K, should be explored both *in vitro* and *in vivo*.

### 7.4.2. The biological and pathological effects of MG in different tissues

MG research has become a "hotspot" in the field of metabolism study from recently. In previous research, very high concentration of MG, compared to physiological levels, were applied to treat animals and cells. In Chapter four and five, we found different expression level of IR and IRS-1 in adipose cells and skeletal muscle cells. In addition, different expression profile was also observed in adipose cells during different adipogenetic stages. When the cells were treated with MG in the pre-adipocyte stage, the PI3K expression and kinase activity were not altered. However, a decreased PI3K activity was detected when differentiated adipose cells were treated with MG. Other than the MG concentration and time duration of treatment, the different physiological condition of

cells might due to the different results. In the future, we will investigate the effects of MG in other tissues, such as liver and neruo cells.

### 7.4.3. To find the most potent MG/AGE inhibitor with minimum side effects

As introduced in Chapter one, a variety of MG inhibitors/breakers have been reported to interfere with the formation of AGE or AGE precursors. Although anti-AGE drugs are also being intensively studied, pharmacological approaches are still in early stages of development. In the present study, NAC, metformin and alagebrium were tested. Each of them to some extend inhibited the effect of MG when administered together. However, their side effects, which limit their clinical use, were not fully evaluated. In the future study, we will try both *in vitro* and *in vivo* system and compare the different effect of these agents. This study will prepare theoretical basis for the preventive and therapeutic use of anti-AGE drugs in clinic.

## REFERENCES


Abdel-Wahab, Y.H., O'Harte, F.P., Barnett, C.R. and Flatt, P.R. (1997a) Characterization of insulin glycation in insulin-secreting cells maintained in tissue culture. *J Endocrinol*, **152**, 59-67.

Abdel-Wahab, Y.H., O'Harte, F.P., Barnett, C.R. and Flatt, P.R. (1997b) Glycation of insulin in a cultured insulin-secreting cell line. *Biochem Soc Trans*, **25**, 128S.

Abdel-Wahab, Y.H., O'Harte, F.P., Boyd, A.C., Barnett, C.R. and Flatt, P.R. (1997c) Glycation of insulin results in reduced biological activity in mice. *Acta Diabetol*, **34**, 265-270.

Abdel-Wahab, Y.H., O'Harte, F.P., Ratcliff, H., McClenaghan, N.H., Barnett, C.R. and Flatt, P.R. (1996) Glycation of insulin in the islets of Langerhans of normal and diabetic animals. *Diabetes*, **45**, 1489-1496.

Abe, R. and Yamagishi, S. (2008) AGE-RAGE system and carcinogenesis. *Curr Pharm Des*, **14**, 940-945.

Accili, D., Frapier, C., Mosthaf, L., McKeon, C., Elbein, S.C., Permutt, M.A., Ramos, E., Lander, E., Ullrich, A. and Taylor, S.I. (1989) A mutation in the insulin receptor gene that impairs transport of the receptor to the plasma membrane and causes insulin-resistant diabetes. *Embo J*, **8**, 2509-2517.

Ahmad, F., Azevedo, J.L., Cortright, R., Dohm, G.L. and Goldstein, B.J. (1997a) Alterations in skeletal muscle protein-tyrosine phosphatase activity and expression in insulin-resistant human obesity and diabetes. *J Clin Invest*, **100**, 449-458.

Ahmad, F., Considine, R.V., Bauer, T.L., Ohannesian, J.P., Marco, C.C. and Goldstein, B.J. (1997b) Improved sensitivity to insulin in obese subjects following weight loss is accompanied by reduced protein-tyrosine phosphatases in adipose tissue. *Metabolism*, **46**, 1140-1145.

Ahmed, M.U., Brinkmann Frye, E., Degenhardt, T.P., Thorpe, S.R. and Baynes, J.W. (1997) N-epsilon-(carboxyethyl)lysine, a product of the chemical modification of proteins by methylglyoxal, increases with age in human lens proteins. *Biochem J*, **324 (Pt 2)**, 565-570.

Ahmed, N. (2005) Advanced glycation endproducts--role in pathology of diabetic complications. *Diabetes Res Clin Pract*, **67**, 3-21.

Ahmed, N., Argirov, O.K., Minhas, H.S., Cordeiro, C.A. and Thornalley, P.J. (2002) Assay of advanced glycation endproducts (AGEs): surveying AGEs by chromatographic assay with derivatization by 6-aminoquinolyl-N-

hydroxysuccinimidyl-carbamate and application to Nepsilon-carboxymethyl-lysine- and Nepsilon-(1-carboxyethyl)lysine-modified albumin. *Biochem J*, **364**, 1-14.

Ahmed, N. and Thornalley, P.J. (2002) Chromatographic assay of glycation adducts in human serum albumin glycated in vitro by derivatization with 6-aminoquinolyl-N-hydroxysuccinimidyl-carbamate and intrinsic fluorescence. *Biochem J*, **364**, 15-24.

Ailhaud, G. (1996) Early adipocyte differentiation. *Biochem Soc Trans*, **24**, 400-402.

Aleksandrovskii, Y.A. (1992) Antithrombin III, C1 inhibitor, methylglyoxal, and polymorphonuclear leukocytes in the development of vascular complications in diabetes mellitus. *Thromb Res*, **67**, 179-189.

Altiok, S., Xu, M. and Spiegelman, B.M. (1997) PPARgamma induces cell cycle withdrawal: inhibition of E2F/DP DNA-binding activity via down-regulation of PP2A. *Genes Dev*, **11**, 1987-1998.

Alzaid, A.A. (1996) Insulin resistance in non-insulin-dependent diabetes mellitus. A review. *Acta Diabetol*, **33**, 87-99.

Amicarelli, F., Colafarina, S., Cattani, F., Cimini, A., Di Ilio, C., Ceru, M.P. and Miranda, M. (2003) Scavenging system efficiency is crucial for cell resistance to ROS-mediated methylglyoxal injury. *Free Radic Biol Med*, **35**, 856-871.

Ardevol, A., Adan, C., Canas, X., Rafecas, I., Esteve, M., Remesar, X., Fernandez-Lopez, J.A. and Alemany, M. (1996) Adipose tissue extraction of circulating insulin in anaesthetized Zucker obese rats. *Int J Obes Relat Metab Disord*, **20**, 837-841.

Asnaghi, L., Bruno, P., Priulla, M. and Nicolin, A. (2004) mTOR: a protein kinase switching between life and death. *Pharmacol Res*, **50**, 545-549.

Babaei-Jadidi, R., Karachalias, N., Ahmed, N., Battah, S. and Thornalley, P.J. (2003) Prevention of incipient diabetic nephropathy by high-dose thiamine and benfotiamine. *Diabetes*, **52**, 2110-2120.

Bai, J.P., Hsu, M.J. and Shier, W.T. (1995) Insulin-degrading enzyme in a human colon adenocarcinoma cell line (Caco-2). *Pharm Res*, **12**, 513-517.

Bailey, C.J. and Turner, R.C. (1996) Metformin. *N Engl J Med*, **334**, 574-579.

Baldwin, D., Jr., Prince, M., Tsai, P., Johnson, C., Lotan, R., Rubenstein, A.H. and Olefsky, J.M. (1981) Insulin binding, internalization, and receptor regulation in cultured human fibroblasts. *Am J Physiol*, **241**, E251-260.

Basta, G., Lazzerini, G., Massaro, M., Simoncini, T., Tanganelli, P., Fu, C., Kislinger, T., Stern, D.M., Schmidt, A.M. and De Caterina, R. (2002) Advanced glycation end products activate endothelium through signal-transduction receptor RAGE: a mechanism for amplification of inflammatory responses. *Circulation*, **105**, 816-822.

Baynes, J.W. (2001) The role of AGEs in aging: causation or correlation. *Exp Gerontol*, **36**, 1527-1537.

Baynes, J.W. and Thorpe, S.R. (2000) Glycoxidation and lipoxidation in atherogenesis. *Free Radic Biol Med*, **28**, 1708-1716.

Beisswenger, P.J., Drummond, K.S., Nelson, R.G., Howell, S.K., Szwergold, B.S. and Mauer, M. (2005) Susceptibility to diabetic nephropathy is related to dicarbonyl and oxidative stress. *Diabetes*, **54**, 3274-3281.

Beisswenger, P.J., Howell, S.K., Touchette, A.D., Lal, S. and Szwergold, B.S. (1999) Metformin reduces systemic methylglyoxal levels in type 2 diabetes. *Diabetes*, **48**, 198-202.

Bevan, P. (2001) Insulin signalling. *J Cell Sci*, **114**, 1429-1430.

Bhattacharya, I. and Ullrich, A. (2006) Endothelin-1 inhibits adipogenesis: role of phosphorylation of Akt and ERK1/2. *FEBS Lett*, **580**, 5765-5771.

Bourajjaj, M., Stehouwer, C.D., van Hinsbergh, V.W. and Schalkwijk, C.G. (2003) Role of methylglyoxal adducts in the development of vascular complications in diabetes mellitus. *Biochem Soc Trans*, **31**, 1400-1402.

Boyd, A.C., Abdel-Wahab, Y.H., McKillop, A.M., McNulty, H., Barnett, C.R., O'Harte, F.P. and Flatt, P.R. (2000) Impaired ability of glycated insulin to regulate plasma glucose and stimulate glucose transport and metabolism in mouse abdominal muscle. *Biochim Biophys Acta*, **1523**, 128-134.

Boyd, D.B. (2003) Insulin and cancer. *Integr Cancer Ther*, **2**, 315-329.

Brady, M.J., Kartha, P.M., Aysola, A.A. and Saltiel, A.R. (1999) The role of glucose metabolites in the activation and translocation of glycogen synthase by insulin in 3T3-L1 adipocytes. *J Biol Chem*, **274**, 27497-27504.

Bray, G.A., Stern, J.S. and Castonguay, T.W. (1992) Effect of adrenalectomy and high-fat diet on the fatty Zucker rat. *Am J Physiol*, **262**, E32-39.

Brownlee, M., Vlassara, H., Kooney, A., Ulrich, P. and Cerami, A. (1986) Aminoguanidine prevents diabetes-induced arterial wall protein cross-linking. *Science*, **232**, 1629-1632.

Brozinick, J.T., Jr., Roberts, B.R. and Dohm, G.L. (2003) Defective signaling through Akt-2 and -3 but not Akt-1 in insulin-resistant human skeletal muscle: potential role in insulin resistance. *Diabetes*, **52**, 935-941.

Buffington, C.K., el-Shiekh, T., Kitabchi, A.E. and Matteri, R. (1986) Phytohemagglutinin (PHA) activated human T-lymphocytes: concomitant appearance of insulin binding, degradation and insulin-mediated activation of pyruvate dehydrogenase (PDH). *Biochem Biophys Res Commun*, **134**, 412-419.

Cantero, A.V., Portero-Otin, M., Ayala, V., Auge, N., Sanson, M., Elbaz, M., Thiers, J.C., Pamplona, R., Salvayre, R. and Negre-Salvayre, A. (2007) Methylglyoxal induces advanced glycation end product (AGEs) formation and dysfunction of PDGF receptor-beta: implications for diabetic atherosclerosis. *Faseb J*, **21**, 3096-3106.

Caro, J.F., Sinha, M.K., Raju, S.M., Ittoop, O., Pories, W.J., Flickinger, E.G., Meelheim, D. and Dohm, G.L. (1987) Insulin receptor kinase in human skeletal muscle from obese subjects with and without noninsulin dependent diabetes. *J Clin Invest*, **79**, 1330-1337.

Ceriello, A. and Motz, E. (2004) Is oxidative stress the pathogenic mechanism underlying insulin resistance, diabetes, and cardiovascular disease? The common soil hypothesis revisited. *Arterioscler Thromb Vasc Biol*, **24**, 816-823.

Chan, W.H., Wu, H.J. and Shiao, N.H. (2007) Apoptotic signaling in methylglyoxal-treated human osteoblasts involves oxidative stress, c-Jun N-terminal kinase, caspase-3, and p21-activated kinase 2. *J Cell Biochem*, **100**, 1056-1069.

Chang, K.C., Paek, K.S., Kim, H.J., Lee, Y.S., Yabe-Nishimura, C. and Seo, H.G. (2002) Substrate-induced up-regulation of aldose reductase by methylglyoxal, a reactive oxoaldehyde elevated in diabetes. *Mol Pharmacol*, **61**, 1184-1191.

Chang, T., Wang, R. and Wu, L. (2005) Methylglyoxal-induced nitric oxide and peroxynitrite production in vascular smooth muscle cells. *Free Radic Biol Med*, **38**, 286-293.

Chang, T. and Wu, L. (2006) Methylglyoxal, oxidative stress, and hypertension. *Can J Physiol Pharmacol*, **84**, 1229-1238.

Chaplen, F.W., Fahl, W.E. and Cameron, D.C. (1996) Detection of methylglyoxal as a degradation product of DNA and nucleic acid components treated with strong acid. *Anal Biochem*, **236**, 262-269.

Chaplen, F.W., Fahl, W.E. and Cameron, D.C. (1998) Evidence of high levels of methylglyoxal in cultured Chinese hamster ovary cells. *Proc Natl Acad Sci U S A*, **95**, 5533-5538.

Cheatham, B. and Kahn, C.R. (1995) Insulin action and the insulin signaling network. *Endocr Rev*, **16**, 117-142.

Chiappe De Cingolani, G.E. and Caldiz, C.I. (2004) Insulin resistance and GLUT-4 glucose transporter in adipocytes from hypertensive rats. *Metabolism*, **53**, 382-387.

Chuang, C.C., Yang, R.S., Tsai, K.S., Ho, F.M. and Liu, S.H. (2007) Hyperglycemia Enhances Adipogenic Induction of Lipid Accumulation: Involvement of Extracellular Signal-Regulated Protein Kinase 1/2, Phosphoinositide 3-Kinase/Akt, and Peroxisome Proliferator-Activated Receptor {gamma} Signaling. *Endocrinology*, **148**, 4267-4275.

Ciechanowski, K., Kedzierska, K., Golembiewska, E., Safranow, K., Bober, J., Domanski, L., Rozanski, J. and Myslak, M. (2005) Impaired synthesis is not the reason for decreased activity of extracellular superoxide dismutase in patients with diabetes. *Arch Med Res*, **36**, 148-153.

Cleasby, M.E., Dzamko, N., Hegarty, B.D., Cooney, G.J., Kraegen, E.W. and Ye, J.M. (2004) Metformin prevents the development of acute lipid-induced insulin resistance in the rat through altered hepatic signaling mechanisms. *Diabetes*, **53**, 3258-3266.

Cooper, R.A. (1984) Metabolism of methylglyoxal in microorganisms. *Annu Rev Microbiol*, **38**, 49-68.

Coughlan, M.T., Forbes, J.M. and Cooper, M.E. (2007) Role of the AGE crosslink breaker, alagebrium, as a renoprotective agent in diabetes. *Kidney Int Suppl*, S54-60.

Creighton, D.J., Migliorini, M., Pourmotabbed, T. and Guha, M.K. (1988) Optimization of efficiency in the glyoxalase pathway. *Biochemistry*, **27**, 7376-7384.

DeFronzo, R.A. and Beckles, A.D. (1979) Glucose intolerance following chronic metabolic acidosis in man. *Am J Physiol*, **236**, E328-334.

Dohm, G.L., Elton, C.W., Friedman, J.E., Pilch, P.F., Pories, W.J., Atkinson, S.M., Jr. and Caro, J.F. (1991) Decreased expression of glucose transporter in muscle from insulin-resistant patients. *Am J Physiol*, **260**, E459-463.

Draznin, B. (2006) Molecular mechanisms of insulin resistance: serine phosphorylation of insulin receptor substrate-1 and increased expression of p85alpha: the two sides of a coin. *Diabetes*, **55**, 2392-2397.

Drolet, R., Richard, C., Sniderman, A.D., Mailloux, J., Fortier, M., Huot, C., Rheaume, C. and Tchernof, A. (2008) Hypertrophy and hyperplasia of abdominal adipose tissues in women. *Int J Obes (Lond)*, **32**, 283-291.

Du, J., Cai, S., Suzuki, H., Akhand, A.A., Ma, X., Takagi, Y., Miyata, T., Nakashima, I. and Nagase, F. (2003) Involvement of MEKK1/ERK/P21Waf1/Cip1 signal transduction pathway in inhibition of IGF-I-mediated cell growth response by methylglyoxal. *J Cell Biochem*, **88**, 1235-1246.

Du, J., Suzuki, H., Nagase, F., Akhand, A.A., Ma, X.Y., Yokoyama, T., Miyata, T. and Nakashima, I. (2001a) Superoxide-mediated early oxidation and activation of ASK1 are important for initiating methylglyoxal-induced apoptosis process. *Free Radic. Biol. Med*, **31**, 469-478.

Du, J., Suzuki, H., Nagase, F., Akhand, A.A., Ma, X.Y., Yokoyama, T., Miyata, T. and Nakashima, I. (2001b) Superoxide-mediated early oxidation and activation of ASK1 are important for initiating methylglyoxal-induced apoptosis process. *Free Radic Biol Med*, **31**, 469-478.

Du, J., Suzuki, H., Nagase, F., Akhand, A.A., Yokoyama, T., Miyata, T., Kurokawa, K. and Nakashima, I. (2000) Methylglyoxal induces apoptosis in Jurkat leukemia T cells by activating c-Jun N-terminal kinase. *J. Cell Biochem*, **77**, 333-344.

Duckworth, W.C., Bennett, R.G. and Hamel, F.G. (1998) Insulin degradation: progress and potential. *Endocr Rev*, **19**, 608-624.

Dumitriu, I.E., Baruah, P., Valentinis, B., Voll, R.E., Herrmann, M., Nawroth, P.P., Arnold, B., Bianchi, M.E., Manfredi, A.A. and Rovere-Querini, P. (2005) Release of high mobility group box 1 by dendritic cells controls T cell activation via the receptor for advanced glycation end products. *J Immunol*, **174**, 7506-7515.

Ebbeling, C.B., Pawlak, D.B. and Ludwig, D.S. (2002) Childhood obesity: public-health crisis, common sense cure. *Lancet*, **360**, 473-482.

Elledge, S.J. (1996) Cell cycle checkpoints: preventing an identity crisis. *Science*, **274**, 1664-1672.

Fajas, L. (2003) Adipogenesis: a cross-talk between cell proliferation and cell differentiation. *Ann Med*, **35**, 79-85.

Fajas, L., Fruchart, J.C. and Auwerx, J. (1998) Transcriptional control of adipogenesis. *Curr Opin Cell Biol*, **10**, 165-173.

Fasshauer, M., Klein, J., Kriauciunas, K.M., Ueki, K., Benito, M. and Kahn, C.R. (2001) Essential role of insulin receptor substrate 1 in differentiation of brown adipocytes. *Mol Cell Biol*, **21**, 319-329.

Feng, L., Xia, Y., Garcia, G.E., Hwang, D. and Wilson, C.B. (1995) Involvement of reactive oxygen intermediates in cyclooxygenase-2 expression induced by interleukin-1, tumor necrosis factor-alpha, and lipopolysaccharide. *J Clin Invest*, **95**, 1669-1675.

Fonseca-Alaniz, M.H., Takada, J., Alonso-Vale, M.I. and Lima, F.B. (2007) Adipose tissue as an endocrine organ: from theory to practice. *J Pediatr (Rio J)*, **83**, S192-203.

Foretz, M., Guichard, C., Ferre, P. and Foufelle, F. (1999) Sterol regulatory element binding protein-1c is a major mediator of insulin action on the hepatic expression of glucokinase and lipogenesis-related genes. *Proc Natl Acad Sci U S A*, **96**, 12737-12742.

Forman, H.J. and Torres, M. (2002) Reactive oxygen species and cell signaling: respiratory burst in macrophage signaling. *Am J Respir Crit Care Med*, **166**, S4-8.

Fosmark, D.S., Torjesen, P.A., Kilhovd, B.K., Berg, T.J., Sandvik, L., Hanssen, K.F., Agardh, C.D. and Agardh, E. (2006) Increased serum levels of the specific advanced glycation end product methylglyoxal-derived hydroimidazolone are associated with retinopathy in patients with type 2 diabetes mellitus. *Metabolism*, **55**, 232-236.

Franke, T.F., Yang, S.I., Chan, T.O., Datta, K., Kazlauskas, A., Morrison, D.K., Kaplan, D.R. and Tsichlis, P.N. (1995) The protein kinase encoded by the Akt proto-oncogene is a target of the PDGF-activated phosphatidylinositol 3-kinase. *Cell*, **81**, 727-736.

Freedman, M.R., Horwitz, B.A. and Stern, J.S. (1986) Effect of adrenalectomy and glucocorticoid replacement on development of obesity. *Am J Physiol*, **250**, R595-607.

Frittitta, L., Youngren, J.F., Sbraccia, P., D'Adamo, M., Buongiorno, A., Vigneri, R., Goldfine, I.D. and Trischitta, V. (1997) Increased adipose tissue PC-1 protein content, but not tumour necrosis factor-alpha gene expression, is associated with a reduction of both whole body insulin sensitivity and insulin receptor tyrosine-kinase activity. *Diabetologia*, **40**, 282-289.

Fukunaga, M., Miyata, S., Higo, S., Hamada, Y., Ueyama, S. and Kasuga, M. (2005) Methylglyoxal induces apoptosis through oxidative stress-mediated activation of p38 mitogen-activated protein kinase in rat Schwann cells. *Ann N Y Acad Sci*, **1043**, 151-157.

Fukunaga, M., Miyata, S., Liu, B.F., Miyazaki, H., Hirota, Y., Higo, S., Hamada, Y., Ueyama, S. and Kasuga, M. (2004) Methylglyoxal induces apoptosis through activation of p38 MAPK in rat Schwann cells. *Biochem Biophys Res Commun*, **320**, 689-695.

Gagnon, A., Dods, P., Roustan-Delatour, N., Chen, C.S. and Sorisky, A. (2001) Phosphatidylinositol-3,4,5-trisphosphate is required for insulin-like growth factor 1-mediated survival of 3T3-L1 preadipocytes. *Endocrinology*, **142**, 205-212.

Galipeau, D., Arikawa, E., Sekirov, I. and McNeill, J.H. (2001) Chronic thromboxane synthase inhibition prevents fructose-induced hypertension. *Hypertension*, **38**, 872-876.

Gallistl, S., Sudi, K., Mangge, H., Erwa, W. and Borkenstein, M. (2000) Insulin is an independent correlate of plasma homocysteine levels in obese children and adolescents. *Diabetes Care*, **23**, 1348-1352.

Garvey, W.T., Maianu, L., Zhu, J.H., Brechtel-Hook, G., Wallace, P. and Baron, A.D. (1998) Evidence for defects in the trafficking and translocation of GLUT4 glucose transporters in skeletal muscle as a cause of human insulin resistance. *J Clin Invest*, **101**, 2377-2386.

Geroldi, D., Falcone, C. and Emanuele, E. (2006) Soluble receptor for advanced glycation end products: from disease marker to potential therapeutic target. *Curr Med Chem*, **13**, 1971-1978.

Giardino, I., Edelstein, D. and Brownlee, M. (1994) Nonenzymatic glycosylation in vitro and in bovine endothelial cells alters basic fibroblast growth factor activity. A model for intracellular glycosylation in diabetes. *J Clin Invest*, **94**, 110-117.

Giardino, I., Edelstein, D. and Brownlee, M. (1996) BCL-2 expression or antioxidants prevent hyperglycemia-induced formation of intracellular advanced glycation endproducts in bovine endothelial cells. *J Clin Invest*, **97**, 1422-1428.

Giardino, I., Fard, A.K., Hatchell, D.L. and Brownlee, M. (1998) Aminoguanidine inhibits reactive oxygen species formation, lipid peroxidation, and oxidant-induced apoptosis. *Diabetes*, **47**, 1114-1120.

Giono, L.E. and Manfredi, J.J. (2007a) Mdm2 is required for inhibition of Cdk2 activity by p21, thereby contributing to p53-dependent cell cycle arrest. *Mol Cell Biol*, **27**, 4166-4178.

Giono, L.E. and Manfredi, J.J. (2007b) Mdm2 plays a positive role as an effector of p53-dependent responses. *Cell Cycle*, **6**, 2143-2147.

Glomb, M.A. and Monnier, V.M. (1995) Mechanism of protein modification by glyoxal and glycolaldehyde, reactive intermediates of the Maillard reaction. *J Biol Chem*, **270**, 10017-10026.

Goldberg, T., Cai, W., Peppa, M., Dardaine, V., Baliga, B.S., Uribarri, J. and Vlassara, H. (2004) Advanced glycoxidation end products in commonly consumed foods. *J Am Diet Assoc*, **104**, 1287-1291.

Goldin, A., Beckman, J.A., Schmidt, A.M. and Creager, M.A. (2006) Advanced glycation end products: sparking the development of diabetic vascular injury. *Circulation*, **114**, 597-605.

Goodyear, L.J., Giorgino, F., Sherman, L.A., Carey, J., Smith, R.J. and Dohm, G.L. (1995) Insulin receptor phosphorylation, insulin receptor substrate-1 phosphorylation, and phosphatidylinositol 3-kinase activity are decreased in intact skeletal muscle strips from obese subjects. *J Clin Invest*, **95**, 2195-2204.

Gorden, P., Carpentier, J.L., Freychet, P., LeCam, A. and Orci, L. (1978) Intracellular translocation of iodine-125-labeled insulin: direct demonstration in isolated hepatocytes. *Science*, **200**, 782-785.

Gould, G.W. and Bell, G.I. (1990) Facilitative glucose transporters: an expanding family. *Trends Biochem Sci*, **15**, 18-23.

Graff, J.R., Konicek, B.W., McNulty, A.M., Wang, Z., Houck, K., Allen, S., Paul, J.D., Hbaiu, A., Goode, R.G., Sandusky, G.E., Vessella, R.L. and Neubauer, B.L. (2000) Increased AKT activity contributes to prostate cancer progression by dramatically accelerating prostate tumor growth and diminishing p27Kip1 expression. *J Biol Chem*, **275**, 24500-24505.

Green, H. and Kehinde, O. (1975) An established preadipose cell line and its differentiation in culture. II. Factors affecting the adipose conversion. *Cell*, **5**, 19-27.

Gregoire, F.M. (2001) Adipocyte differentiation: from fibroblast to endocrine cell. *Exp Biol Med (Maywood)*, **226**, 997-1002.

Gugliucci, A., Mehlhaff, K., Kinugasa, E., Ogata, H., Hermo, R., Schulze, J. and Kimura, S. (2007) Paraoxonase-1 concentrations in end-stage renal disease patients increase after hemodialysis: correlation with low molecular AGE adduct clearance. *Clin Chim Acta*, **377**, 213-220.

Hager, A., Sjostrm, L., Arvidsson, B., Bjorntorp, P. and Smith, U. (1977) Body fat and adipose tissue cellularity in infants: a longitudinal study. *Metabolism*, **26**, 607-614.

Hallfrisch, J., Ellwood, K.C., Michaelis, O.E.t., Reiser, S., O'Dorisio, T.M. and Prather, E.S. (1983) Effects of dietary fructose on plasma glucose and hormone responses in normal and hyperinsulinemic men. *J Nutr*, **113**, 1819-1826.

Hammes, H.P., Martin, S., Federlin, K., Geisen, K. and Brownlee, M. (1991) Aminoguanidine treatment inhibits the development of experimental diabetic retinopathy. *Proc Natl Acad Sci U S A*, **88**, 11555-11558.

Handberg, A., Vaag, A., Damsbo, P., Beck-Nielsen, H. and Vinten, J. (1990) Expression of insulin regulatable glucose transporters in skeletal muscle from type 2 (non-insulin-dependent) diabetic patients. *Diabetologia*, **33**, 625-627.

Harada, H., Tsujino, T., Watari, Y., Nonaka, H., Emoto, N. and Yokoyama, M. (2004) Oral taurine supplementation prevents fructose-induced hypertension in rats. *Heart Vessels*, **19**, 132-136.

Hausman, D.B., DiGirolamo, M., Bartness, T.J., Hausman, G.J. and Martin, R.J. (2001) The biology of white adipocyte proliferation. *Obes Rev*, **2**, 239-254.

Hirano, M., Arima, H. and Oiso, Y. (2008) Immunological insulin resistance due to insulin antibodies developed after cessation of insulin therapy in a patient with type 2 diabetes. *Diabetes Care*, **31**, e84.

Hirsch, J. and Batchelor, B. (1976) Adipose tissue cellularity in human obesity. *Clin Endocrinol Metab*, **5**, 299-311.

Hofmann, M.A., Drury, S., Fu, C., Qu, W., Taguchi, A., Lu, Y., Avila, C., Kambham, N., Bierhaus, A., Nawroth, P., Neurath, M.F., Slattery, T., Beach, D., McClary, J., Nagashima, M., Morser, J., Stern, D. and Schmidt, A.M. (1999) RAGE mediates a novel proinflammatory axis: a central cell surface receptor for S100/calgranulin polypeptides. *Cell*, **97**, 889-901.

Hofmann, M.A., Drury, S., Hudson, B.I., Gleason, M.R., Qu, W., Lu, Y., Lalla, E., Chitnis, S., Monteiro, J., Stickland, M.H., Bucciarelli, L.G., Moser, B., Moxley, G., Itescu, S., Grant, P.J., Gregersen, P.K., Stern, D.M. and Schmidt, A.M. (2002) RAGE and arthritis: the G82S polymorphism amplifies the inflammatory response. *Genes Immun*, **3**, 123-135.

Hovorka, R., Powrie, J.K., Smith, G.D., Sonksen, P.H., Carson, E.R. and Jones, R.H. (1993) Five-compartment model of insulin kinetics and its use to investigate action of chloroquine in NIDDM. *Am J Physiol*, **265**, E162-175.

Huang, S.M., Hancock, M.K., Pitman, J.L., Orth, A.P. and Gekakis, N. (2009) Negative regulators of insulin signaling revealed in a genome-wide functional screen. *PLoS One*, **4**, e6871.

Hunter, S.J., Boyd, A.C., O'Harte, F.P., McKillop, A.M., Wiggam, M.I., Mooney, M.H., McCluskey, J.T., Lindsay, J.R., Ennis, C.N., Gamble, R., Sheridan, B., Barnett, C.R., McNulty, H., Bell, P.M. and Flatt, P.R. (2003) Demonstration of glycated insulin in human diabetic plasma and decreased biological activity assessed by euglycemic-hyperinsulinemic clamp technique in humans. *Diabetes*, **52**, 492-498.

Iavarone, A. and Massague, J. (1997) Repression of the CDK activator Cdc25A and cell-cycle arrest by cytokine TGF-beta in cells lacking the CDK inhibitor p15. *Nature*, **387**, 417-422.

Iezzi, M., Escher, G., Meda, P., Charollais, A., Baldini, G., Darchen, F., Wollheim, C.B. and Regazzi, R. (1999) Subcellular distribution and function of Rab3A, B, C, and D isoforms in insulin-secreting cells. *Mol Endocrinol*, **13**, 202-212.

Ikeda, K., Higashi, T., Sano, H., Jinnouchi, Y., Yoshida, M., Araki, T., Ueda, S. and Horiuchi, S. (1996) N (epsilon)-(carboxymethyl)lysine protein adduct is a major immunological epitope in proteins modified with advanced glycation end products of the Maillard reaction. *Biochemistry*, **35**, 8075-8083.

Jana, C.K., Das, N. and Sohal, R.S. (2002) Specificity of age-related carbonylation of plasma proteins in the mouse and rat. *Arch Biochem Biophys*, **397**, 433-439.

Jia, X., Olson, D.J., Ross, A.R. and Wu, L. (2006) Structural and functional changes in human insulin induced by methylglyoxal. *Faseb J*, **20**, 1555-1557.

Jo, J., Gavrilova, O., Pack, S., Jou, W., Mullen, S., Sumner, A.E., Cushman, S.W. and Periwal, V. (2009) Hypertrophy and/or Hyperplasia: Dynamics of Adipose Tissue Growth. *PLoS Comput Biol*, **5**, e1000324.

Jochen, A., Hays, J. and Lee, M. (1989) Kinetics of insulin internalization and processing in adipocytes: effects of insulin concentration. *J Cell Physiol*, **141**, 527-534.

Jones, C.N., Abbasi, F., Carantoni, M., Polonsky, K.S. and Reaven, G.M. (2000) Roles of insulin resistance and obesity in regulation of plasma insulin concentrations. *Am J Physiol Endocrinol Metab*, **278**, E501-508.

Kahn, S.E., Hull, R.L. and Utzschneider, K.M. (2006) Mechanisms linking obesity to insulin resistance and type 2 diabetes. *Nature*, **444**, 840-846.

Kalapos, M.P. (1994) Methylglyoxal toxicity in mammals. *Toxicol Lett*, **73**, 3-24.

Kalapos, M.P. (1999) Methylglyoxal in living organisms: chemistry, biochemistry, toxicology and biological implications. *Toxicol Lett*, **110**, 145-175.

Kalapos, M.P. (2007a) Can ageing be prevented by dietary restriction? *Mech Ageing Dev*, **128**, 227-228.

Kalapos, M.P. (2007b) Possible mechanism for the effect of ketogenic diet in cases of uncontrolled seizures The reconsideration of acetone theory. *Med Hypotheses*, **68**, 1382-1388.

Kalapos, M.P. (2008) The tandem of free radicals and methylglyoxal. *Chem Biol Interact*, **171**, 251-271.

Kalapos, M.P., Garzo, T., Antoni, F. and Mandl, J. (1992) Accumulation of S-D-lactoylglutathione and transient decrease of glutathione level caused by methylglyoxal load in isolated hepatocytes. *Biochim Biophys Acta*, **1135**, 159-164.

Kang, J.H. (2003) Modification and inactivation of human Cu,Zn-superoxide dismutase by methylglyoxal. *Mol Cells*, **15**, 194-199.

Kani, S., Nakayama, E., Yoda, A., Onishi, N., Sougawa, N., Hazaka, Y., Umeda, T., Takeda, K., Ichijo, H., Hamada, Y. and Minami, Y. (2007) Chk2 kinase is required for methylglyoxal-induced G2/M cell-cycle checkpoint arrest: implication of cell-cycle checkpoint regulation in diabetic oxidative stress signaling. *Genes Cells*, **12**, 919-928.

Kern, P.A., Ranganathan, S., Li, C., Wood, L. and Ranganathan, G. (2001) Adipose tissue tumor necrosis factor and interleukin-6 expression in human obesity and insulin resistance. *Am J Physiol Endocrinol Metab*, **280**, E745-751.

Khwaja, A., Rodriguez-Viciana, P., Wennstrom, S., Warne, P.H. and Downward, J. (1997) Matrix adhesion and Ras transformation both activate a phosphoinositide 3-OH kinase and protein kinase B/Akt cellular survival pathway. *Embo J*, **16**, 2783-2793.

Kikuchi, S., Shinpo, K., Moriwaka, F., Makita, Z., Miyata, T. and Tashiro, K. (1999) Neurotoxicity of methylglyoxal and 3-deoxyglucosone on cultured cortical neurons: synergism between glycation and oxidative stress, possibly involved in neurodegenerative diseases. *J Neurosci Res*, **57**, 280-289.

Kim, J.B., Sarraf, P., Wright, M., Yao, K.M., Mueller, E., Solanes, G., Lowell, B.B. and Spiegelman, B.M. (1998) Nutritional and insulin regulation of fatty acid synthetase and leptin gene expression through ADD1/SREBP1. *J Clin Invest*, **101**, 1-9.

Kim, J.B. and Spiegelman, B.M. (1996) ADD1/SREBP1 promotes adipocyte differentiation and gene expression linked to fatty acid metabolism. *Genes Dev*, **10**, 1096-1107.

Kim, M.S., Yoon, C.Y., Jang, P.G., Park, Y.J., Shin, C.S., Park, H.S., Ryu, J.W., Pak, Y.K., Park, J.Y., Lee, K.U., Kim, S.Y., Lee, H.K., Kim, Y.B. and Park, K.S. (2004) The mitogenic and antiapoptotic actions of ghrelin in 3T3-L1 adipocytes. *Mol Endocrinol*, **18**, 2291-2301.

Kim, Y.B., Nikoulina, S.E., Ciaraldi, T.P., Henry, R.R. and Kahn, B.B. (1999) Normal insulin-dependent activation of Akt/protein kinase B, with diminished activation

of phosphoinositide 3-kinase, in muscle in type 2 diabetes. *J Clin Invest*, **104**, 733-741.

Kitamura, T., Kitamura, Y., Kuroda, S., Hino, Y., Ando, M., Kotani, K., Konishi, H., Matsuzaki, H., Kikkawa, U., Ogawa, W. and Kasuga, M. (1999) Insulin-induced phosphorylation and activation of cyclic nucleotide phosphodiesterase 3B by the serine-threonine kinase Akt. *Mol Cell Biol*, **19**, 6286-6296.

Kitamura, T., Ogawa, W., Sakaue, H., Hino, Y., Kuroda, S., Takata, M., Matsumoto, M., Maeda, T., Konishi, H., Kikkawa, U. and Kasuga, M. (1998) Requirement for activation of the serine-threonine kinase Akt (protein kinase B) in insulin stimulation of protein synthesis but not of glucose transport. *Mol Cell Biol*, **18**, 3708-3717.

Klip, A., Tsakiridis, T., Marette, A. and Ortiz, P.A. (1994) Regulation of expression of glucose transporters by glucose: a review of studies in vivo and in cell cultures. *Faseb J*, **8**, 43-53.

Koff, A., Cross, F., Fisher, A., Schumacher, J., Leguellec, K., Philippe, M. and Roberts, J.M. (1991) Human cyclin E, a new cyclin that interacts with two members of the CDC2 gene family. *Cell*, **66**, 1217-1228.

Koh, H., Lee, K.H., Kim, D., Kim, S., Kim, J.W. and Chung, J. (2000) Inhibition of Akt and its anti-apoptotic activities by tumor necrosis factor-induced protein kinase C-related kinase 2 (PRK2) cleavage. *J Biol Chem*, **275**, 34451-34458.

Koop, D.R. and Casazza, J.P. (1985) Identification of ethanol-inducible P-450 isozyme 3a as the acetone and acetol monooxygenase of rabbit microsomes. *J Biol Chem*, **260**, 13607-13612.

Kosaki, A., Pillay, T.S., Xu, L. and Webster, N.J. (1995) The B isoform of the insulin receptor signals more efficiently than the A isoform in HepG2 cells. *J Biol Chem*, **270**, 20816-20823.

Kosaki, A. and Webster, N.J. (1993) Effect of dexamethasone on the alternative splicing of the insulin receptor mRNA and insulin action in HepG2 hepatoma cells. *J Biol Chem*, **268**, 21990-21996.

Koschinsky, T., He, C.J., Mitsuhashi, T., Bucala, R., Liu, C., Buenting, C., Heitmann, K. and Vlassara, H. (1997) Orally absorbed reactive glycation products (glycotoxins): an environmental risk factor in diabetic nephropathy. *Proc Natl Acad Sci U S A*, **94**, 6474-6479.

Krook, A., Roth, R.A., Jiang, X.J., Zierath, J.R. and Wallberg-Henriksson, H. (1998) Insulin-stimulated Akt kinase activity is reduced in skeletal muscle from NIDDM subjects. *Diabetes*, **47**, 1281-1286.

Kuhla, B., Luth, H.J., Haferburg, D., Boeck, K., Arendt, T. and Munch, G. (2005) Methylglyoxal, glyoxal, and their detoxification in Alzheimer's disease. *Ann N Y Acad Sci*, **1043**, 211-216.

Laight, D.W., Desai, K.M., Gopaul, N.K., Anggard, E.E. and Carrier, M.J. (1999) Pro-oxidant challenge in vivo provokes the onset of NIDDM in the insulin resistant obese Zucker rat. *Br J Pharmacol*, **128**, 269-271.

Lander, H.M., Tauras, J.M., Ogiste, J.S., Hori, O., Moss, R.A. and Schmidt, A.M. (1997) Activation of the receptor for advanced glycation end products triggers a p21(ras)-dependent mitogen-activated protein kinase pathway regulated by oxidant stress. *J Biol Chem*, **272**, 17810-17814.

Lau, D.C., Schillabeer, G., Li, Z.H., Wong, K.L., Varzaneh, F.E. and Tough, S.C. (1996) Paracrine interactions in adipose tissue development and growth. *Int J Obes Relat Metab Disord*, **20 Suppl 3**, S16-25.

Lazar, D.F. and Saltiel, A.R. (2006) Lipid phosphatases as drug discovery targets for type 2 diabetes. *Nat Rev Drug Discov*, **5**, 333-342.

Lee, H.K., Seo, I.A., Suh, D.J., Lee, H.J. and Park, H.T. (2009) A novel mechanism of methylglyoxal cytotoxicity in neuroglial cells. *J Neurochem*, **108**, 273-284.

Leoncini, G. (1979) The role of alpha-ketoaldehydes in biological systems. *Ital J Biochem*, **28**, 285-294.

Leoncini, G. and Poggi, M. (1996) Effects of methylglyoxal on platelet hydrogen peroxide accumulation, aggregation and release reaction. *Cell Biochem Funct*, **14**, 89-95.

Levacher, C., Sztalryd, C., Kinebanyan, M.F. and Picon, L. (1984) Effects of thyroid hormones on adipose tissue development in Sherman and Zucker rats. *Am J Physiol*, **246**, C50-56.

Li Calzi, S., Choice, C.V. and Najjar, S.M. (1997) Differential effect of pp120 on insulin endocytosis by two variant insulin receptor isoforms. *Am J Physiol*, **273**, E801-808.

Li, Y., Soos, T.J., Li, X., Wu, J., Degennaro, M., Sun, X., Littman, D.R., Birnbaum, M.J. and Polakiewicz, R.D. (2004) Protein kinase C Theta inhibits insulin signaling by phosphorylating IRS1 at Ser(1101). *J Biol Chem*, **279**, 45304-45307.

Li, Y.M., Steffes, M., Donnelly, T., Liu, C., Fuh, H., Basgen, J., Bucala, R. and Vlassara, H. (1996) Prevention of cardiovascular and renal pathology of aging by the advanced glycation inhibitor aminoguanidine. *Proc Natl Acad Sci U S A*, **93**, 3902-3907.

Lindsay, J.R., McKillop, A.M., Mooney, M.H., O'Harte, F.P., Bell, P.M. and Flatt, P.R. (2003) Demonstration of increased concentrations of circulating glycated insulin in human Type 2 diabetes using a novel and specific radioimmunoassay. *Diabetologia*, **46**, 475-478.

Liu, B.F., Miyata, S., Hirota, Y., Higo, S., Miyazaki, H., Fukunaga, M., Hamada, Y., Ueyama, S., Muramoto, O., Uriuhara, A. and Kasuga, M. (2003) Methylglyoxal induces apoptosis through activation of p38 mitogen-activated protein kinase in rat mesangial cells. *Kidney Int*, **63**, 947-957.

Lizcano, J.M., Deak, M., Morrice, N., Kieloch, A., Hastie, C.J., Dong, L., Schutkowski, M., Reimer, U. and Alessi, D.R. (2002) Molecular basis for the substrate specificity of NIMA-related kinase-6 (NEK6). Evidence that NEK6 does not phosphorylate the hydrophobic motif of ribosomal S6 protein kinase and serum- and glucocorticoid-induced protein kinase in vivo. *J Biol Chem*, **277**, 27839-27849.

Lo, T.W., Westwood, M.E., McLellan, A.C., Selwood, T. and Thornalley, P.J. (1994) Binding and modification of proteins by methylglyoxal under physiological conditions. A kinetic and mechanistic study with N alpha-acetylarginine, N alpha-acetylcysteine, and N alpha-acetyllysine, and bovine serum albumin. *J Biol Chem*, **269**, 32299-32305.

Lord, J.M., Flight, I.H. and Norman, R.J. (2003) Metformin in polycystic ovary syndrome: systematic review and meta-analysis. *Bmj*, **327**, 951-953.

Lupsa, B.C., Chong, A.Y., Cochran, E.K., Soos, M.A., Semple, R.K. and Gorden, P. (2009) Autoimmune forms of hypoglycemia. *Medicine (Baltimore)*, **88**, 141-153.

Lutsey, P.L., Steffen, L.M. and Stevens, J. (2008) Dietary intake and the development of the metabolic syndrome: the Atherosclerosis Risk in Communities study. *Circulation*, **117**, 754-761.

Lyles, G.A. (1996) Mammalian plasma and tissue-bound semicarbazide-sensitive amine oxidases: biochemical, pharmacological and toxicological aspects. *Int J Biochem Cell Biol*, **28**, 259-274.

Lyles, G.A. and Chalmers, J. (1992) The metabolism of aminoacetone to methylglyoxal by semicarbazide-sensitive amine oxidase in human umbilical artery. *Biochem Pharmacol*, **43**, 1409-1414.

MacDougald, O.A. and Lane, M.D. (1995) Transcriptional regulation of gene expression during adipocyte differentiation. *Annu Rev Biochem*, **64**, 345-373.

Magun, R., Burgering, B.M., Coffer, P.J., Pardasani, D., Lin, Y., Chabot, J. and Sorisky, A. (1996) Expression of a constitutively activated form of protein kinase B (c-Akt)

in 3T3-L1 preadipose cells causes spontaneous differentiation. *Endocrinology*, **137**, 3590-3593.

Matthaei, S., Stumvoll, M., Kellerer, M. and Haring, H.U. (2000) Pathophysiology and pharmacological treatment of insulin resistance. *Endocr Rev*, **21**, 585-618.

McLellan, A.C., Thornalley, P.J., Benn, J. and Sonksen, P.H. (1994) Glyoxalase system in clinical diabetes mellitus and correlation with diabetic complications. *Clin Sci (Lond)*, **87**, 21-29.

Mei, B., Zhao, L., Chen, L. and Sul, H.S. (2002) Only the large soluble form of preadipocyte factor-1 (Pref-1), but not the small soluble and membrane forms, inhibits adipocyte differentiation: role of alternative splicing. *Biochem J*, **364**, 137-144.

Menghini, R., Marchetti, V., Cardellini, M., Hribal, M.L., Mauriello, A., Lauro, D., Sbraccia, P., Lauro, R. and Federici, M. (2005) Phosphorylation of GATA2 by Akt increases adipose tissue differentiation and reduces adipose tissue-related inflammation: a novel pathway linking obesity to atherosclerosis. *Circulation*, **111**, 1946-1953.

Miele, C., Riboulet, A., Maitan, M.A., Oriente, F., Romano, C., Formisano, P., Giudicelli, J., Beguinot, F. and Van Obberghen, E. (2003) Human glycated albumin affects glucose metabolism in L6 skeletal muscle cells by impairing insulin-induced insulin receptor substrate (IRS) signaling through a protein kinase C alpha-mediated mechanism. *J Biol Chem*, **278**, 47376-47387.

Miller, A.G., Smith, D.G., Bhat, M. and Nagaraj, R.H. (2006) Glyoxalase I is critical for human retinal capillary pericyte survival under hyperglycemic conditions. *J Biol Chem*, **281**, 11864-11871.

Mizutani, K., Ikeda, K., Kawai, Y. and Yamori, Y. (1999) Biomechanical properties and chemical composition of the aorta in genetic hypertensive rats. *J Hypertens*, **17**, 481-487.

Mohamed-Ali, V., Pinkney, J.H. and Coppack, S.W. (1998) Adipose tissue as an endocrine and paracrine organ. *Int J Obes Relat Metab Disord*, **22**, 1145-1158.

Monnier, V.M. and Cerami, A. (1981) Nonenzymatic browning in vivo: possible process for aging of long-lived proteins. *Science*, **211**, 491-493.

Monnier, V.M., Stevens, V.J. and Cerami, A. (1981) Maillard reactions involving proteins and carbohydrates in vivo: relevance to diabetes mellitus and aging. *Prog Food Nutr Sci*, **5**, 315-327.

Mooney, R.A., Senn, J., Cameron, S., Inamdar, N., Boivin, L.M., Shang, Y. and Furlanetto, R.W. (2001) Suppressors of cytokine signaling-1 and -6 associate with and inhibit the insulin receptor. A potential mechanism for cytokine-mediated insulin resistance. *J Biol Chem*, **276**, 25889-25893.

Morgan, P.E., Dean, R.T. and Davies, M.J. (2002) Inactivation of cellular enzymes by carbonyls and protein-bound glycation/glycoxidation products. *Arch Biochem Biophys*, **403**, 259-269.

Mostafa, A.A., Randell, E.W., Vasdev, S.C., Gill, V.D., Han, Y., Gadag, V., Raouf, A.A. and El Said, H. (2007) Plasma protein advanced glycation end products, carboxymethyl cysteine, and carboxyethyl cysteine, are elevated and related to nephropathy in patients with diabetes. *Mol Cell Biochem*, **302**, 35-42.

Mosthaf, L., Vogt, B., Haring, H.U. and Ullrich, A. (1991) Altered expression of insulin receptor types A and B in the skeletal muscle of non-insulin-dependent diabetes mellitus patients. *Proc Natl Acad Sci U S A*, **88**, 4728-4730.

Munch, G., Deuther-Conrad, W. and Gasic-Milenkovic, J. (2002) Glycoxidative stress creates a vicious cycle of neurodegeneration in Alzheimer's disease--a target for neuroprotective treatment strategies? *J Neural Transm Suppl*, 303-307.

Murga, C., Laguinge, L., Wetzker, R., Cuadrado, A. and Gutkind, J.S. (1998) Activation of Akt/protein kinase B by G protein-coupled receptors. A role for alpha and beta gamma subunits of heterotrimeric G proteins acting through phosphatidylinositol-3-OH kinasegamma. *J Biol Chem*, **273**, 19080-19085.

Naaz, A., Holsberger, D.R., Iwamoto, G.A., Nelson, A., Kiyokawa, H. and Cooke, P.S. (2004) Loss of cyclin-dependent kinase inhibitors produces adipocyte hyperplasia and obesity. *Faseb J*, **18**, 1925-1927.

Nagaraj, R.H., Sarkar, P., Mally, A., Biemel, K.M., Lederer, M.O. and Padayatti, P.S. (2002) Effect of pyridoxamine on chemical modification of proteins by carbonyls in diabetic rats: characterization of a major product from the reaction of pyridoxamine and methylglyoxal. *Arch Biochem Biophys*, **402**, 110-119.

Naitoh, T., Kitahara, M. and Tsuruzoe, N. (2001) Tumor necrosis factor-alpha is induced through phorbol ester--and glycated human albumin-dependent pathway in THP-1 cells. *Cell Signal*, **13**, 331-334.

Neeper, M., Schmidt, A.M., Brett, J., Yan, S.D., Wang, F., Pan, Y.C., Elliston, K., Stern, D. and Shaw, A. (1992) Cloning and expression of a cell surface receptor for advanced glycosylation end products of proteins. *J Biol Chem*, **267**, 14998-15004.

Nishikawa, T., Edelstein, D., Du, X.L., Yamagishi, S., Matsumura, T., Kaneda, Y., Yorek, M.A., Beebe, D., Oates, P.J., Hammes, H.P., Giardino, I. and Brownlee, M. (2000)

Normalizing mitochondrial superoxide production blocks three pathways of hyperglycaemic damage. *Nature*, **404**, 787-790.

Nolan, J.J., Freidenberg, G., Henry, R., Reichart, D. and Olefsky, J.M. (1994) Role of human skeletal muscle insulin receptor kinase in the in vivo insulin resistance of noninsulin-dependent diabetes mellitus and obesity. *J Clin Endocrinol Metab*, **78**, 471-477.

Ogawa, W., Matozaki, T. and Kasuga, M. (1998) Role of binding proteins to IRS-1 in insulin signalling. *Mol Cell Biochem*, **182**, 13-22.

Olefsky, J.M. and Kolterman, O.G. (1981) Mechanisms of insulin resistance in obesity and noninsulin-dependent (type II) diabetes. *Am J Med*, **70**, 151-168.

Ota, K., Nakamura, J., Li, W., Kozakae, M., Watarai, A., Nakamura, N., Yasuda, Y., Nakashima, E., Naruse, K., Watabe, K., Kato, K., Oiso, Y. and Hamada, Y. (2007) Metformin prevents methylglyoxal-induced apoptosis of mouse Schwann cells. *Biochem Biophys Res Commun*, **357**, 270-275.

Ou, P., Wolff,S.P. (1993) Aminoguanidine: A drug proposed for prophylaxis in diabetes inhibits catalase and generates hydrogen peroxide in vitro. In *Biochem Pharmacol*, Vol. 46, pp. 1139-1144.

Oya, T., Hattori, N., Mizuno, Y., Miyata, S., Maeda, S., Osawa, T. and Uchida, K. (1999) Methylglyoxal modification of protein. Chemical and immunochemical characterization of methylglyoxal-arginine adducts. *J Biol Chem*, **274**, 18492-18502.

Papoulis, A., al-Abed, Y. and Bucala, R. (1995) Identification of N2-(1-carboxyethyl)guanine (CEG) as a guanine advanced glycosylation end product. *Biochemistry*, **34**, 648-655.

Park, L., Raman, K.G., Lee, K.J., Lu, Y., Ferran, L.J., Jr., Chow, W.S., Stern, D. and Schmidt, A.M. (1998) Suppression of accelerated diabetic atherosclerosis by the soluble receptor for advanced glycation endproducts. *Nat Med*, **4**, 1025-1031.

Peng, X.D., Xu, P.Z., Chen, M.L., Hahn-Windgassen, A., Skeen, J., Jacobs, J., Sundararajan, D., Chen, W.S., Crawford, S.E., Coleman, K.G. and Hay, N. (2003) Dwarfism, impaired skin development, skeletal muscle atrophy, delayed bone development, and impeded adipogenesis in mice lacking Akt1 and Akt2. *Genes Dev*, **17**, 1352-1365.

Permutt, M.A., Wasson, J. and Cox, N. (2005) Genetic epidemiology of diabetes. *J Clin Invest*, **115**, 1431-1439.

Phillips, S.A. and Thornalley, P.J. (1993) The formation of methylglyoxal from triose phosphates. Investigation using a specific assay for methylglyoxal. *Eur J Biochem*, **212**, 101-105.

Pi, J., Bai, Y., Zhang, Q., Wong, V., Floering, L.M., Daniel, K., Reece, J.M., Deeney, J.T., Andersen, M.E., Corkey, B.E. and Collins, S. (2007) Reactive Oxygen Species as a Signal in Glucose-Stimulated Insulin Secretion. *Diabetes*.

Picard, F., Kapur, S., Perreault, M., Marette, A. and Deshaies, Y. (2001) Nitric oxide mediates endotoxin-induced hypertriglyceridemia through its action on skeletal muscle lipoprotein lipase. *Faseb J*, **15**, 1828-1830.

Pickup, J.C. (2004) Inflammation and activated innate immunity in the pathogenesis of type 2 diabetes. *Diabetes Care*, **27**, 813-823.

Poggioli, S., Bakala, H. and Friguet, B. (2002) Age-related increase of protein glycation in peripheral blood lymphocytes is restricted to preferential target proteins. *Exp Gerontol*, **37**, 1207-1215.

Polonsky, K. (1995) Secretion and metabolism of insulin, proinsulin, and C-peptide. In DeGroot, L. (ed.), *Endocrinology*. WB Saunders Philadelphia, U. S. A, p. 1354.

Portero-Otin, M., Bellmunt, M.J., Requena, J.R. and Pamplona, R. (2003) Protein modification by advanced Maillard adducts can be modulated by dietary polyunsaturated fatty acids. *Biochem Soc Trans*, **31**, 1403-1405.

Portero-Otin, M., Pamplona, R., Bellmunt, M.J., Ruiz, M.C., Prat, J., Salvayre, R. and Negre-Salvayre, A. (2002) Advanced glycation end product precursors impair epidermal growth factor receptor signaling. *Diabetes*, **51**, 1535-1542.

Powers, A.C., Solomon, S.S. and Duckworth, W.C. (1980) Insulin degradation by mononuclear cells. *Diabetes*, **29**, 27-32.

Price, C.L. and Knight, S.C. (2007) Advanced glycation: a novel outlook on atherosclerosis. *Curr Pharm Des*, **13**, 3681-3687.

Price, C.L., Sharp, P.S., North, M.E., Rainbow, S.J. and Knight, S.C. (2004) Advanced glycation end products modulate the maturation and function of peripheral blood dendritic cells. *Diabetes*, **53**, 1452-1458.

Procaccini, R.L., DeFanti, D.R. and DeFeo, J.J. (1971) Inhibition of in vitro histone acetylation in a cell free rat uterine system by methylglyoxal and phenylglyoxal. *Biochem Biophys Res Commun*, **43**, 684-687.

Proud, C.G. (2006) Regulation of protein synthesis by insulin. *Biochem Soc Trans*, **34**, 213-216.

Qi, L. and Cho, Y.A. (2008) Gene-environment interaction and obesity. *Nutr Rev*, **66**, 684-694.

Racker, E. (1951) The mechanism of action of glyoxalase. *J Biol Chem*, **190**, 685-696.

Rahbar, S., Natarajan, R., Yerneni, K., Scott, S., Gonzales, N. and Nadler, J.L. (2000a) Evidence that pioglitazone, metformin and pentoxifylline are inhibitors of glycation. *Clin Chim Acta*, **301**, 65-77.

Rahbar, S., Yerneni, K.K., Scott, S., Gonzales, N. and Lalezari, I. (2000b) Novel inhibitors of advanced glycation endproducts (part II). *Mol Cell Biol Res Commun*, **3**, 360-366.

Rahman, A., Shahabuddin and Hadi, S.M. (1990) Formation of strand breaks and interstrand cross-links in DNA by methylglyoxal. *J Biochem Toxicol*, **5**, 161-166.

Randle, P.J., Garland, P.B., Hales, C.N. and Newsholme, E.A. (1963) The glucose fatty-acid cycle. Its role in insulin sensitivity and the metabolic disturbances of diabetes mellitus. *Lancet*, **1**, 785-789.

Ray, S. and Ray, M. (1981) Isolation of methylglyoxal synthase from goat liver. *J Biol Chem*, **256**, 6230-6233.

Reiser, S., Powell, A.S., Scholfield, D.J., Panda, P., Fields, M. and Canary, J.J. (1989) Day-long glucose, insulin, and fructose responses of hyperinsulinemic and nonhyperinsulinemic men adapted to diets containing either fructose or high-amylose cornstarch. *Am J Clin Nutr*, **50**, 1008-1014.

Rett, K. (1999) The relation between insulin resistance and cardiovascular complications of the insulin resistance syndrome. *Diabetes Obes Metab*, **1 Suppl 1**, S8-16.

Riboulet-Chavey, A., Pierron, A., Durand, I., Murdaca, J., Giudicelli, J. and Van Obberghen, E. (2006) Methylglyoxal impairs the insulin signaling pathways independently of the formation of intracellular reactive oxygen species. *Diabetes*, **55**, 1289-1299.

Richard, J.P. (1991) Kinetic parameters for the elimination reaction catalyzed by triosephosphate isomerase and an estimation of the reaction's physiological significance. *Biochemistry*, **30**, 4581-4585.

Richard, J.P. (1993) Mechanism for the formation of methylglyoxal from triosephosphates. *Biochem Soc Trans*, **21**, 549-553.

Roden, M., Price, T.B., Perseghin, G., Petersen, K.F., Rothman, D.L., Cline, G.W. and Shulman, G.I. (1996) Mechanism of free fatty acid-induced insulin resistance in humans. *J Clin Invest*, **97**, 2859-2865.

Rosca, M.G., Mustata, T.G., Kinter, M.T., Ozdemir, A.M., Kern, T.S., Szweda, L.I., Brownlee, M., Monnier, V.M. and Weiss, M.F. (2005) Glycation of mitochondrial proteins from diabetic rat kidney is associated with excess superoxide formation. *Am J Physiol Renal Physiol*, **289**, F420-430.

Rosen, E.D., Walkey, C.J., Puigserver, P. and Spiegelman, B.M. (2000) Transcriptional regulation of adipogenesis. *Genes Dev*, **14**, 1293-1307.

Ross, S.E., Hemati, N., Longo, K.A., Bennett, C.N., Lucas, P.C., Erickson, R.L. and MacDougald, O.A. (2000) Inhibition of adipogenesis by Wnt signaling. *Science*, **289**, 950-953.

Ruggiero-Lopez, D., Lecomte, M., Moinet, G., Patereau, G., Lagarde, M. and Wiernsperger, N. (1999) Reaction of metformin with dicarbonyl compounds. Possible implication in the inhibition of advanced glycation end product formation. *Biochem Pharmacol*, **58**, 1765-1773.

Sajan, M.P., Standaert, M.L., Miura, A., Bandyopadhyay, G., Vollenweider, P., Franklin, D.M., Lea-Currie, R. and Farese, R.V. (2004) Impaired activation of protein kinase C-zeta by insulin and phosphatidylinositol-3,4,5-(PO4)3 in cultured preadipocyte-derived adipocytes and myotubes of obese subjects. *J Clin Endocrinol Metab*, **89**, 3994-3998.

Sakamoto, H., Mashima, T., Yamamoto, K. and Tsuruo, T. (2002) Modulation of heat-shock protein 27 (Hsp27) anti-apoptotic activity by methylglyoxal modification. *J Biol Chem*, **277**, 45770-45775.

Sakaue, H., Ogawa, W., Takata, M., Kuroda, S., Kotani, K., Matsumoto, M., Sakaue, M., Nishio, S., Ueno, H. and Kasuga, M. (1997) Phosphoinositide 3-kinase is required for insulin-induced but not for growth hormone- or hyperosmolarity-induced glucose uptake in 3T3-L1 adipocytes. *Mol Endocrinol*, **11**, 1552-1562.

Saltiel, A.R. and Kahn, C.R. (2001) Insulin signalling and the regulation of glucose and lipid metabolism. *Nature*, **414**, 799-806.

Sandu, O., Song, K., Cai, W., Zheng, F., Uribarri, J. and Vlassara, H. (2005) Insulin resistance and type 2 diabetes in high-fat-fed mice are linked to high glycotoxin intake. *Diabetes*, **54**, 2314-2319.

Sanger, F. and Tuppy, H. (1951) The amino-acid sequence in the phenylalanyl chain of insulin. 2. The investigation of peptides from enzymic hydrolysates. *Biochem J*, **49**, 481-490.

Santomauro, A.T., Boden, G., Silva, M.E., Rocha, D.M., Santos, R.F., Ursich, M.J., Strassmann, P.G. and Wajchenberg, B.L. (1999) Overnight lowering of free fatty

acids with Acipimox improves insulin resistance and glucose tolerance in obese diabetic and nondiabetic subjects. *Diabetes*, **48**, 1836-1841.

Santos, R.F., Nomizo, R., Bopsco, A., Wajchenberg, B.L., Reaven, G.M. and Azhar, S. (1997) Effect of metformin on insulin-stimulated tyrosine kinase activity of erythrocytes from obese women with normal glucose tolerance. *Diabetes Metab*, **23**, 143-148.

Sasaki, N., Fukatsu, R., Tsuzuki, K., Hayashi, Y., Yoshida, T., Fujii, N., Koike, T., Wakayama, I., Yanagihara, R., Garruto, R., Amano, N. and Makita, Z. (1998) Advanced glycation end products in Alzheimer's disease and other neurodegenerative diseases. *Am J Pathol*, **153**, 1149-1155.

Sato, H., Terasaki, T., Mizuguchi, H., Okumura, K. and Tsuji, A. (1991) Receptor-recycling model of clearance and distribution of insulin in the perfused mouse liver. *Diabetologia*, **34**, 613-621.

Schagger, H. and von Jagow, G. (1987) Tricine-sodium dodecyl sulfate-polyacrylamide gel electrophoresis for the separation of proteins in the range from 1 to 100 kDa. *Anal Biochem*, **166**, 368-379.

Schiekofer, S., Andrassy, M., Chen, J., Rudofsky, G., Schneider, J., Wendt, T., Stefan, N., Humpert, P., Fritsche, A., Stumvoll, M., Schleicher, E., Haring, H.U., Nawroth, P.P. and Bierhaus, A. (2003) Acute hyperglycemia causes intracellular formation of CML and activation of ras, p42/44 MAPK, and nuclear factor kappaB in PBMCs. *Diabetes*, **52**, 621-633.

Schmidt, A.M., Mora, R., Cao, R., Yan, S.D., Brett, J., Ramakrishnan, R., Tsang, T.C., Simionescu, M. and Stern, D. (1994) The endothelial cell binding site for advanced glycation end products consists of a complex: an integral membrane protein and a lactoferrin-like polypeptide. *J Biol Chem*, **269**, 9882-9888.

Schmidt, A.M., Yan, S.D., Brett, J., Mora, R., Nowygrod, R. and Stern, D. (1993) Regulation of human mononuclear phagocyte migration by cell surface-binding proteins for advanced glycation end products. *J Clin Invest*, **91**, 2155-2168.

Sebekova, K., Schinzel, R., Munch, G., Krivosikova, Z., Dzurik, R. and Heidland, A. (1999) Advanced glycation end-product levels in subtotally nephrectomized rats: beneficial effects of angiotensin II receptor 1 antagonist losartan. *Miner Electrolyte Metab*, **25**, 380-383.

Sechi, L.A. and Bartoli, E. (1997) Mechanisms of insulin resistance leading to hypertension: what we can learn from experimental models. *J Investig Med*, **45**, 238-251.

Shamsi, F.A., Partal, A., Sady, C., Glomb, M.A. and Nagaraj, R.H. (1998) Immunological evidence for methylglyoxal-derived modifications in vivo. Determination of antigenic epitopes. *J Biol Chem*, **273**, 6928-6936.

Sherr, C.J. and Roberts, J.M. (1999) CDK inhibitors: positive and negative regulators of G1-phase progression. *Genes Dev*, **13**, 1501-1512.

Shimomura, I., Bashmakov, Y., Ikemoto, S., Horton, J.D., Brown, M.S. and Goldstein, J.L. (1999) Insulin selectively increases SREBP-1c mRNA in the livers of rats with streptozotocin-induced diabetes. *Proc Natl Acad Sci U S A*, **96**, 13656-13661.

Shinohara, M., Thornalley, P.J., Giardino, I., Beisswenger, P., Thorpe, S.R., Onorato, J. and Brownlee, M. (1998) Overexpression of glyoxalase-I in bovine endothelial cells inhibits intracellular advanced glycation endproduct formation and prevents hyperglycemia-induced increases in macromolecular endocytosis. *J Clin Invest*, **101**, 1142-1147.

Singh, R., Barden, A., Mori, T. and Beilin, L. (2001) Advanced glycation end-products: a review. *Diabetologia*, **44**, 129-146.

Smit, A.J. and Lutgers, H.L. (2004) The clinical relevance of advanced glycation endproducts (AGE) and recent developments in pharmaceutics to reduce AGE accumulation. *Curr Med Chem*, **11**, 2767-2784.

Smith, I. (1971) Model of an insulin dimer and tetramer, and a hypothetical proinsulin. *Biochem J*, **125**, 81P.

Smith, P.K., Krohn, R.I., Hermanson, G.T., Mallia, A.K., Gartner, F.H., Provenzano, M.D., Fujimoto, E.K., Goeke, N.M., Olson, B.J. and Klenk, D.C. (1985) Measurement of protein using bicinchoninic acid. *Anal Biochem*, **150**, 76-85.

Song, D., Arikawa, E., Galipeau, D., Battell, M. and McNeill, J.H. (2004) Androgens are necessary for the development of fructose-induced hypertension. *Hypertension*, **43**, 667-672.

Soulis-Liparota, T., Cooper, M., Papazoglou, D., Clarke, B. and Jerums, G. (1991) Retardation by aminoguanidine of development of albuminuria, mesangial expansion, and tissue fluorescence in streptozocin-induced diabetic rat. *Diabetes*, **40**, 1328-1334.

Spalding, K.L., Arner, E., Westermark, P.O., Bernard, S., Buchholz, B.A., Bergmann, O., Blomqvist, L., Hoffstedt, J., Naslund, E., Britton, T., Concha, H., Hassan, M., Ryden, M., Frisen, J. and Arner, P. (2008) Dynamics of fat cell turnover in humans. *Nature*, **453**, 783-787.

Steiner, D.F., Clark, J.L., Nolan, C., Rubenstein, A.H., Margoliash, E., Aten, B. and Oyer, P.E. (1969) Proinsulin and the biosynthesis of insulin. *Recent Prog Horm Res*, **25**, 207-282.

Steiner, D.F., Tager, H.S., Chan, S.J., Nanjo, K., Sanke, T. and Rubenstein, A.H. (1990) Lessons learned from molecular biology of insulin-gene mutations. *Diabetes Care*, **13**, 600-609.

Stirban, A., Negrean, M., Stratmann, B., Gawlowski, T., Horstmann, T., Gotting, C., Kleesiek, K., Mueller-Roesel, M., Koschinsky, T., Uribarri, J., Vlassara, H. and Tschoepe, D. (2006) Benfotiamine prevents macro- and microvascular endothelial dysfunction and oxidative stress following a meal rich in advanced glycation end products in individuals with type 2 diabetes. *Diabetes Care*, **29**, 2064-2071.

Stith, B.J., Goalstone, M.L., Espinoza, R., Mossel, C., Roberts, D. and Wiernsperger, N. (1996) The antidiabetic drug metformin elevates receptor tyrosine kinase activity and inositol 1,4,5-trisphosphate mass in Xenopus oocytes. *Endocrinology*, **137**, 2990-2999.

Stitt, A.W., Bucala, R. and Vlassara, H. (1997) Atherogenesis and advanced glycation: promotion, progression, and prevention. *Ann N Y Acad Sci*, **811**, 115-127; discussion 127-119.

Tanaka, Y., Uchino, H., Shimizu, T., Yoshii, H., Niwa, M., Ohmura, C., Mitsuhashi, N., Onuma, T. and Kawamori, R. (1999) Effect of metformin on advanced glycation endproduct formation and peripheral nerve function in streptozotocin-induced diabetic rats. *Eur J Pharmacol*, **376**, 17-22.

Taylor, S.I., Kadowaki, T., Kadowaki, H., Accili, D., Cama, A. and McKeon, C. (1990) Mutations in insulin-receptor gene in insulin-resistant patients. *Diabetes Care*, **13**, 257-279.

Thorburn, A.W., Storlien, L.H., Jenkins, A.B., Khouri, S. and Kraegen, E.W. (1989) Fructose-induced in vivo insulin resistance and elevated plasma triglyceride levels in rats. *Am J Clin Nutr*, **49**, 1155-1163.

Thornalley, P.J. (1993) The glyoxalase system in health and disease. *Mol Aspects Med*, **14**, 287-371.

Thornalley, P.J. (2005) Glycation free adduct accumulation in renal disease: the new AGE. *Pediatr Nephrol*, **20**, 1515-1522.

Thornalley, P.J., Hooper, N.I., Jennings, P.E., Florkowski, C.M., Jones, A.F., Lunec, J. and Barnett, A.H. (1989) The human red blood cell glyoxalase system in diabetes mellitus. *Diabetes Res Clin Pract*, **7**, 115-120.

Thornalley, P.J., Yurek-George, A. and Argirov, O.K. (2000) Kinetics and mechanism of the reaction of aminoguanidine with the alpha-oxoaldehydes glyoxal, methylglyoxal, and 3-deoxyglucosone under physiological conditions. *Biochem Pharmacol*, **60**, 55-65.

Tsuchida, K., Makita, Z., Yamagishi, S., Atsumi, T., Miyoshi, H., Obara, S., Ishida, M., Ishikawa, S., Yasumura, K. and Koike, T. (1999) Suppression of transforming growth factor beta and vascular endothelial growth factor in diabetic nephropathy in rats by a novel advanced glycation end product inhibitor, OPB-9195. *Diabetologia*, **42**, 579-588.

Tucker, J.D., Taylor, R.T., Christensen, M.L., Strout, C.L., Hanna, M.L. and Carrano, A.V. (1989) Cytogenetic response to 1,2-dicarbonyls and hydrogen peroxide in Chinese hamster ovary AUXB1 cells and human peripheral lymphocytes. *Mutat Res*, **224**, 269-279.

Vaca, C.E., Fang, J.L., Conradi, M. and Hou, S.M. (1994) Development of a 32P-postlabelling method for the analysis of 2'-deoxyguanosine-3'-monophosphate and DNA adducts of methylglyoxal. *Carcinogenesis*, **15**, 1887-1894.

Valet, P., Pages, C., Jeanneton, O., Daviaud, D., Barbe, P., Record, M., Saulnier-Blache, J.S. and Lafontan, M. (1998) Alpha2-adrenergic receptor-mediated release of lysophosphatidic acid by adipocytes. A paracrine signal for preadipocyte growth. *J Clin Invest*, **101**, 1431-1438.

Vander Jagt, D.L., Hunsaker, L.A., Vander Jagt, T.J., Gomez, M.S., Gonzales, D.M., Deck, L.M. and Royer, R.E. (1997) Inactivation of glutathione reductase by 4-hydroxynonenal and other endogenous aldehydes. *Biochem Pharmacol*, **53**, 1133-1140.

Vasan, S., Foiles, P. and Founds, H. (2003) Therapeutic potential of breakers of advanced glycation end product-protein crosslinks. *Arch Biochem Biophys*, **419**, 89-96.

Vasan, S., Zhang, X., Zhang, X., Kapurniotu, A., Bernhagen, J., Teichberg, S., Basgen, J., Wagle, D., Shih, D., Terlecky, I., Bucala, R., Cerami, A., Egan, J. and Ulrich, P. (1996) An agent cleaving glucose-derived protein crosslinks in vitro and in vivo. *Nature*, **382**, 275-278.

Vasdev, S., Ford, C.A., Longerich, L., Parai, S., Gadag, V. and Wadhawan, S. (1998) Aldehyde induced hypertension in rats: prevention by N-acetyl cysteine. *Artery*, **23**, 10-36.

Vlassara, H. (1996) Advanced glycation end-products and atherosclerosis. *Ann Med*, **28**, 419-426.

Wada, R., Nishizawa, Y., Yagihashi, N., Takeuchi, M., Ishikawa, Y., Yasumura, K., Nakano, M. and Yagihashi, S. (2001) Effects of OPB-9195, anti-glycation agent, on experimental diabetic neuropathy. *Eur J Clin Invest*, **31**, 513-520.

Wang, H., Liu, J. and Wu, L. (2009) Methylglyoxal-induced mitochondrial dysfunction in vascular smooth muscle cells. *Biochem Pharmacol*, **77**, 1709-1716.

Wang, H., Meng, Q.H., Chang, T. and Wu, L. (2006) Fructose-induced peroxynitrite production is mediated by methylglyoxal in vascular smooth muscle cells. *Life Sci*, **79**, 2448-2454.

Wang, H., Meng, Q.H., Gordon, J.R., Khandwala, H. and Wu, L. (2007a) Proinflammatory and proapoptotic effects of methylglyoxal on neutrophils from patients with type 2 diabetes mellitus. *Clin Biochem*, **40**, 1232-1239.

Wang, X., Chang, T., Jiang, B., Desai, K. and Wu, L. (2007b) Attenuation of hypertension development by aminoguanidine in spontaneously hypertensive rats: role of methylglyoxal. *Am J Hypertens*, **20**, 629-636.

Wang, X., Desai, K., Chang, T. and Wu, L. (2005) Vascular methylglyoxal metabolism and the development of hypertension. *J Hypertens*, **23**, 1565-1573.

Wang, X., Desai, K., Clausen, J.T. and Wu, L. (2004) Increased methylglyoxal and advanced glycation end products in kidney from spontaneously hypertensive rats. *Kidney Int*, **66**, 2315-2321.

Wang, X., Jia, X., Chang, T., Desai, K. and Wu, L. (2008) Attenuation of hypertension development by scavenging methylglyoxal in fructose-treated rats. *J Hypertens*, **26**, 765-772.

Wautier, M.P., Chappey, O., Corda, S., Stern, D.M., Schmidt, A.M. and Wautier, J.L. (2001) Activation of NADPH oxidase by AGE links oxidant stress to altered gene expression via RAGE. *Am J Physiol Endocrinol Metab*, **280**, E685-694.

Weiner, F.R., Smith, P.J., Wertheimer, S. and Rubin, C.S. (1991) Regulation of gene expression by insulin and tumor necrosis factor alpha in 3T3-L1 cells. Modulation of the transcription of genes encoding acyl-CoA synthetase and stearoyl-CoA desaturase-1. *J Biol Chem*, **266**, 23525-23528.

Wellen, K.E. and Hotamisligil, G.S. (2005) Inflammation, stress, and diabetes. *J Clin Invest*, **115**, 1111-1119.

Wells-Knecht, K.J., Brinkmann, E., Wells-Knecht, M.C., Litchfield, J.E., Ahmed, M.U., Reddy, S., Zyzak, D.V., Thorpe, S.R. and Baynes, J.W. (1996) New biomarkers of Maillard reaction damage to proteins. *Nephrol Dial Transplant*, **11 Suppl 5**, 41-47.

Westwood, M.E. and Thornalley, P.J. (1995) Molecular characteristics of methylglyoxal-modified bovine and human serum albumins. Comparison with glucose-derived advanced glycation endproduct-modified serum albumins. *J Protein Chem*, **14**, 359-372.

White, M.F. and Kahn, C.R. (1994) The insulin signaling system. *J Biol Chem*, **269**, 1-4.

Wolffenbuttel, B.H., Boulanger, C.M., Crijns, F.R., Huijberts, M.S., Poitevin, P., Swennen, G.N., Vasan, S., Egan, J.J., Ulrich, P., Cerami, A. and Levy, B.I. (1998) Breakers of advanced glycation end products restore large artery properties in experimental diabetes. *Proc Natl Acad Sci U S A*, **95**, 4630-4634.

Wu, L. (2005) The pro-oxidant role of methylglyoxal in mesenteric artery smooth muscle cells. *Can J Physiol Pharmacol*, **83**, 63-68.

Wu, L. (2006) Is methylglyoxal a causative factor for hypertension development? *Can J Physiol Pharmacol*, **84**, 129-139.

Wu, L. and Juurlink, B.H. (2002) Increased methylglyoxal and oxidative stress in hypertensive rat vascular smooth muscle cells. *Hypertension*, **39**, 809-814.

Wu, L., Noyan Ashraf, M.H., Facci, M., Wang, R., Paterson, P.G., Ferrie, A. and Juurlink, B.H. (2004) Dietary approach to attenuate oxidative stress, hypertension, and inflammation in the cardiovascular system. *Proc Natl Acad Sci U S A*, **101**, 7094-7099.

Xu, B., Goulding, E.H., Zang, K., Cepoi, D., Cone, R.D., Jones, K.R., Tecott, L.H. and Reichardt, L.F. (2003) Brain-derived neurotrophic factor regulates energy balance downstream of melanocortin-4 receptor. *Nat Neurosci*, **6**, 736-742.

Yamauchi, T., Tobe, K., Tamemoto, H., Ueki, K., Kaburagi, Y., Yamamoto-Honda, R., Takahashi, Y., Yoshizawa, F., Aizawa, S., Akanuma, Y., Sonenberg, N., Yazaki, Y. and Kadowaki, T. (1996) Insulin signalling and insulin actions in the muscles and livers of insulin-resistant, insulin receptor substrate 1-deficient mice. *Mol Cell Biol*, **16**, 3074-3084.

Yan, S.D., Schmidt, A.M. and Stern, D. (2001) Alzheimer's disease: inside, outside, upside down. *Biochem Soc Symp*, 15-22.

Yang, Q., Graham, T.E., Mody, N., Preitner, F., Peroni, O.D., Zabolotny, J.M., Kotani, K., Quadro, L. and Kahn, B.B. (2005) Serum retinol binding protein 4 contributes to insulin resistance in obesity and type 2 diabetes. *Nature*, **436**, 356-362.

Yano, S., Tokumitsu, H. and Soderling, T.R. (1998) Calcium promotes cell survival through CaM-K kinase activation of the protein-kinase-B pathway. *Nature*, **396**, 584-587.

Yao, D., Taguchi, T., Matsumura, T., Pestell, R., Edelstein, D., Giardino, I., Suske, G., Ahmed, N., Thornalley, P.J., Sarthy, V.P., Hammes, H.P. and Brownlee, M. (2006) Methylglyoxal modification of mSin3A links glycolysis to angiopoietin-2 transcription. *Cell*, **124**, 275-286.

Yao, D., Taguchi, T., Matsumura, T., Pestell, R., Edelstein, D., Giardino, I., Suske, G., Rabbani, N., Thornalley, P.J., Sarthy, V.P., Hammes, H.P. and Brownlee, M. (2007) High glucose increases angiopoietin-2 transcription in microvascular endothelial cells through methylglyoxal modification of mSin3A. *J Biol Chem*, **282**, 31038-31045.

Yeh, W.C., Cao, Z., Classon, M. and McKnight, S.L. (1995) Cascade regulation of terminal adipocyte differentiation by three members of the C/EBP family of leucine zipper proteins. *Genes Dev*, **9**, 168-181.

Youngstrom, T.G. and Bartness, T.J. (1998) White adipose tissue sympathetic nervous system denervation increases fat pad mass and fat cell number. *Am J Physiol*, **275**, R1488-1493.

Yu, P.H. (2001) Involvement of cerebrovascular semicarbazide-sensitive amine oxidase in the pathogenesis of Alzheimer's disease and vascular dementia. *Med Hypotheses*, **57**, 175-179.

Yu, P.H., Wang, M., Fan, H., Deng, Y. and Gubisne-Haberle, D. (2004) Involvement of SSAO-mediated deamination in adipose glucose transport and weight gain in obese diabetic KKAy mice. *Am J Physiol Endocrinol Metab*, **286**, E634-641.

Yu, P.H., Wright, S., Fan, E.H., Lun, Z.R. and Gubisne-Harberle, D. (2003) Physiological and pathological implications of semicarbazide-sensitive amine oxidase. *Biochim Biophys Acta*, **1647**, 193-199.

Zhou, B.P., Liao, Y., Xia, W., Spohn, B., Lee, M.H. and Hung, M.C. (2001) Cytoplasmic localization of p21Cip1/WAF1 by Akt-induced phosphorylation in HER-2/neu-overexpressing cells. *Nat Cell Biol*, **3**, 245-252.

Zierath, J.R., He, L., Guma, A., Odegoard Wahlstrom, E., Klip, A. and Wallberg-Henriksson, H. (1996) Insulin action on glucose transport and plasma membrane GLUT4 content in skeletal muscle from patients with NIDDM. *Diabetologia*, **39**, 1180-1189.